Image Quality

A Comparison of Photographic and Television Systems

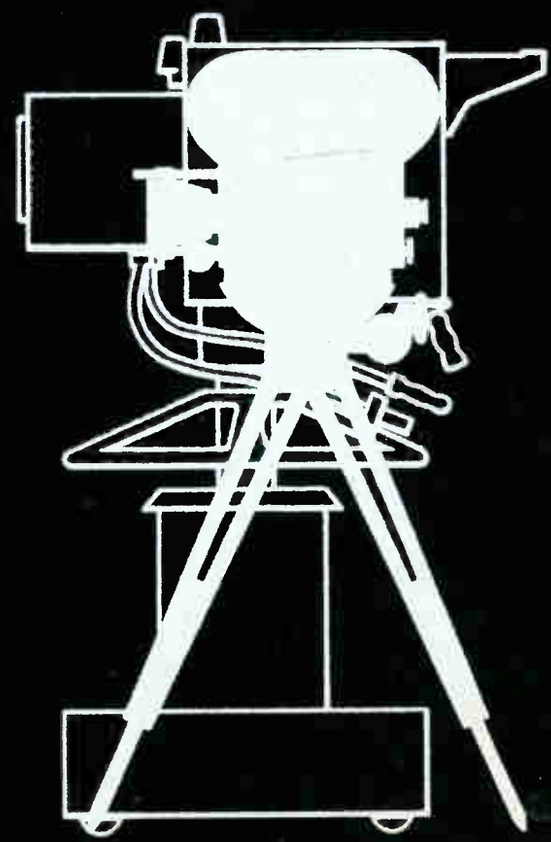

Otto H. Schade, Sr.

Image Quality

A Comparison of Photographic and Television Systems

Otto H. Schade, Sr.

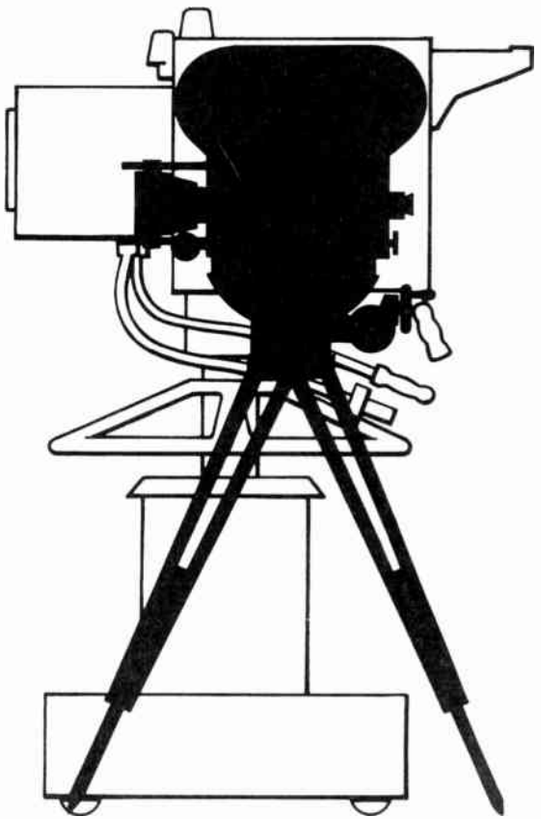

Published by RCA Laboratories, Princeton, New Jersey 08540

Foreword

It is not often that one has the occasion to indulge in superlatives without fear of abusing the language. This is such an occasion.

Otto Schade's career in television and the allied imaging sciences is unique. Many of the concepts that one takes for granted had their origin in his pioneering work in the 1940's and 1950's. At that time the television, photographic, optical, and visual systems each had its own method for evaluating its imaging properties. And the methods were generally non-commensurable. Schade introduced a set of criteria common to all of these systems, a set that is now universally accepted. His modulation transfer functions and equivalent line numbers can be applied equally to amplifiers, lenses, and the human eye. He recorded the first measurements, in these terms, on the human visual system.

It was Schade's intimate knowledge of and contributions to all parts of the television chain from camera to viewer that made possible his unparalleled demonstrations of picture quality. Many of these photographs are scattered through his publications and some have not appeared in print. It is for this reason that a number of his colleagues felt that a compilation of these photographs in a single volume would constitute a valuable service to the art and science of imaging. It would also, we felt, establish the television system as a versatile imaging tool confined not alone to the constraints of the commercial broadcast standards but capable as well of unusually high-quality renditions.

The impact of well executed photographs bespeaks volumes. Hence, the slender profile of this collection.

Albert Rose
Princeton, N.J., 15 April 1975

Preface

Image quality is a subjective judgment made by a mental comparison of an external image with image impressions stored and remembered more or less distinctly by the observer, who allows for a loss of detail in areas too small to be resolved by the eye. The quality of a photographic print is judged by its gray scale, definition, and graininess; the subjective ranking of the image as "poor," "good," or "excellent" depends, of course, on the size of the image and the viewing distance. Moreover, the rating of a given image may be greatly influenced by the availability of a much better image for comparison purposes. A study of intensity transfer functions, modulation transfer functions, and granularity or noise levels permits the determination of objective criteria for image quality that will correlate with visual observations. Nevertheless, viewing conditions remain important parameters, and a picture is far more instructive than a set of numbers or functions describing the image.

The collection of pictures grouped at the end of this volume were taken by the writer over a period of two decades. They illustrate far better than words the quality of television and photographic images obtained with specific electric and optical system parameters. The text describes these parameters and gives a brief account of the methods used for evaluation of objective image criteria and equivalents developed during this span of time.

The writer has enjoyed in this work the stimulation and guidance of many scientists in RCA and the Eastman Kodak Company, and is particularly indebted to A. Rose, D. O. North, and E. G. Ramberg of RCA Laboratories, Princeton, N.J. for many discussions and help in the analysis and formulation of the objective measures. I would like to thank Charles C. Foster and Ralph F. Ciafone for their generous help in preparing the text and reproductions for publication.

Otto H. Schade, Sr.

Contents

Image Quality—A Comparison of Photographic and Television Systems

Introduction

One of the most difficult problems in the early stages of television was to produce a system that could pick-up and reproduce live images with acceptable detail and low flicker, because these two characteristics are determined by the number of picture elements and the rate at which they are transmitted over an electrical frequency channel. It was indeed a tremendous task to build a system that could transmit 5 million picture elements or thirty 441-line images in one second, because it required a bandwidth equal to that of 500 sound broadcast channels. It is not surprising that the quality of a television picture was judged then, and even now, by its resolution, implied by the number of scan lines. It was recognized quite early that the bandwidth-limited resolution of a television image was something quite different from the grain-limited resolution of a motion picture. In motion pictures, the detail contrast decreases steadily towards zero, whereas a bandwidth-limited system can maintain a high detail contrast close to its limit of resolution. The resolving power used as a criterion of image sharpness in photography cannot be directly applied to commercial television images, which, by subjective tests, appear considerably sharper than indicated by the moderate resolving power of the system. One may well ask if this difference alters the general appearance of the image and, if so, in what ways the appearance differs from that of a good photograph. The answer to these questions depends to a degree on the subject material and requires a more detailed analysis.

The "perfect" picture should, in a practical sense, look like a piece of the real world to the unaided eye. The broad term "image quality" encompasses much more than resolution or sharpness. It includes three basic parameters:

(1) The gray scale, which is determined by the intensity transfer function. Continuity of the intensity in the vertical coordinate of a TV image is of particular concern because the continuous optical image from the camera lens is sampled and reproduced in discrete increments by a line raster. It will be shown that continuity in the vertical coordinate of the image can be restored by proper choice of the scanning spots in the camera and in the display tube.
(2) Sharpness and definition, which are determined by the modulation transfer function.
(3) Granularity or noise, which is controlled by the particle or quantum density that can be stored in the sensor of the camera.

These characteristics should be uniform within the format of the image, a condition that implies isotropy, absence of geometric distortion, shading, and other image defects.

The photographs used to illustrate image quality, Figs. 27 through 72, are grouped together following the text. In the text, these numbers are given in bold face to distinguish them from those figures that are included with the text. It is hoped that this arrangement will aid the reader in perceiving, by direct comparisons of these photographs, the visual significance of such characteristics as number of lines, bandwidth, noise, and gray scale as they affect image quality.

1. The Gray Scale

The reproduction of a natural gray scale ranks first in importance. It was known from photography that the overall transfer function of the system (plotted in log-log units) should depart from a straight line, representing a linear function with a slope or "gamma" of unity, and

be somewhat S-shaped for a most pleasing reproduction. The gamma in the center range should be in the order of 1.2 and fall off towards the ends of the range. The range itself should be at least 100 to 1. This range is difficult to achieve in a paper print; it can be exceeded considerably in the display on a cathode-ray tube (CRT) in a dark room or with transparencies; and in a motion-picture projection it is limited to somewhat less than 100 to 1 by lens flare and ambient light.

The gray scale and gamma of early TV systems were fixed by the transfer functions of the sensor and the display tube (CRT) and yielded a short range, going rapidly into black. Thus, gray-scale range could be controlled only by lighting all darker areas in the studio scene to reduce the gamma of the scene itself. This cannot be done for outdoor scenes or in the reproduction of motion-picture film. An intensive study of television and motion-picture transfer functions[1] led to the concept of "gamma correction" in the electrical video channel, where the normally linear signal transfer can be manipulated by nonlinear networks. It was found that these gamma-correction circuits could change any combination of transfer functions in the sensor (camera), display tube, and the scene picked up by the camera to a desirable overall transfer function, including the transfer from a motion-picture film.

The effectiveness of gamma correction by electrical means was demonstrated to the motion-picture industry in 1950 by a side-by-side comparison between an optical projection of a series of 2 × 2-inch transparencies and a television display of duplicate slides picked up by a light-spot scanner with gamma correction. The correction circuits could be adjusted to obtain a nearly exact match of gamma in the optical and television images, or to expand or compress the shadow region or the highlight region of the gray scale. Copies made with a 4 × 5-inch view camera of the optically projected image and of the television image reproduced over a 525-line 4.25-MHz channel are shown in Figs. **27** through **30**. The exposure in the view camera was 1.5 seconds at f:16 to minimize image degradation in the photographic copying process. This time exposure integrates noise from the TV process, and the apparent grain in these pictures is caused by the stationary grain structure of the CRT screen in the light-spot scanner.

Pictures of a live pickup made at the same time with an image-orthicon camera (4½-inch face plate) over a 4.25-MHz 525-line channel and over a 625-line 8-MHz channel are reproduced in Figs. **31** and **32**. It was demonstrated that the direct-view television images could be given more "sparkle" in the highlights than seen in the optical projections of the slides. The expanded highlights, however, are not reproduced by the photographic copying process owing to saturation in the film, which is more pronounced when copying a TV line structure from a CRT display. (The density range in the film is much higher than indicated by the gray scale range because of the light concentration into the fine scanning lines.)

The Sampled Image

The intensity distribution of a television image is reproduced in the vertical coordinate by a sampling process. The structure of the line raster should be no more visible than the dot structure in a good halftone print at normal viewing distances. Raster structures are carrier frequencies of the sampling process, which, like noise, interfere with the detection of fine detail and must be filtered out by low-pass filters preceding and following the raster process. In fact, a somewhat lengthy analysis[2] indicates that the modulation frequencies from the camera and in the final image should be limited to one-half the frequency of the raster carrier, or sampling frequency, to eliminate all unwanted modulation products, which are sum and difference frequencies of the modulation with all harmonics of the pulse carrier frequency. The sampling frequency f_s of a line raster is the raster line number $n_r = f_s$, and for a 500-line raster, the modulation frequency should go to zero at 250 cycles, or $N_v = 500$ TV lines. This "Nyquist" limit is difficult to satisfy with the normally gaussian spot shapes of television tubes without incurring an excessive loss of modulation transfer. The theoretically most desirable modulation transfer function (MTF) is rectangular up to the Nyquist limit and requires a $(\sin x)/x$ spot cross section with first zeros on adjacent raster lines. This exotic spot shape can be approached by vertical aperture correction using delay lines that are now commercially available.[3] A compromise design for gaussian spots aims at filtering out the raster carrier to eliminate a visible line structure but retains an MTF of 38% at the Nyquist limit; it is called the "flat field" condition. The gaussian line profiles extend over two line spacings, which is sufficient to produce a uniform intensity in the vertical direction in the display and prevent unscanned interline spaces in the camera. The latter would decrease sensitivity and can cause instability of the raster and strong "aliasing" which cannot be removed by post filtering in the display. The nonzero response at the Nyquist limit produces a maximum spu-

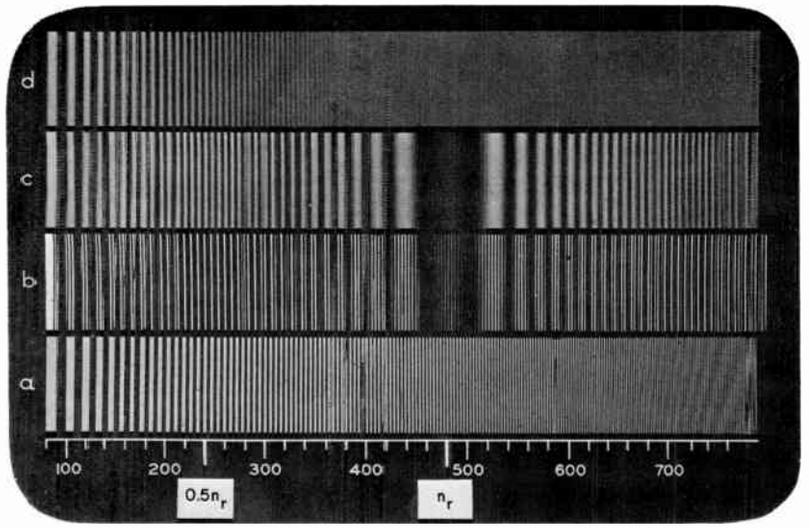

Fig. 1—Repetitive frequency spectrum (aliasing) generated by an optical line-raster process without input filtering (camera MTF very high compared to Nyquist limit, 0.5 n_r): (a) test pattern, (b) very small display aperture does not filter out raster frequency, (c) larger display aperture filters out raster carrier, and (d) raster plate removed shows spectrum of display aperture and eliminates aliasing.

rious signal amplitude of $(0.38)^2$, or 14%, which occurs only occasionally and can be tolerated.

For applications such as reconnaisance, where maximum resolving power is essential, a higher sampling frequency (four samples per spread function) is recommended, which corresponds to an MTF not larger than 5% at the Nyquist limit. Stated mathematically in terms of TV lines,

$$\mathrm{MTF}_{cv} = \mathrm{MTF}_{(d+e)v} \leqq 0.38 \text{ at } N = n_r \qquad [1]$$

and

$$N_{e(c)v} = N_{e(d+e)v} \leqq 0.64 n_r$$

where $N_{e(c)v}$ is the noise-equivalent pass band calculated from the MTF of the camera (pre-filter) and $N_{e(d+e)v}$ is the noise-equivalent pass band* for the post-filter. The latter consists of the cascaded MTF value $\mathrm{MTF}_{(d+e)v}$ for the display system and the eye in the vertical direction of the image. Thus, the MTF of the display device (CRT) alone can be higher than specified by Eq. [1] for larger viewing distances, where filtering by the eye can be sufficient.

The strong aliasing produced by an optical raster process and a very small sampling spot in the camera ($N_{e(c)v} \gg n_r$) is illustrated by Fig. 1. A raster plate containing very fine vertical slits having a frequency $f_r = n_r = 480$ lines was placed over a linearly increasing frequency pattern (a) to produce the sampled image (b). The repetitive frequency spectrum extends far beyond the normal frequency response of the Nyquist limit $f = 0.5\, f_r$. Integration by a post-filter (c) eliminates the sampling frequency (fine white lines) but not the aliasing. The response of the post filter is shown by (d), obtained by removing the raster plate. The post-filter MTF is zero at the sampling frequency f_r. Similar pre-filtering is necessary to decrease the generation of alien frequencies, as stated by Eq. [1].

Assuming that the requirements for the gray scale and sampling have been met, we can proceed to a discussion of the MTF and the equivalent pass band (N_e) that determine definition and sharpness of the image.

2. Modulation Transfer, Definition, and Sharpness

The accuracy in the reproduction of detail is determined in principle by the diameter and intensity distribution of the point image of the process. When the first point image from the lens is reproduced, every point is expanded into a finite size; the second point image is increased in size and its intensity distribution is usually different from that of the first point image. Practical point images are in general not sharply defined but have a bright nucleus surrounded by a haze disc of gradually decreasing intensity. Beyond the diameter where the haze disc intensity decreases to less than 1% of that of the bright center, it cannot be seen any longer, but the total light flux in the haze component at this and lower intensities may represent a large fraction of the total flux in the point image. For this reason a specification of the point spread function must have an accuracy far better than 1%. Successive point images are generated by considering the second point image as an "aperture" of nonuniform transmittance that scans the first point images, a process called "convolution."

* Discussed in section dealing with the modulation transfer function of the visual system (Eq. [3]).

The intensity products within the scanning aperture, plotted as a function of displacement (Δx, Δy), yield the point image of the two processes. Edge transitions can be generated similarly. The method can be applied to any type of intensity distribution that, no matter how complex, can be broken down by a Fourier analysis into a series of sine-wave components having certain amplitudes and phase relations. A complete specification of the "aperture effect" of point images can therefore be given by evaluating the Fourier transform of the aperture by a convolution with sinusoidally varying intensity functions of different spatial frequencies in the direction of scanning (and uniform in the perpendicular direction). This sine-wave response function or, as it is now called, the modulation transfer function, may have different values for different directions of scanning when the aperture is not circular. Being an integral of the total flux distribution in two-dimensional products, the accuracy of measured MTF's is better than obtained by calculation from measured point images.

The concept of representing the spread functions of all components in photographic and TV systems by their "aperture response" i.e., by their frequency transforms (the sine-wave response or modulation transfer function), arose from the need to determine the contribution of individual system components in a multi-stage process to the blurring of the final image. Recordings of original TV images on motion-picture film were needed for networking purposes, and the quality of the originals was severely degraded in the process. Data on spot sizes or on the aperture response of lenses, display tubes, and photographic film were non-existent. It was thus necessary to develop instrumentation for measuring the MTF or the square-wave response[4–6] of these components and establish experimental proof of the two-dimensional transform theory. The combined MTF of any number of components could then be obtained by simple multiplication. It followed immediately that a given response factor for a system with n components requires that the response of every stage be the nth root of the desired response. For example, a moderate MTF of 32% at the output of a 5-stage system requires an MTF of 80% in every stage! The idea of correcting deficiencies in the horizontal MTF of the TV system "aperture" by a boost of high frequencies met with instant success,[4,6] whereas aperture correction in the vertical direction was hampered by the unavailability of delay lines until a much later time.[3,7] The effectively smaller aperture obtained by such correction circuits is traded for increased noise. The noise increases to its normal value consistent with the smaller aperture when the correction is made for apertures following a noise source, but it is higher than the normal noise when the correction is made for a low-MTF element preceding a noise source, which puts stringent requirements on the camera lens. The rms noise is inversely proportional to the diameter of the sampling aperture. It follows that high-resolution systems have basically a higher noise level than systems with moderate resolution and, therefore, require a higher exposure and photon density in the sensor to maintain the same quantum count and signal-to-noise ratio in the smaller sampling aperture.

Before going further into the subject of noise, it is appropriate to discuss the evaluation of a modulation transfer function for the visual process that must be included in any assessment of image definition and sharpness.

2.1 Modulation Transfer Function of the Visual System

It is logical that an external image will be judged to be perfectly sharp when all spatial frequencies within the visual pass band are reproduced with an MTF of unity. It is also logical that all frequencies beyond the visual pass band can be cut off by a filter without effect on the visual impression. Therefore, a cutoff within the visual pass band or an attenuation of the MTF in some part of the visual frequency response cannot be assessed properly without knowledge of the MTF of the eye.

The square-wave flux response function $r\bar{\Delta}(N)$ of the eye was derived in 1948 from measurements of its contrast sensitivity to square-wave line patterns[4] by a method used for measuring the frequency response of amplifiers, namely by adjusting the input signal to maintain a constant output signal at different frequencies. The sine-wave response was calculated with Eq. [7] (see Sec. 2.2, Sharpness and Texture).

Direct measurements of the response of the eye to sine-wave fields, i.e., the luminance MTF of the eye, were made in 1955.[8] A set of these MTF's normalized to unity at $f = 0$ is shown in Fig. 2. The MTF is expressed in cycles/mm (f) at the retina of the eye, which has an effective focal length of 17 mm. Thus for a given viewing ratio, ρ = viewing distance divided by the vertical picture dimension, the corresponding TV line number is

$$N_{\rho(\text{eye})} = 34f/\rho. \qquad [2]$$

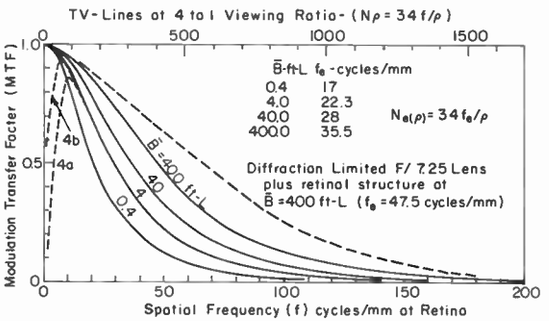

Fig. 2—Modulation transfer functions of visual system (at retina).

The MTF calculated with Eq. [7] from the square-wave flux response of the earlier measurement is in good agreement with the MTF shown in Fig. 2 for the average field brightness $\bar{B}$ of 4 ft-L. The actually measured MTF's (see Ref. 8) for *stationary* sine-wave fields, however, show a loss of low frequencies as indicated by curve 4a and need further discussion. It is well known that the eye must vibrate (ocular tremor) to see fine detail, i.e., to generate ac signals from contours and small objects. Its dc response is very low, and is restored in the brain by a complex correlation with other sensor inputs and the vast stored information acquired in a lifetime of picture processing. The amplitude of the ocular tremor is quite small, about 6 μm,[9] so that the ac signals decrease for frequencies smaller than 80 cycles/mm. However, in terms of "sensation" units, the decrease is compensated to a large extent by the increasing signal-to-noise ratio for larger objects, and for very low frequencies by the jerky motion of the eyeball. Curve 4a was measured with a short time of observation, providing no time for eyeball motion. A second set of observations was therefore made with sine-wave fields drifting at a rate of one cycle per second at low frequencies, which increased the low-frequency response as shown by curve 4b for $\bar{B}$ = 4 ft-L. A long observation time during which the eye scans the image increases the low-frequency response.* The low-frequency response to square-wave test patterns is on the order of 80% at zero frequency because of the steep sides of this waveform, which is more common in natural scenes than a low-frequency sine wave. A representative MTF should take into account the signal processing in the retina–brain combination, and is better represented by an MTF normalized to unity at zero frequency. These MTF's are lower than the MTF of the optic of the eye because they include the loss in the sampling structure of the retina and the ocular tremor.

The MTF increases at higher light levels, partly because of the automatic iris that stops the lens down to f:7.25 at $\bar{B}$ = 400 ft-L (reduced aberrations) and partly because of reduced integration in the retinal signal processing. A broken-line curve indicates an upper limit calculated for a diffraction-limited f:7.25 lens in cascade with a 2.2-μm cone structure and the ocular tremor. The actual MTF for $\bar{B}$ = 400 ft-L indicates an aberration of approximately 0.4 wavelength of light, which is indeed good performance for a lens–sensor combination.

Because of the signal processing and memory in the brain, the eye will recognize nearly all departures from a normal MTF in an external image, and will judge the image to be unnatural when its low-frequency response is depressed, or if a sharp cutoff or "image crispening" produces an overemphasis of contours or visible transients in the retinal image, or when the image contains an artificial line or dot structure. These faults can be seen in many TV images at a normal viewing distance, and are interpreted as typical "TV image quality" compared to a good photograph.

2.2 Sharpness and Texture (Equivalent Pass Bands)

Clearly the diameter of the sampling aperture or its corresponding frequency transform determines the sharpness of an image. The differences in aperture transmittance and MTF's indicate the desirability of a measure such as an equivalent aperture and MTF, which can be specified by a single number. A random grain structure or "white" noise is a very useful test object because its frequency components have a flat spectrum with random phase relations. When this noise spectrum is passed through an aperture, one measures the MTF of the aperture. The squared value of the MTF is a measure of the total sine-wave energy. The area under the squared MTF of the aperture can be represented by a rectangle—an equivalent MTF_e of constant response up to a frequency f_e or line number N_e where the MTF_e drops abruptly to zero. This constant-amplitude pass band is called

* The low-frequency loss disappears for extremely short exposures, i.e., transient excitation.

the "noise-equivalent pass band" [5,6] of the aperture defined by

$$f_e = \int_0^\infty \mathrm{MTF}_{(f)}{}^2 df \qquad [3]$$

or

$$N_e = \int_0^\infty \mathrm{MTF}_{(N)}{}^2 dN$$

and yields the following equivalents: For a square aperture of area $\bar{a}$, $N_e = 1/\sqrt{\bar{a}}$; for a gaussian aperture of diameter $\delta = 4r_0$, $N_e = 1.6/\delta$; and for a round aperture of uniform transmittance and diameter δ, $N_e = 1.08/\delta$. It can be demonstrated that the equivalent pass band of a multistage process can be computed with good accuracy* from the individual N_e values of the stages with

$$N_{e(p)} = 1/(N_{e1}{}^{-2} + N_{e2}{}^{-2} + \ldots)^{1/2}. \qquad [4]$$

This simple rule derives from the fact that the MTF's of different spot shapes or apertures are similar in the region $N \leq N_e$ when plotted in normalized units N/N_e, as illustrated by Fig. 3, and that the differences at high frequencies are greatly attenuated in the MTF product of a multistage process.

The square-wave amplitude response ($\hat{r}(N)$) measured with bar-pattern test charts can be converted to a (sine-wave) MTF by the following equation†

$$\mathrm{MTF}_{(N)} \simeq \frac{\pi}{4}\left(\hat{r}_N + \frac{1}{3}\hat{r}_{3N} - \frac{1}{5}\hat{r}_{5N} + \frac{1}{7}\hat{r}_{7N} + \frac{1}{11}\hat{r}_{11N} - \frac{1}{13}\hat{r}_{13N}\right) \qquad [5]$$

The waveform from a square-wave pattern degenerates into trapezoids and finally into sine waves in the upper two thirds of a square-wave response function because of the loss of harmonics. The change of waveform is not recognized by the eye at higher frequencies, because its own MTF eliminates the harmonics of fine-line objects, which are judged by their effective contrast, i.e., by their equivalent mean square-wave amplitude. *The equivalent square-wave flux* response ($r\bar{\Delta}_N$) at a line number (N) is defined by the flux ratio $\Delta\psi_{(N)}/\Delta\psi_{(N=0)}$ where $\Delta\psi$ is the mean intensity of the half-wave as measured with a rectifier type meter. The square-wave flux response can be calculated from the MTF by

$$r\bar{\Delta}_N = \frac{8}{\pi^2}\left(\mathrm{MTF}_N + \frac{1}{9}\mathrm{MTF}_{3N} + \frac{1}{25}\mathrm{MTF}_{5N} - \ldots\right) \qquad [6]$$

Conversely the MTF can be calculated from the square-wave flux response with

$$\mathrm{MTF}_N = \frac{\pi^2}{8}r\bar{\Delta}_N - \frac{1}{9}\mathrm{MTF}_{3N} - \frac{1}{25}\mathrm{MTF}_{5N} - \ldots \qquad [7]$$

For evaluation, one starts with high line numbers for which the 3rd-harmonic response is negligible. The MTF for lower line numbers can then be computed with the now available MTF's of the higher order terms.[6]

It is found further that the edge transitions of apertures having equal noise-equivalent pass bands are reasonably equivalent. This condition is illustrated in Fig. 4 for the MTF of a lens and a $\cos^2$ spot having equal values N_e. The edge transition of the lens has a some-

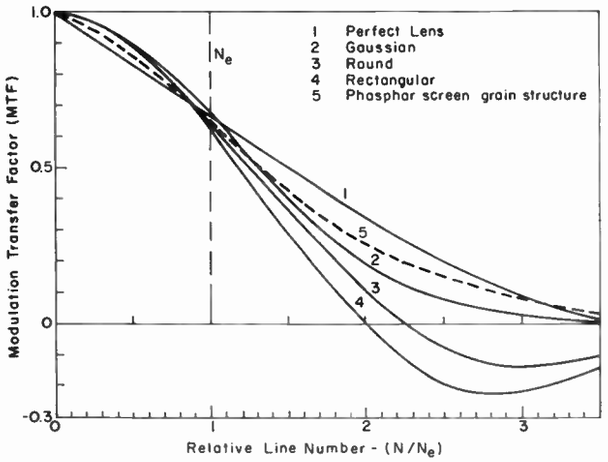

Fig. 3—Modulation transfer functions of sampling apertures. The spatial frequency is the line number in relative units (N/N_e): for the perfect lens, $N_e = 1.322/\delta$, ($\delta = 2.44\lambda \times$ f/number); gaussian, $N_e = 1.6/\delta$, ($\delta = 4r_0$ and $\tau = \exp\{-[r/r_0]^2\}$); round, $N_e = 1.08/\delta$, ($\delta = 2r$); and for a rectangular aperture, $N_e = 1/\sqrt{a}$ (where a is the area).

* Exceptions are the abnormal MTF's of aperture correction circuits or filters which require evaluation with Eq. [3] when included in a process.

† Note that the term for $9N$ does not appear in the series.

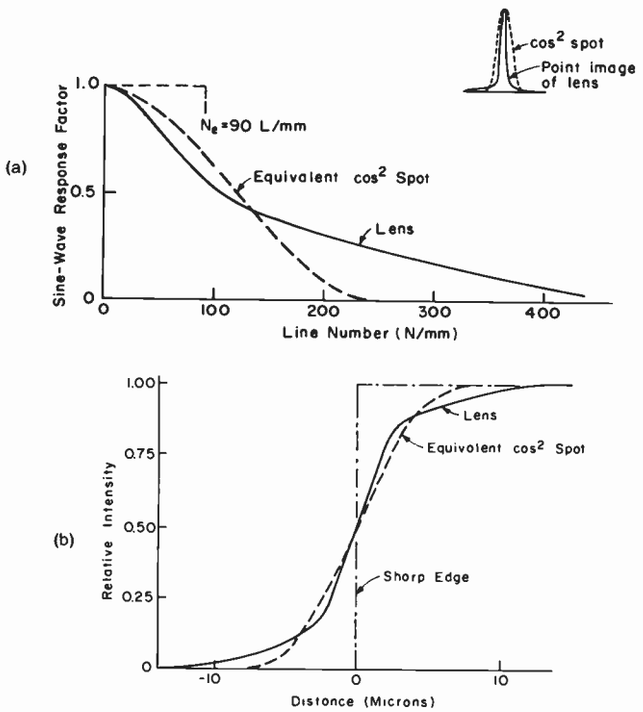

Fig. 4—(a) MTF of a camera lens and a $\cos^2$ aperture having identical equivalent pass bands (N_e) and (b) edge transitions for the apertures.

what steeper slope at the center of the transition, but the total length of the transition curve is longer than for the equivalent $\cos^2$ aperture. These differences compensate one another, and the noise-equivalent pass band emerges as a good measure for ranking general image sharpness as illustrated by the photographs Figs. **33** and **34**. It is evident from Eq. [3] that a long high-frequency tail of low amplitude in an MTF contributes little to the integral N_e.

Although the edge sharpness of the images Fig. **33** and **34** may be alike, there remain subtle differences because of faint high-frequency detail from the aperture having a high limiting resolution. This is called "texture," which is missing in an image having a short high-frequency spectrum ($\cos^2$ spot). One image shows faintly the texture of the ropes, whereas the other one does not. These small differences are important in reconnaissance images where texture can give a clue to the nature of the objects. A relatively small amount of noise or granularity, however, can easily obscure the texture. Photography has not had in the past the flexibility available in television to manipulate the shape of the modulation transfer function. Higher resolution is obtained by going to larger formats and a finer grain structure, which increases the scale factor of the MTF but does not change its shape. Image processing and manipulation of the MTF should be looked at with caution because it can destroy the natural balance in good normal photography. Nevertheless, a general sharpness rating of imaging processes by a single number is of considerable interest. Such a rating is very accurate when the shape of the overall MTF at the retina of the eye is reaonably constant.

2.3 Sharpness Rating of Images

A barely detectable difference in sharpness, i.e., a "liminal" unit of sharpness, was determined in 1940 by Baldwin[10] in terms of the detectable change in the number of picture elements (figures of confusion) in images produced with a calibrated out-of-focus projector having a well-defined spread function. Translated into just perceptible differences in N_e values, this liminal unit turned out to be a change of 3.5% in N_e or in the effective length of an edge transition in the retinal image, calculated from the MTF products of the total process and the MTF of the visual system.[4,11] Expressed in log units the sharpness is given by

$$S = -66.7 \log(N_{e(e)}/\overline{N}_{e(p+e)}), \qquad [8]$$

where $N_{e(e)}$ is the eye's equivalent pass band and $\bar{N}_{e(p+e)}$ is the combined pass band of the external image and the eye. It is often more convenient to refer the pass band of the eye to the external image plane. The pass band $N_{e(e)p}$ of the eye referred to an external image depends on the viewing ratio (ρ) and is given by

$$N_{e(e)p} = 34 f_{e(e)}/\rho \quad \text{(see Fig. 2 for } f_{e(e)}) \qquad [9]$$

and

$$N_{e(p+e)} = [N_{e(e)p}^{-2} + N_{e(p)}^{-2}]^{-1/2}$$

A graph of the above equation with ρ as parameter is shown in Fig. 5 for a mean image luminance $\bar{B}$ of 4 to 7 ft-L ($f_{e(e)}$ = 22.3 cycles/mm). The highlight luminance of the image is generally 4 to 6 times the

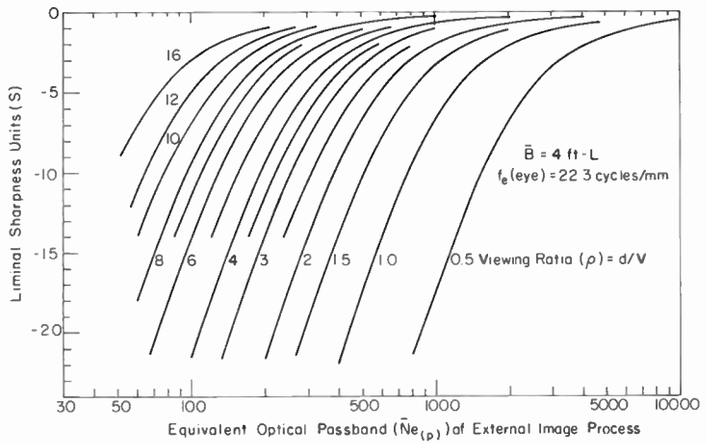

Fig. 5—Image sharpness (liminal units, see Eq. [8]) plotted as a function of the equivalent pass band ($\bar{N}_{e(p)}$) of the external image with viewing ratio (ρ) as parameter for a mean image luminance $\bar{B}$ = 4 ft-L.

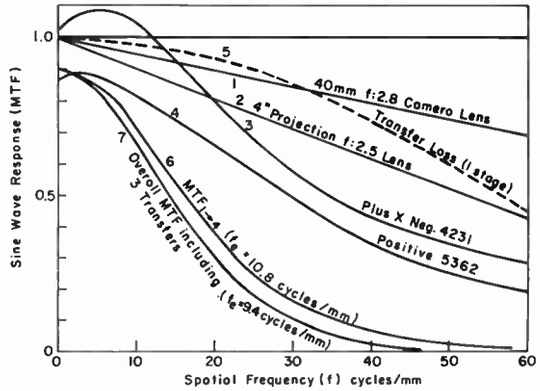

Fig. 6—MTF's of a motion picture process. Curves 1–5 are for the various components of the system, curve 5 shows the transfer loss (for one stage), curve 6 the MTF products of 1–4, and curve 7 includes the three transfer losses in the motion picture system.

mean value. The sharpness rating is very accurate when the overall MTF (including the eye) has a consistent shape. This condition is approached, with few exceptions, for normal viewing distances because the product of a large number of component MTF's tends towards a gaussian function, even though the MTF's of individual components may differ substantially in shape.

A set of photographs with known N_e values made in 1952 with a calibrated defocusable projector is shown in Figs. 35 through 40 to illustrate image sharpness as a function of the equivalent pass band of the image. The photographs with N_e ratings of 270 lines and 350 lines differ according to Fig. 5 by only two liminal units at ρ = 4. They should look equally sharp at ρ = 8, where they differ by less than one liminal unit, and the sharpness difference of 4½ units at ρ = 2 should be quite apparent. A TV reproduction of the same object is shown in Fig. 41. Its N_e rating is 360 lines and it was reproduced with a 625-line raster over an 8-MHz frequency channel. This image should be viewed at a distance of at least 2 times the vertical dimension in order to prevent the visibility of the raster lines.

A more accurately controlled test for comparing television and photographic images was made for the purpose of establishing the constants for a theater TV system[12] that would have the same sharpness as a high-quality 35-mm motion picture, in which Plus X negative film (4231) and high-contrast positive film (5362) are used with a good 40-mm f:2.8 camera lens and an excellent 4-inch f:2.5 projection lens. The MTF's of the process are shown in Fig. 6 by curves 1 through 5.* Their product is curve 6.

The total pass band is then $N_{e(p)0}$ = 21.7 l/mm. This theoretical pass band is reduced by focusing errors in the intermittant film

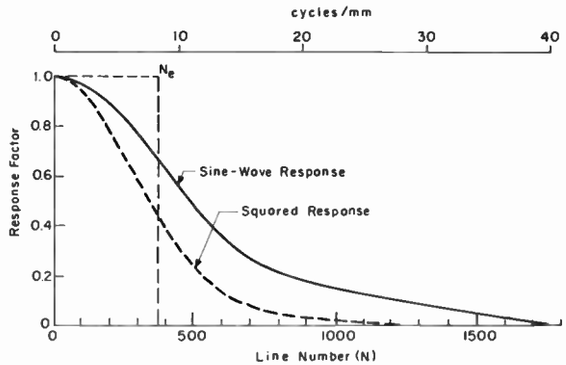

Fig. 7—Measured MTF of photographic slide-duplicating process simulating a 35-mm motion picture process.

* Film data from Eastman Kodak Co.

Fig. 8—Test plate for evaluation of Fig. 7

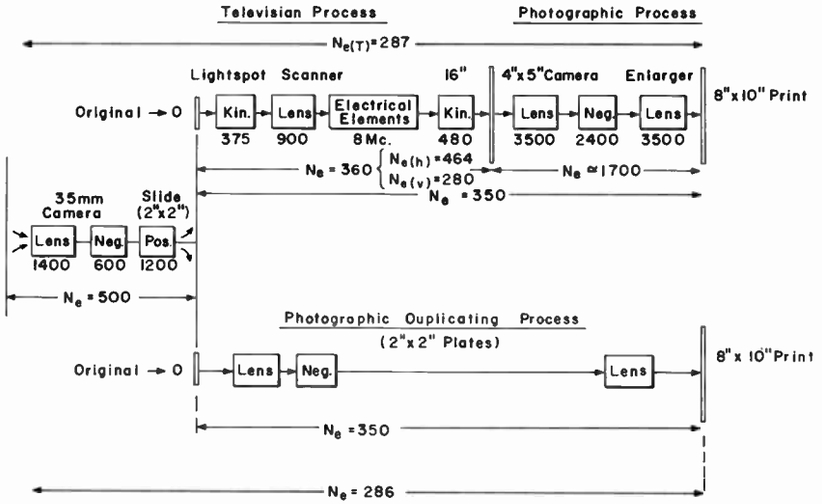

Fig. 9—Block diagram of the television and photographic duplicating processes and their N_e values.

Fig. 10—Test plate for television process (see Fig. 11).

transport mechanisms and by diffusion in printing processes that have been investigated more recently.[13] The transfer loss in a step contact printer in perfect adjustment is shown by curve 5, and the transfer losses in the camera and projector mechanisms are similar. The three transfers in the above system (see Fig. 12) reduce the overall MTF to curve 7 and decrease the equivalent pass band of the complete motion-picture system to $N_{e(p)}$ = 18.8 l/mm. For the 15.7-mm dimension of a standard motion picture frame this corresponds to $N_{e(p)}$ = 295 TV lines on the projection screen for an original master print. Release prints are made from duplicate negatives that degrade the process to $N_{e(p)} \simeq 280$ lines in the vertical format dimension.

To ensure a similar quality for comparative tests, measurements were made with resolution test plates reproduced by the same process used for making photographic copies of a series of excellent 2 × 2-inch transparencies made with a good 35-mm camera. The sine-wave MTF of the photographic duplicating process simulating the motion picture is shown in Fig. 7, and a print of the test plate (which was measured with a microphotometer) is shown in Fig. 8. A block diagram of the photographic and television duplicating processes and their N_e values is shown in Fig. 9. The test plate copy for the TV process and its MTF's are reproduced in Fig. 10 and Fig. 11. All N_e

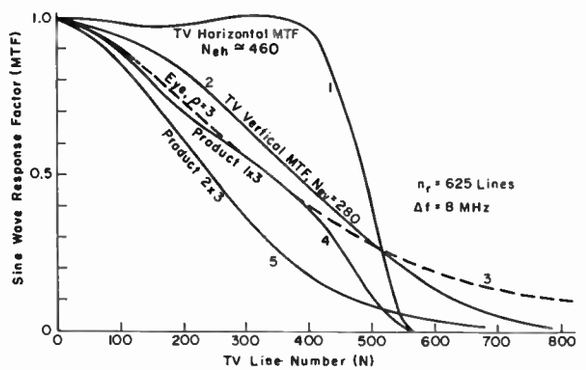

Fig. 11—MTF's of 625-line 8-MHz television system (light spot scanner) at the display screen (curves 1 and 2), MTF of the eye (curve 3) reflected onto the display screen for ρ = 3, and overall product MTF's (curves 4 and 5).

values are given in the block diagram, including those for the original 35-mm transparencies and the final photographic recording process on 8 × 10-inch paper prints, which must be included in the overall sharpness evaluation of the prints. The diagram shows that the N_e ratings of the TV and photographic duplicating processes have the same values and agree with the values calculated above for a 35-mm motion-picture process. Two sets of pictures reproduced by the two systems are shown in Figs. **42** and **43**. The test proved conclusively that a 625-line TV system with a mean equivalent pass band $\bar{N}_{e(p)} = (N_{e(h)} \cdot N_{e(v)})_p^{1/2} = 360$ lines can provide a picture equal in sharpness to a 35-mm motion-picture process for a minimum viewing distance three times the vertical frame dimension, although the MTF reveals that the resolving power of the motion picture is in the order of 1400 lines compared to 550 lines in the TV image. The reproduced pictures *do not* represent the relative noise level of the processes because of the larger format of the originals and the integration of "live" noise by the time exposure in the 4 × 5-inch copy camera. The granularity visible in the TV images is caused by the stationary grain structure of the phosphor screen in the light-spot scanner, which is not integrated out by a time exposure.

3. Granularity and Noise

The noise modulation of a gray-scale level is caused by random fluctuations or deviations in the number of quanta integrated within the sampling aperture of the process. It can be measured with a microphotometer. The dc current from the average light flux passing through the sampling aperture is the signal from the gray-scale level, and the fluctuations in the current, measured with an rms meter, are the rms noise; their ratio is the signal-to-noise ratio (SNR_0) of the gray-scale level. The effective size and noise-equivalent pass band of the aperture sampling the noise is determined by the MTF product following the noise source, and depends on the location of the noise source in the system. The pass bands for noise are thus, in general, larger than for the signal and may differ from one another. The noise must, therefore, be determined separately for each noise source, and the total noise at a point of observation is obtained by an addition of mean-squared noise values or, expressed by signal-to-noise ratios,

$$SNR_{tot} = (SNR_1^{-2} + SNR_2^{-2} + \ldots + SNR_n^{-2})^{-1/2} \qquad [10]$$

Signal-to-noise ratios measured in the video channel of a TV system or at the films of a photographic process do not completely define the visual appearance and magnitudes of the noise, because they are taken in mid-system and do not include the low-pass filtering in the display device and the eye. Most television systems contain high-pass filters or aperture-correction stages that have the opposite effect on noise from that of a low-pass filter, and their effect on the noise spectrum in the video channel is quite different from that at the retina of the eye,[2,4] that is, a high-pass filter accentuates noise, whereas a low-pass filter reduces noise.

Another important parameter controlling the noise of a gray-scale level is the (intensity) transfer function of the system which, in general, has a different transfer ratio ($\dot{\gamma}$) for noise and signals in different stages and gray-scale levels. The "point-gamma" ($\dot{\gamma}$) at a gray-scale level is the slope of the transfer function in log-log coordinates and equal to the ratio of the small-signal to the large-signal transfer factors. Thus, a signal-to-noise ratio $SNR_{1,4}$ originating in stage one and transferred to stage four must be divided by the product $\dot{\gamma}_2\dot{\gamma}_3\dot{\gamma}_4$ of the stages following the noise source.[2,13(a)]

3.1 Noise in Photographic Processes

Photographic film is measured with a round sampling aperture of 48-μm diameter. Eastman Kodak specifies the noise by a granularity number $G = 1000\ \sigma_{(D)}$, where $\sigma_{(D)} = 0.4343/SNR_m$ is the standard deviation in density at a net density $D = 1$. The value SNR_m is measured with the aperture pass band $\bar{N}_{em} = 1080/48 = 22.5$ l/mm. The signal-to-noise ratio at any density and for different sampling apertures can be computed with

$$SNR_0 = SNR_m \frac{\bar{N}_{em}}{\bar{N}_e D^{0.45}} = 9.77 \frac{10^3}{G\bar{N}_e D^{0.45}} \qquad [11]$$

where $\bar{N}_e$ is the equivalent pass band of the sampling aperture expressed in TV-lines/mm. The gray-scale level is expressed by the photographic density D = −log transmittance, and the exponent (0.45) applies to films with mixed grain sizes such as TRI-X, Panatomic-X, Plus-X and Super-XX films. It has a value of 0.5 for single-grain-size films (high-resolution types).[14]

The evaluation of signal-to-noise ratios for a 35-mm motion-picture process may serve as an example. The motion-picture process

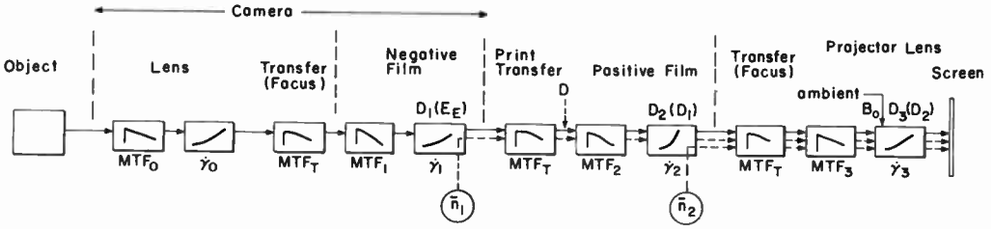

Motion Picture Process

Fig. 12—Block diagram of transfers and noise sources ($\bar{n}$) in motion picture process.

contains two principal noise sources generating "white" noise for pass bands of interest,[14] as illustrated by the block diagram in Fig. 12. Additional noise may be introduced by a negative duplicating process inserted at point D for making release prints. The noise generated by the source ($\bar{n}_1$) in the negative film is transferred by the positive film and the projection lens to the external image plane and from there into the visual system. For the transfer to the projection screen, the

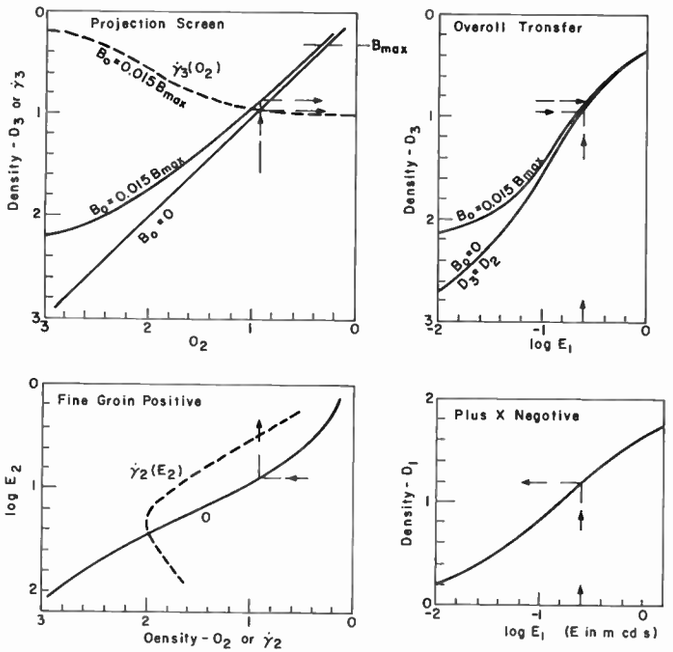

Fig. 13—Transfer functions of motion picture process.

equivalent pass band has the value

$$N_{e(2,3)} = \int_0^\infty (\mathrm{MTF_2 \cdot MTF_T^2 \cdot MTF_3})^2 \, dN$$

calculated in TV-lines/mm for use in Eq. [11] and the SNR in the external projection image is given by

$$\mathrm{SNR}_{(1,3)} = \frac{\mathrm{SNR}_{0,\mathrm{neg}}}{\dot{\gamma}_2\dot{\gamma}_3} = \frac{9770}{G_1\bar{N}_{e(2,3)}D_1^{0.45}\dot{\gamma}_2\dot{\gamma}_3} \qquad [12]$$

where the gamma values are determined at coordinated operating points, or gray-scale densities, D_2 and D_3 of the transfer functions shown in Fig. 13. The gamma ($\dot{\gamma}_3$) of the projection lens is unity if a complete absence of lens flare and ambient illumination is assumed. It decreases near the black level for the more realistic assumption of 1.5% ambient illumination ($B_0 = 0.015\ B_{max}$) as illustrated in Fig. 13.

The $\mathrm{SNR}_{(1,3)}$ calculated, for the granularity $G = 10$ of Plus-X negative film* and $N_{e(2,3)} = 27.2$ l/mm, with Eq [12] and Fig. 13 is shown as a function of gray scale (D_3) by curve 1 in Fig. 14. The noise ($\bar{n}_2$) from the positive film ($G = 6.5$) is sampled by the apertures of the projection lens and one transfer ($\mathrm{MTF_T}$), yielding $N_{e(3)} = 43.7$ l/mm. The $\mathrm{SNR}_{(2,3)}$ is calculated similarly and combined according to Eq. [10] with $\mathrm{SNR}_{(1,3)}$ to obtain the total $\mathrm{SNR_p}$ in the projected image, shown by the solid curve 2 for $B_0 = 0.015\ B_{max}$ in Fig. 14.

The SNR_r in the retinal image is most important for a comparison of different processes. After selection of the viewing ratio, the MTF

* Film data from Eastman Kodak Co.

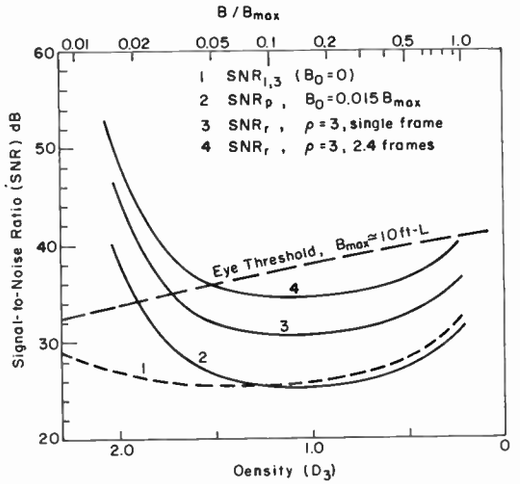

Fig. 14—Signal-to-noise ratios of motion-picture process at the display screen (SNR_p) and at the retina of the eye (SNR_r) for a viewing ratio $\rho = 3$.

of the eye can be expressed in TV-lines/mm at the film plane by

$$N_{(\rho)e} = \frac{34f}{\rho V}, \qquad [13]$$

where f is the spatial frequency at the retina, $V = 15.7$ is the vertical frame dimension of 35-mm film. Also

$$N_{e(\rho)e} = \frac{34f_{e(e)}}{\rho V}. \qquad [14]$$

Signal-to-noise ratios and N_e values expressed in TV-lines/mm for the noise pass bands of the two film noise sources are evaluated separately before combining them with Eq [10]. For the viewing ratio $\rho = 3$, the $SNR_{1,4}$ from the negative noise is increased over $SNR_{1,3}$ by a factor of 1.69, whereas $SNR_{2,4}$ is increased over $SNR_{2,3}$ by a factor of 2.7 at the retina of the eye. The total SNR_r at the retina (curve 3 in Fig. 14) is 5.0 dB higher than the external value SNR_p. A further increase by $\sqrt{2.4}$ occurs in the eye, which integrates 2.4 frames of a running motion picture that shows 24 frames per second (each frame is shown twice to reduce flicker). This SNR_r is curve 4 in Fig. 14. The broken curve marked "Eye Threshold" indicates the approximate threshold signal-to-noise ratio where noise can just be seen.[8] Noise is visible for all values below this threshold and agrees with the observation that the 35-mm motion picture is noisy in the highlights and middle tones and noise free in the blacks. The SNR_r does, of course, increase for larger viewing distances (the curves move up). The computed values do not include noise caused by film wear, which is very noticeable after relatively few runs.

3.2 Noise in Television Processes

The evaluation of signal-to-noise ratios for a television system is similar.[2] However, the vertical and horizontal noise-equivalent pass bands are no longer alike, as in a motion-picture process, and must be determined separately. In addition, the system (see block diagram Fig. 15) contains a raster process, aperture-correction circuits, and an electrical cutoff filter limiting the pass band to a definite value $N_{c,h}$ in the horizontal direction. The system contains three basic noise

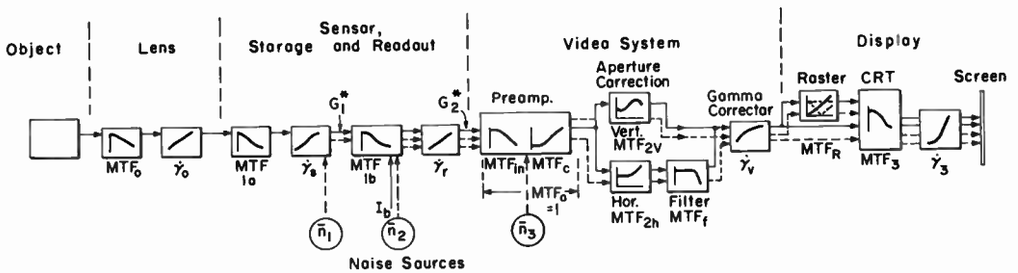

Television Process

Fig. 15—Block diagram of transfers and noise sources ($\bar{n}$) in television process.

sources. The noise source ($\bar{n}_1$) represents photoelectron noise generated in the sensor. Excess noise is injected by the "readout" system ($\bar{n}_2$)† and by the preamplifier ($\bar{n}_3$). Depending on the type of camera tube and sensor, a multiplication of charges may take place before storage which introduces a gain G_1* (image intensifier stage) before readout. In this case the noise source $\bar{n}_1$ becomes the dominating noise generator when G_1* is sufficiently large.

Camera tubes of the vidicon type have no prestorage gain. For a direct target readout, beam transfer and target noise ($\bar{n}_2$) are negligible, and the predominant noise source is preamplifier noise ($\bar{n}_3$), which is injected between a low-pass MTF caused by capacitive input loading of the amplifier and a correction MTF_c that restores a constant MTF for the signals‡ but changes the white-noise spectrum of the source ($\bar{n}_3$) to a triangular "peaked" noise spectrum. A third type of camera tube contains an electron multiplier, and the storage surface is read out by the return beam (image orthicon, return-beam vidicon). The multiplier introduces a high gain G_2*, which makes beam and multiplier noise ($\bar{n}_2$) the dominating noise source, because it is larger than $\bar{n}_1$ when G_1* is small or unity. The noise spectrum from $\bar{n}_2$ is then flat (white noise).

The MTF's for the signal transfer in an 8-MHz 625-line system containing a modern lead-oxide vidicon camera tube are shown in Figs. 16a and 16b. The MTF_h for the horizontal coordinate is the product of all MTF's in the system shown by curves 3 and 4 (Fig. 16a) for the display screen (CRT) and the retina of the eye, respectively. The MTF_v for the vertical coordinate (Fig. 16b) is curve 1, requiring vertical aperture correction with two delay-line sections[3,7] to increase the MTF to curve 2 and curve 3 at the retina of the eye for $\rho = 3$.

The MTF's following the dominant amplifier noise source $\bar{n}_3$ (Fig. 15) are shown in Figs. 17a and 17b and require explanation. The total noise at the display screen is essentially amplifier noise, and the signal-to-noise ratio can be computed as a function of screen luminance with

$$SNR_p(B/B_{max}) = \frac{SNR_{o,max}(I_B/I_{max})}{(\alpha\cdot\beta)^{1/2}\dot{\gamma}_v\dot{\gamma}_d}, \qquad [15]$$

† $\bar{n}_2$ is a combination of as many as four noise sources.

‡ The method of correcting for a capacitive roll-off of the input MTF (high peaking in a separate stage or feedback) is immaterial.

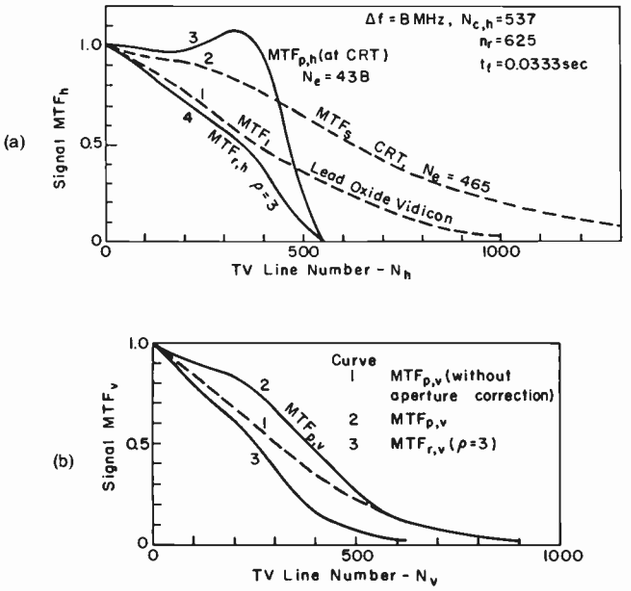

Fig. 16—MTF's for signal transfer in an 8-MHz 625-Line system with lead oxide vidicon. (a) For the horizontal component: curve 1 is MTF of camera tube, 2 is MTF of display tube, 3 is overall MTF at display screen, and 4 is overall MTF at retina for viewing ratio $\rho = 3$. (b) For the vertical component: curve 1 is overall MTF at display screen without aperture correction, 2 is MTF at screen with aperture correction, and 3 is overall MTF at the retina of the eye for $\rho = 3$.

where $\alpha = N_{e(n)h}/N_{c,h}$ and $\beta = N_{e(n)v}/n_r$ are the horizontal and vertical bandwidth reduction factors for noise, and $N_{c,h}$ and n_r are the aperture pass bands for the electrical channel used for measuring or calculating the signal-to-noise ratio $SNR_{o,max}$ at the amplifier output (n_r is the active raster line number). The signal current is proportional to the input exposure (E) for a lead oxide vidicon (Fig. 18), which requires gamma correction (a low $\dot{\gamma}_v$) to achieve a normal gray-scale reproduction in combination with the high-gamma display tube. The current I_B corresponding to the screen luminance (B) is determined by the system transfer functions. The transfer function of the display tube is basically a 3rd-power characteristic changed by a 1% ambient light level and a 13% black-level setup to the function shown in Fig. 18.

Electrical noise sources are one-dimensional, and the second dimension (V) is generated artificially by the raster process as dis-

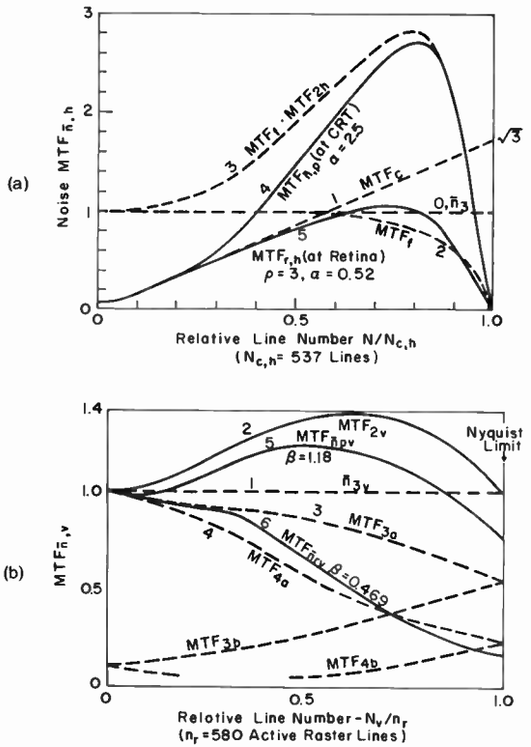

Fig. 17—Noise spectra and MTF's for dominant amplifier noise source ($\bar{n}_3$ in Fig. 15) in an 8-MHz 625-line system with lead oxide vidicon. (a) For horizontal component: curve 0 is spectrum of noise source $\bar{n}_3$, 1 is noise spectrum after input compensation, 2 is MTF of filter, 3 is MTF of filter with aperture correction, 4 is noise spectrum at display screen, and 5 is noise spectrum at retina of eye for $\rho = 3$. (b) For vertical component: curve 1 is noise spectrum after sampling, 2 is after aperture correction, 3 is folded MTF of display tube, 4 is folded MTF of eye ($\rho = 3$), 5 is noise spectrum at display screen, and 6 is noise spectrum at retina ($\rho = 3$).

cussed subsequently. The essentially white-noise spectrum of the amplifier noise source $\bar{n}_3$ is changed to a peaked-noise spectrum (curve 1 in Fig. 17a) having the normalized value $\sqrt{3}$ at the cutoff line number $N_{c,h} = 537$ lines of the 8-MHz channel. (The N_e value of curve 1 is unity in relative units.) For the horizontal direction this MTF_c is multiplied by the MTF_f of the cutoff filter, the MTF_{2h} of the horizontal aperture correction circuit, and the MTF_3 of the display tube to obtain the $MTF_{\bar{n},p}$ of the noise spectrum at the display screen

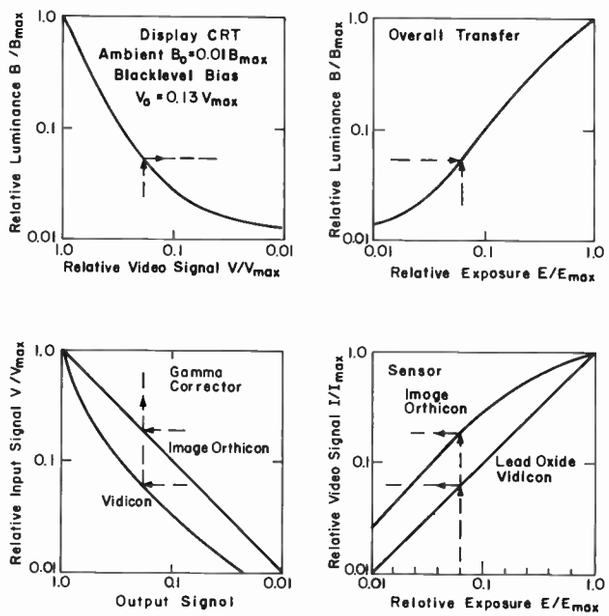

Fig. 18—Transfer functions of television process.

(curve 4). This spectrum multiplied by the MTF of the eye for the selected viewing ratio ($\rho = 3$) yields curve 5, and integration of the squared overall MTF's yields the equivalent pass bands $N_{e(\bar{n})h}$ and $N_{e(\bar{n})e,v}$ for noise at the display screen and at the retina of the eye.

The artificially generated noise spectrum for the vertical coordinate of any electrical noise source is a "flat" noise spectrum. The wide-band noise of the source is sampled at line-frequency rate for any vertical section in the display. Without filtering, the low sampling rate (18.75 kHz for 625 lines) heterodynes the peaked wide-band noise into the low-frequency range limited by the line frequency, yielding a highly repetitive spectrum (aliasing).[2] Summing of like frequencies by a quadratic addition results in a flat noise spectrum within the "Nyquist" limit $N_v = 0$ to n_r indicated in Fig. 17b by the straight line $\bar{n}_{3,v}$. Because of the spectrum aliasing, the MTF's following the noise source are "folded" into the range $N_v = 0$ to n_r to calculate the rms noise spectra

$$MTF_{npv} = (MTF_{3a}^2 + MTF_{3b}^2)^{1/2} MTF_{2v}$$

$$MTF_{nrv} = [(MTF_{3a} MTF_{4a})^2 + (MTF_{3b} MTF_{4b})^2]^{1/2} MTF_{2v}$$

at the display and at the retina of the eye and the bandwidth reduction factor β.

The signal-to-noise ratios calculated with Eq. [15] are for the integration time ($\frac{1}{30}$ second) of a single TV-frame, and must be multiplied by $\sqrt{3}$ to account for the integration of 3 frames by the eye. The functions $SNR_p(B/B_{max})$ on the CRT screen and $SNR_r(B/B_{max})$ at the retina are shown by curves 1 and 2 in Fig. 19. The low-pass filtering of the peaked noise spectrum by the eye causes a drastic reduction of the noise (10.8 dB).

The value $SNR_{0,max} = 90$ is used for the lead oxide vidicon and 8-MHz channel, and corresponds to $SNR_{0,max} = 180$ (45 dB) in a 5-MHz channel. For a standard 525-line 4.25-MHz system, the curves 1 and 2 are displaced up by approximately 8 dB, and the retinal image at a 3-to-1 viewing ratio is practically noise free.

An image orthicon camera tube has a lower gamma in the highlight region (Fig. 18) and does not require gamma correction. The noise is predominantly beam noise ($\bar{n}_2$) because of the high multiplier gain (G_2* in Fig. 15). The 4½-inch image orthicon has a higher MTF than the lead oxide vidicon and requires less aperture correction. The horizontal noise spectrum is flat, and although $SNR_{0,max}$ is somewhat lower, the signal-to-noise ratios at the display screen and at the retina are substantially higher (curves 3 and 4 in Fig. 19) and comparable to 35-mm motion-picture noise for "live" images.

One additional comment should be made with respect to the appearance of television noise from a system with "peaked" noise ($\bar{n}_3$). The image has sharper "grains" than the motion picture because of the larger high-frequency content of the horizontal noise component, curve 5 Fig. 17a, at the retina of the eye, which psychologically increases the impression of a sharper picture when compared with the more blurry noise from a system containing only low-pass filters. The above evaluation is made for a relatively close viewing distance and the SNR_r obviously increases in all cases for larger viewing distances, where the noise becomes invisible.

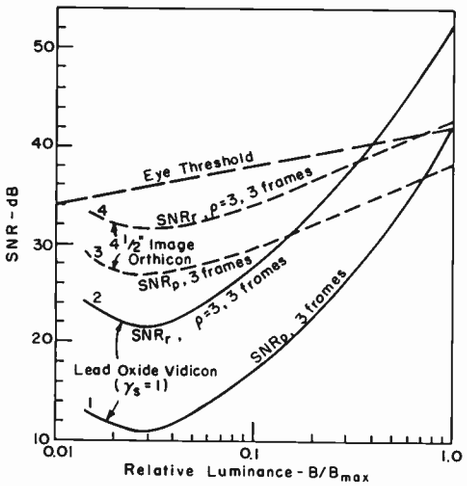

Fig. 19—Signal-to-noise ratios for television process: for lead oxide vidicon, curve 1 is at the display screen and curve 2 is at the retina of the eye ($\rho = 3$); for the image orthicon, curve 3 is at the display and curve 4 is at the retina.

4. Format Size and Image Quality

The effects of a smaller format size of the motion-picture film can be analyzed by simple reasoning. Assume that the format is reduced by placing a rectangular mask in front of the negative film in the camera to restrict the exposed area. For the same film types, neither the exposure nor the processing in the system are affected by the frame size reduction. *The MTF's in l/mm and the SNR_p (Eqs. [11] and [12]) remain unchanged!* The projected image, however, will be smaller and for the same viewing *distance* looks equally sharp and has the same noise level at the retina because the viewing *ratio* (ρ) has increased. A half-size 16-mm frame, for example, contains only one half the total resolution $N_{e(p)} = 150$ lines compared to $N_{e(p)} = 300$ lines for the 35-mm frame. Fig. 5 shows that the sharpness ratings for $\rho = 3$ and $N_{e(p)} = 300$, or for $\rho = 6$ and $N_{e(p)} = 150$ are both −8 liminal units. However, when the projected image from the 16-mm film is increased to normal size by increasing the projector magnification for a viewing ratio of 3, the sharpness rating of the 16-mm film decreases to −19.2 liminal units and the granularity is coarser because of the higher magnification to the retina of the eye. The SNR_r computed for this condition is 3.5 dB lower than the curves 3 or 4 in Fig. 14 for 35-mm film. Similarly for an 8-mm film (¼ size format), $N_{e(p)}$ decreases to 75 lines. Sharpness and noise in the small image appear the same for a viewing ratio of 12, but the sharpness decreases to −36.4 liminal units at $\rho = 3$ when the projected picture is increased to full size. The SNR_r at the retina is 5.1 dB below curves 3 or 4 in Fig. 14 and the diameter of the grains has increased four times!

The actual formats of 16- and 8-mm films are somewhat smaller than used in the examples, and the signal-to-noise ratios at the retina are approximately 0.4 dB lower. In addition, the focal lengths of the lenses used for smaller formats are smaller and the N_e value of the projection lens in particular may be somewhat higher. The sharpness rating is slightly higher but so is the noise. (A similar exchange occurs for reversal films.)

The signal-to-noise ratio in the displayed image is independent of format size for given film types and MTF's in a photographic system. This condition is duplicated in a TV system when the dominant noise sources are $\bar{n}_1$ or $\bar{n}_2$ (Fig. 15), provided the bandwidth of the video channel is proportional to the frame area. It applies exactly to the case of simply masking the format of the sensor down to a smaller exposed format without making any other change in the system, including the display, which then shows a smaller picture in a dark frame of the original size. Assume for example an image orthicon camera, which is beam-noise limited ($\bar{n}_2$). When the sensor is masked down to one-half format size (¼ area) nothing happens until the scanned area in the sensor is reduced to the smaller format to restore the full picture size in the display. The signal current then decreases to one fourth, the beam current can be reduced to one fourth, and the SNR decreases to one half. When the video pass band is reduced to one fourth (which can be done because the MTF is now theoretically one half), the original SNR_p in the display is restored. This does not work out the same when the system is amplifier-noise limited because this noise is proportional to the 1.5 power of the bandwidth. Thus, for a frame area of one fourth, the signal current is again reduced to one fourth, but the bandwidth reduction decreases the noise by a factor $(4)^{1.5}$, the SNR_p has twice the value, and the bandwidth need be reduced only to 1/2.5 to maintain the original value. The opposite happens when the format size is increased.

It is pointed out that the examples do not account for effects caused by beam-current changes on the MTF or the capacitance change when a camera tube is scaled up or down. Nor do they account for the bandwidth limitation of the MTF. The general result is that the quality of the image from smaller TV camera tubes does not decrease as much as indicated by the simple theory compared to smaller photographic frames, and that it does not increase in proportion to the frame area in the same manner as photographic film, unless the system components are changed.

The noise in TV images is generally lower than in photographic images of the same sensor format (in the camera) because the quantum efficiency of film is less than 1%, whereas the quantum efficiency of TV sensors ranges from 20% to close to 100%. Note that a standard vidicon format is very close to a 16-mm film format.

Table 1—Pass bands ($N_{e(p)}$), sharpness (S), and signal-to-noise ratios of motion pictures (Plus X, F.G.Pos) reproduced by a 525-line 4.25-MHz TV system at $B/B_{max} = 0.15$, $\rho = 3$ with low-gamma (0.6) vidicon, $I_{max} = 300$ nA.

System	$\bar{N}_c$	$\bar{N}_{e(p)}$	S	SNR_p	SNR_r*	Remarks
TV alone	400	270	−9.2	38.0	115.0	(peaked noise)
TV & 35-mm M.P.	400	183	−15.2	39.0	85	M.P. noise only
				27.2	68.3	total noise
TV & 8-mm M.P.	350	67	−39.4	20.3	33.8	M.P. noise only
				17.9	32.4	total noise

* Includes frame integration by eye

5. Image Quality of Motion Pictures Reproduced by a Standard 525-Line TV System

A standard 525-line TV system limited by a 4.25-MHz channel has a limiting resolution of 340 lines in the horizontal direction and 490 lines in the vertical direction. The mean equivalent pass band of the image on the CRT display screen calculated for a vidicon camera is $\bar{N}_{e(p)} = 270$ lines. Clearly, the sharpness of a motion picture reproduced by the TV system will be lower than this value, and motion-picture noise will be visible because of the lower signal-to-noise ratio in 35-mm and smaller film formats.

The results of a numerical evaluation* are listed in Table 1 *for a gray-scale level* (B/B_{max}) of 0.15 near the center of the logarithmic gray scale (see Figs. 14 and 18). The resolution (N_c) of the 35-mm film is limited by the TV system to a mean value of 400 lines, whereas the MTF of 8-mm film is essentially inside the TV pass band and is not limited by the reproduction. The sharpness values (S, liminal units) are reduced substantially compared to the TV system alone. (The sharpness of the 8-mm motion picture is only 3 liminal units lower than the sharpness of a direct projection of this film, $S = -36.4$). The signal-to-noise ratios at the CRT screen (SNR_p) are

* Film data from Eastman Kodak Co.

dominated by film noise and more so at the retina of the eye (SNR_r) at the close viewing ratio of 3, where the peaked noise of the TV system is greatly attenuated. The film noise will be relatively more visible when the viewing distance is increased to a more normal value (a ρ of 4 to 6) where the TV noise becomes invisible. The values of SNR_r include noise integration over 3 frames for the TV system noise and over 2.4 frames for the motion-picture film noise. The noise pass bands at the retina ($\rho = 3$) for TV, 35-mm motion pictures, and 8-mm motion pictures are $N_{e\bar{n},r} = 250$, 148 and 90 TV lines, respectively, and indicate relative grain sizes of 1:1.7:2.8. The complete functions SNR_r (B/B_{max}) are plotted in Fig. 20.

The signal-to-noise ratio SNR_{max} in Eq. [15] at the camera output before signal processing in the video channel has the value $SNR_{o,max} = 230$ for $I_{max} = 300$ nA for the TV system without motion-picture noise. The corresponding value at the retina of the eye for $\rho = 3$ is $SNR_r = 580$, five times higher than at $B/B_{max} = 0.15$, whereas the SNR_r of the motion picture increases only by a factor of two. The high-light noise in a 35-mm film reproduction is 3.6 times higher than the TV system noise and the high-light noise from an 8-mm film is 8.7 times higher than the TV system noise.

6. High-Definition Systems

A larger sensor format increases the total definition. The focal lengths of the lenses must be increased to cover the format and their N_e values decrease somewhat so that the increase in the overall pass band $N_{e(p)}$ of the process is not proportional to the increase in format size. This condition is particularly pronounced in TV systems because of the electron optics and different noise sources. A detailed analysis[15,16] is beyond the scope of this paper.

A moderate increase in resolution can be obtained in a TV system by simply increasing the bandwidth and raster line number. Larger increases require, in addition, an increase of the sensor format, a selection of sensors having a higher resolution density (cycles/mm), a decrease of the scanning-beam diameter in the readout system, and redesign of the electron optics to cover a larger format with low aberrations, uniform focus, and high MTF.[15] In all cases, a smaller sampling aperture (a smaller picture element) demands a higher quantum efficiency or an increase of exposure to restore a quantum count for adequate signal-to-noise ratios. The pass band of the electrical video system increases as the square of the total resolution for a given

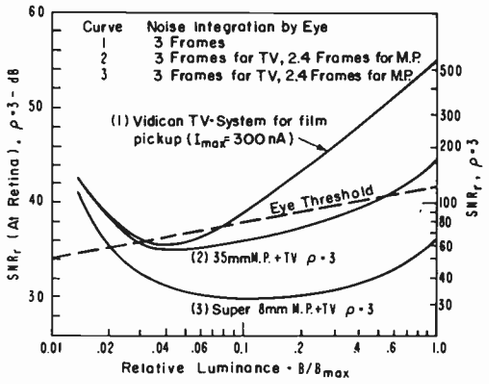

Fig. 20—Signal-to-noise ratios at the retina, for a viewing ratio $\rho = 3$, of motion pictures reproduced by a 525-line 4.25 MHz TV system.

frame rate, and so does the required beam current. It therefore becomes necessary to decrease the frame rate and go to a slow-scan readout, because even a 100-MHz bandwidth requires a readout time of 0.7 second for a single frame of a 10,000-line system in a square format (10^8 picture elements). Available video pass bands are generally lower and increase the frame time to several seconds. These high-resolution images are recorded on a large-format film exposed directly by an electron beam or a laser beam. A direct-view image requires a faster readout and is then bandwidth limited in resolution by the available channel. The detail in the image can, however, be inspected by reading out a small fraction of the total format area (electronic zoom).

A high-resolution return-beam vidicon camera (50 × 50-mm ASOS sensor) and CRT monitor at the Harrison, N.J. laboratory of RCA Electronic Components was available to demonstrate the effects on the resolution of the TV images of varying the sensor format, line number, bandwidth, and other system parameters. Readout time, scan rates, and bandwidth of the system could be varied over a wide range, as could the scanned format area. The photographs in Figs. 44–45 were taken with a 4 × 5-inch view camera of the pictures displayed on the 17-inch CRT monitor (10 × 10-inch format).

A test-pattern reproduction by an excellent 600-line system is shown in Fig. 44. The resolution is given in TV lines by multiplying the numbers on the wedges in the large circles by 20 and the numbers on the small wedges and in the small circles by 50. The scanning lines

are not visible because spot wobble was used to obtain a "flat field." The effect of the raster can be seen by the spurious patterns in the horizontal wedges, where the raster carrier produces a diamond-shaped pattern at the number 60, corresponding to 1200 lines and a sampling frequency f_r of 600 cycles. The zero beat at the sampling frequency is seen in the linear vertical frequency strip pattern at the number 6 (the pattern goes to 2000 lines at 10). The Nyquist limit (600 lines) occurs at 3, where the response from the camera should be cut off. The spurious response beyond this number is the aliasing of the raster process, i.e., the sideband modulation of the carrier by the difference frequencies f_r-f_m when the response of the camera is finite at the Nyquist limit.

The fine detail of the test pattern is resolved much better by a 1000-line system, Fig. **45**. Note that the Nyquist limit has moved up to 1000 lines (5 in the strip chart) and the zero beat with the raster carrier occurs at 2000 lines (10 in the strip chart).

The direct photograph of the test pattern with the view camera on Panatomic-X film (65 × 65 mm), Fig. **46**, has a resolution limit of 4000 to 4500 lines (80 to 90 in the small wedges and small circles) seen better in the enlargement Fig. **47**. The sharpness is increased substantially, but the small type in the newspaper is not readable, because this requires a resolution in the order of 8000 lines.

The full resolution of the 4½-inch return-beam vidicon is 80 to 100 cycles/mm (8000 to 10000 lines for the 50 × 50-mm format). To show this resolution, the object distance of the test pattern was doubled to make the numbers in the small circle of the test pattern direct reading in cycles/mm (Fig. **48**) and the scanned area was reduced to prevent bandwidth limitation by the 60-MHz video channel. The faint diagonal dot and line structure is caused by the field mesh in the camera tube, which should have a finer ruling.

The bandwidth-limited resolution of a 100-MHz video system is shown in Fig. **49**. The full format was scanned with 1870 lines, 20 frames/s, 3 to 1 interlaced. The CRT display was expanded and an enlargement is necessary to reproduce the 100-MHz cutoff at 3600 lines (72 in the small circle). Fig. **50** shows that the small newspaper print in the test pattern is definitely readable when the bandwidth limitation is removed by underscanning in the camera.

The photographs Figs. **51** through **55** were made with a scanning raster of 1870 lines, 20 frames/s, 3-to-1 interlaced and a 60-MHz bandwidth. Raster lines are not visible because a "flat field" was obtained by spot wobble in the display tube. The full format pictures Fig. **51**, **52**, and **54**) are bandwidth-limited 1870-line reproductions of aerial photographs (9 × 9-inch contact prints on paper) picked up by the camera. The detail in the actual image stored in the sensor is shown in the remaining figures by 1870-line pictures of small areas in the stored image (approximately $\frac{1}{30}$ of the format area in the sensor). This detail can be read out by a single slow scan of the full format into a tape storage or into a high-resolution recorder to make a hard copy.

Gray scale, definition, and granularity in an image are controlled basically by the total number of quanta (photons, electrons, grains) that can be stored in the sensor format of the camera. The number of quanta in the sampling area or picture element determines gray scale and noise level, and the number of picture elements in the sensor format determines the total definition in the image.

The loss of image quality resulting from a format reduction of the sensor is illustrated by the following two series of pictures. The image quality decreases at first slowly and then more rapidly because of the limited resolving power of the eye. A larger viewing distance (or smaller image) is required for a poor picture to reduce its apparent graininess and improve the apparent resolution.

The first set of pictures (Fig. **57** to **63**) were made with television cameras, starting with a larger sensor format and a high quantum density that were then decreased to smaller values and lower electrical pass bands. The original master print copied with these cameras is a very sharp contact paper print from an 8 × 10-inch negative film taken with a large view camera by a professional photographer. This print has an excellent gray scale, a limiting resolution of 5400 lines, and an equivalent pass band (N_e) of the order of 2200 lines. A photographic copy of the master print was made with a 4 × 5-inch camera, which decreased the resolution to 3000 lines with $N_e \simeq 1200$. The printed reproduction shown in Fig. **56**, made with a 150-line/inch printing raster, further reduces N_e to roughly 800 lines.

Fig. **57** is the reproduction of a 1760-line TV image picked up with a high-resolution return-beam vidicon and displayed on a 17-inch CRT monitor. The originally bandwidth-limited MTF is degraded severely by copying the CRT image; N_e is degraded substantially to perhaps 600 lines and further by the printing process. The fact that the image definition is limited by the 60 MHz pass band and copying process and not by the return-beam vidicon camera is demonstrated by Fig. **58**. The high quality of the original master print and excellent definition of the image stored in the sensor of the camera tube are

visible in this figure, which shows a section of the image electronically enlarged 3.2 times. This magnification was obtained by reducing the scanned area in the camera to 10% of the full format area.

An experiment was made in 1951 to generate a 1000-line TV image with a high equivalent pass band by assembling a picture from four 500-line TV images. The assembly was rephotographed and is reproduced in Fig. **59**. The estimated N_e value is 650 lines.

Figs. **60** through **63** show the same scene reproduced by systems operating at 625 lines, 9 MHz, 30 frames per second; 525 lines, 7.5 MHz, 30 frames per second; 625 lines, 5 MHz, 25 frames per second (European standards); and 525 lines, 4.25 MHz, 30 frames per second (U.S. standards). One can follow the reduction in image sharpness as the number of lines and the bandwidth are reduced.

It should be pointed out that the gray scale in these images, taken in 1951, suffered in the copying process. The noise level seen on the direct-view CRT images was quite low, but is not reproduced in the illustrations, as it is integrated out by the various copying processes.

The second set of pictures (Figs. **64** to **72**) illustrates loss of image quality and increasing coarseness of the grain structure resulting from a format reduction in a photographic process in which the noise level is considerably higher for small formats than in TV images. The 8 × 10-inch original paper print used for the previous series was copied with an Exacta miniature camera (f:2 Schneider Xenon, 50 mm, stopped to f:5.6) on 35-mm, 16-mm, and super-8-mm motion picture formats. Three sets of 8 × 10-inch enlargements were made: (1) with the same lens for the 35-mm motion-picture format, (2) with a 13-mm f:1.5 wide-angle Elgeet lens stopped to f:4 for the 16-mm film format, and (3) with the Elgeet lens stopped to f:2.8 for the 8-mm motion-picture format.

The excellent sharpness of the grain structure in the enlargements testifies to the high quality of the enlarger. Figs. **64** through **69** were taken on Plus-X negative film, and Figs. **70** through **72** were taken on Tri-X film. This film has roughly the same MTF as Plus-X film but 1.6 times the granularity because of its higher speed (ASA400 compared to ASA125 for Plus-X). The loss of definition and increase in granularity by the progressive reduction from 35-mm to 8-mm motion-picture frame sizes is very evident, particularly for the Tri-X film, which must be used with a large-aperture lens to approach the sensitivity of a normal TV camera. The reader may compare the visual image quality of the Plus-X series with the data given in the preceding numerical evaluation.

7. Resolving Power

The oldest measure of image quality is the resolving power. As a subjective measure it requires no knowledge of the physical factors involved in an imaging process. The international standard test object is an assembly of periodic line patterns. The chart contains pairs of 3-bar line patterns of progressively decreasing size (see Fig. 21). The resolving power is specified by the frequency or line number (N_r) of the smallest pair of patterns in which 3 bars are resolved in at least one pattern of the pair, and all larger patterns are resolved.

The objective criterion for the detection of a "signal" in a noisy background is a detail-signal-to-noise ratio which must have a certain value (k) for a given probability of detection.[17,18] The signal from an object area (such as a disc or rectangle) in a noisy background is basically the difference of the quantum count in the object area ($\bar{a}_0$) and the mean quantum count in the background taken with the same area, i.e., the object area is regarded as the sampling aperture for measuring the signal and the noise in the background. This concept implies that the noise must be integrated within the object area by the imaging system. The system must be matched by a two-dimensional filter to the spectrum of the object area under observation. A normal imaging system has a small sampling aperture and clearly resolves the noise in larger areas. It follows that a larger object in a very noisy background may not be visible at close viewing distances or with higher magnification, whereas it may be easily detected when the magnification is reduced to a value where the sampling aperture of the eye (or of any other detector) matches the object area. This fact is illustrated by the set of pictures in Fig. 21 and by the enlargements of selected pictures in Figs. 22, 23, and 24. The resolving power in picture #3, Fig. 21, for example, is best seen when observed with a hand magnifier, whereas pattern 2.5 in the magnified image, Fig. 23, is resolved more clearly from a larger viewing distance. The requirement for optimum filtering is particularly evident for the low-contrast picture #14 in Fig 21, where the fairly large pattern number 1.1 (see Table 2) is just resolved at a normal viewing distance of 25 cm, but cannot be detected in the 4.6 times larger image, Fig. 24a, unless the viewing distance is increased to 5.6 feet. The reader can verify that the exact distance is not critical.

The optimum matching condition occurs when the equivalent pass band of the eye equals the equivalent pass band of the object, in this case the reciprocal bar width ($1/w$) of the pattern. For a luminance in

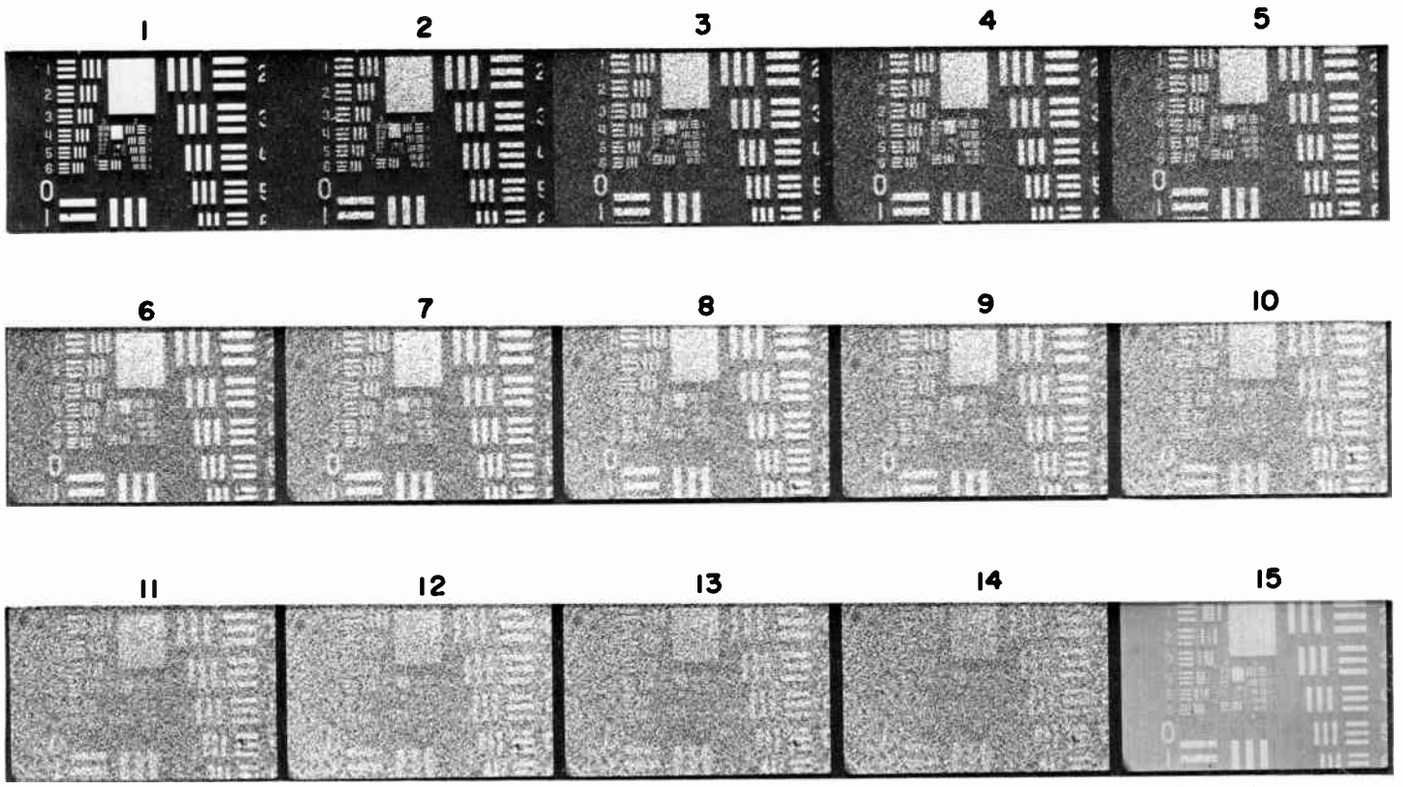

Fig. 21—Standard test patterns showing resolving power (lines/mm) in noisy images as a function of contrast (see Table 2 for data).

Table 2—Resolving power (N_r), contrast (C), and image detail contrast (C_{Ni}) for photographs in Fig. 21.

Photo	1	2	3	4	5	6	7	8	9	10	11	12	13	14	15
N_r	25	7	6.1	5.8	5.5	5.0	4.7	4.4	4.1	3.6	3.2	2.8	2.6	2.1	
C	1	1	.91	.87	.83	.77	.71	.67	.62	.55	.5	.43	.4	.33	.33
C_{Ni}	.88	.88	.8	.75	.72	.66	.61	.56	.53	.47	.42	.36	.34	.29	.29
Pattern Number		2.6	2.5	2.4	2.4	2.3	2.3	2.2	2.1	1.6	1.5	1.4	1.3	1.1	nearest number

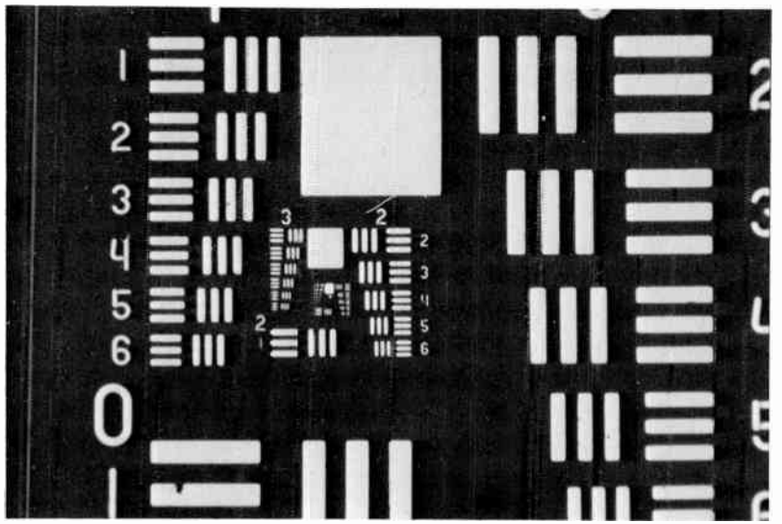

Fig. 22—Enlargement of picture 1 of Fig. 21 showing resolving power of system without noise at high contrast (C = 1) where N_r = 600 lines or 25 lines/mm.

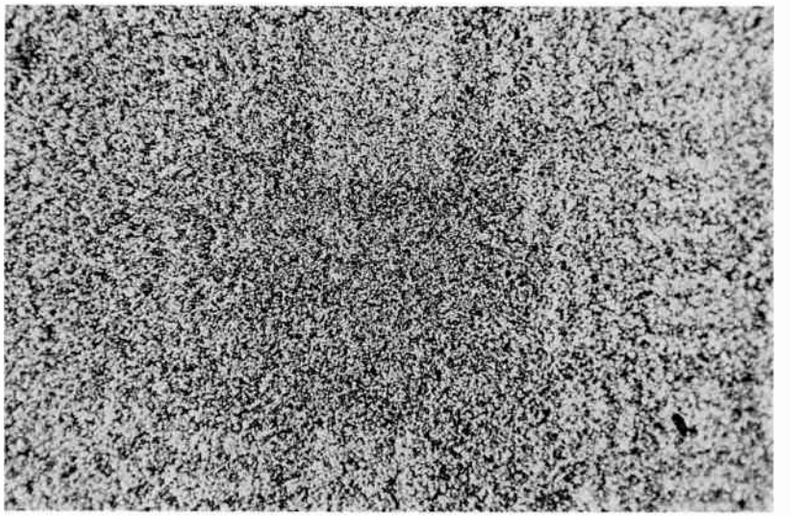

Fig. 24a—Enlargement of picture 14 of Fig. 21, contrast C = 0.33, N_r = 2.1 lines/mm. Pattern is visible at a viewing distance of 4 feet or more.

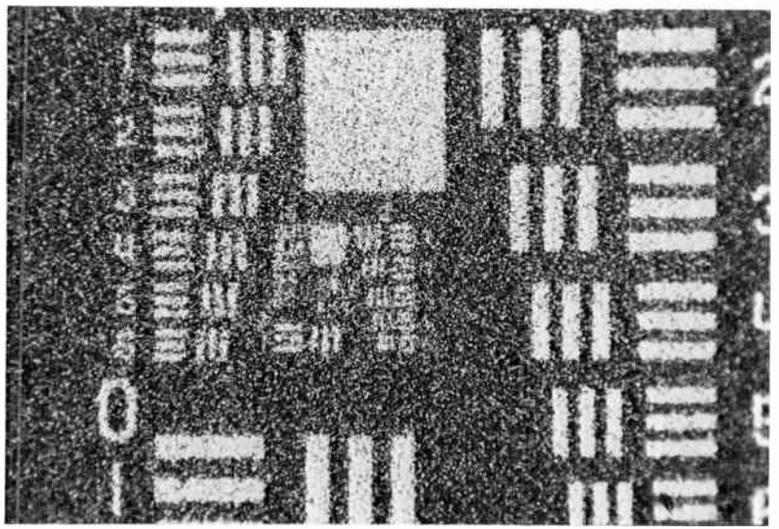

Fig. 23—Enlargement of picture 3 of Fig. 21, where contrast is reduced to C = 0.91 and noise added (N_r = 6.1 lines/mm, determined at pattern 2.5).

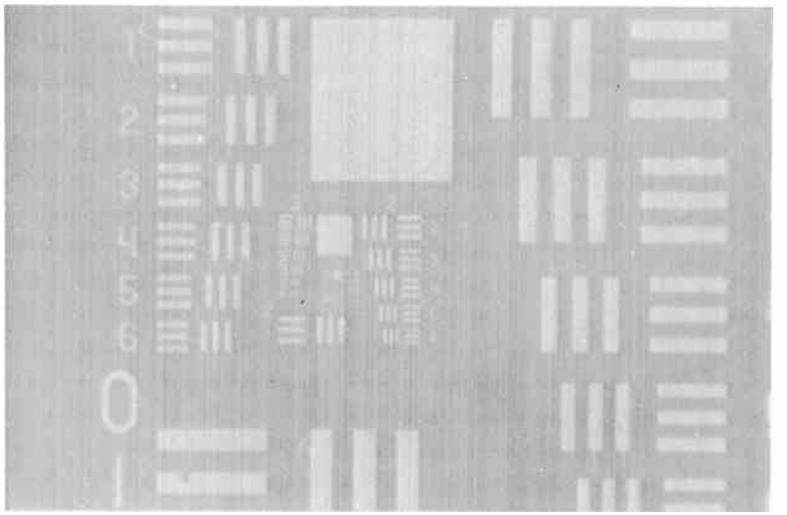

Fig. 24b—Same as Fig. 24a, but with noise removed to show definition hidden by noise.

the range of 4 to 40 ft-L and a normal viewing distance of 25 cm, the best match occurs when the test pattern frequency is 1 to 1.5 cycles/mm or $N = 2$ to 3 l/mm. The optimum magnification for a visual detection has therefore the value $M_{opt} \simeq N_r/3$, where N_r is the resolving power in lines/mm.

The set of pictures was made by projecting a high-contrast test pattern image on a photographic grain plate which introduces the noise. The contrast was varied by adding a uniform light bias to the test pattern light via a semitransparent mirror in the projection path. The noise plate was mounted on a scanning table, so that the noise could be removed by integration, i.e., by applying a scanning motion to the noise plate during exposure of the film in the recording camera.[14] This feature was used to focus the projector and is illustrated by the picture pairs (#1, #2) and (#14, #15). The noise seen in picture #2 was removed by scanning to produce the noise-free picture #1 enlarged in Fig. 22. Similarly the noise in the low-contrast picture #14 was remove by scanning to obtain picture #15 and to show the actual image hidden by noise. The enlargement, Fig. 24b, shows fine scratches caused by incomplete integration of the noise by the scanning motion.

The original purpose for generating pictures with accurately known noise levels and contrasts by an optical synthesis was the determination of the threshold value (k) for the resolving-power test object.[14] With this value it is possible to calculate the resolving power from the constants of the imaging system and the object contrast. The detail-signal-to-noise ratio ($SNR_{\Delta,N}$) is calculated for the image area ($\bar{a}_i$) of a single bar of the periodic image with

$$SNR_{\Delta,N} = SNR_{(1)}\dot{\gamma}a_i^{1/2}(\Delta B_0/\bar{B}_0)r\bar{\Delta}_N(l_0/l_i) \qquad [16]$$

where $\dot{\gamma}$ is the sensor gamma (unity in this case), and the ratio $(\Delta B_0/\bar{B}_0)$ is the peak-to-peak signal modulation of the bar pattern. The mean gray-scale signal $\bar{B}_0$, which determines the noise measured or calculated for this level, is expressed by the signal-to-noise ratio $SNR_{(1)}$ for the unit area of one mm^2. The product $r\bar{\Delta}_N(l_0/l_i)$ specifies the amplitude reduction of the object signal by the square-wave flux response factor ($r\bar{\Delta}_N$) in the periodic direction and by the reciprocal spread factor of the imaging system (l_0/l_i) in the direction of the bar length. Substitution of equivalent pass bands yields

$$SNR_{\Delta,N} = SNR_{(1)}\dot{\gamma}(5/Nb^{1/2})(\Delta B_0/\bar{B}_0)r\bar{\Delta}_N \qquad [17]$$

where $b = [25 + (N^2/N_{e(s)}^2)]^{1/2}$ and $N_{e(s)}$ is the equivalent pass band of the complete imaging system. For visual observations, the square-wave flux response factor can be calculated from the system MTF with $r\bar{\Delta}_N = 0.81\text{MTF}_N$.

The threshold value for $SNR_{\Delta,N}$ determined by observation of resolving powers in the above and other test series is $k = 3.6$. With this value substituted for $SNR_{\Delta,N}$, Eq. [17] can be solved for N as a function of the known detail contrast $(\Delta B_0/\bar{B}_0)$ of the test object, given the MTF and the large area signal-to-noise ratio $SNR_{(1)}$ for one mm^2 of the imaging system.

Table 2 lists the calculated resolving power (N_r) for the pictures shown in Fig. 21 in TV-lines/mm (total picture height is 24 mm) and the corresponding pattern number as well as the large-area contrast $C = \Delta B_0/B_{max}$ and the actual detail contrast $C_{Ni} \simeq (\Delta B_0/\bar{B}_0)r\bar{\Delta}_N$ in the image. The reader can verify by observation (with suitable magnification) that observed and calculated values are in agreement, allowing for normal statistical variations. Exceptions are pictures #2 and, to some extent, #3, where the noise simulation by optically additive grain noise is inaccurate.

Expressed in TV units, the noise-free image #1 has a limiting resultion of 600 lines in the frame dimension of 24 mm ($N_r = 25$ l/mm). The signal-to-noise ratio $SNR_{(1)}$ for a sampling area of one mm^2 is 12.52 in all pictures containing noise, at any gray-scale level, because of the method of optical noise addition.

The threshold value for a TV reproduction of the test object with 30 frames/s is $k = 2$ because of the frame integration by the eye in a live image.

The resolving power in the photographs in Figs. **64, 66,** and **68** was calculated with Eq. [17] for the standard 3-bar resolving power test object and the threshold value $SNR_{\Delta,N} = k = 3.6$. The MTF of the system is the product for 2 lenses (curve 1 squared in Fig. 6), the negative film (curve 3), and the transfer MTF (curve 5). The MTF of the printing paper can be neglected because of the large magnification.

The resolving power (N_r) in TV-lines/mm is plotted in Fig. 25 as a function of detail contrast for several gray-scale densities (D_1) of the negative film. Corresponding exposure levels ($\bar{E}/E_{max}$) are listed in the figure. Additional scales indicate the resolving power in TV-lines per format dimension for 35-mm, 16-mm, and 8-mm film formats. The resolving power in Figs. **64** and **66** can be observed on the periodic windows of a number of buildings. The observed range is indicated in Fig. 25 and refers to different gray-scale levels in the original and

different contrasts. Absolute blacks rarely occur in a real scene or in a print having a good gray scale.

The detail signal-to-noise ratio at the display screen of a normal TV system using a lead oxide vidicon camera (controlled by amplifier noise) is given closely by

$$\mathrm{SNR}_{\Delta(N)} = \bar{I}(\Delta E_0/\bar{E}_0)0.81\mathrm{MTF}_N/(\bar{i}_{n(a_0)}\sqrt{\alpha}) \qquad [18]$$

where $\bar{I}$ is the gray-scale current at the target, MTF_N is the response factor of the system at the line number N, and the denominator is the rms noise current of the preamplifier calculated for the area $\bar{a}_0 = 5/N^2$ of one bar in the resolving-power test object. The noise current of the amplifier is closely

$$\bar{i}_{n(a_0)} = 0.56[(X/Y)0.2N^2/(2bt_f)]^{3/2}C_{in}/g_m{}^{1/2}, \quad \text{nA} \qquad [19]$$

For $X/Y = 4/3$, $t_f = 1/30$, $b = 0.784$ (blanking factor), $C_{\mathrm{in}} = 20$ pF and $g_m = 0.0065$, Eq. [19] reduces to $\bar{i}_{n(a_0)} = 1.6 \cdot 10^{-9}\, N^3$ nA. The bandwidth factor $\alpha^{1/2}$ is calculated as discussed in connection with Eq. [15] for each assumed value N.

The resolving power for a live TV image is obtained by letting $\mathrm{SNR}_{\Delta,(N)}$ equal the threshold value $k = 2$ and solving for the exposure contrast $\Delta E_0/\bar{E}_0$:

$$\Delta E_0/\bar{E}_0 = 3.95\cdot 10^{-9}\sqrt{\alpha}N_r{}^3/\bar{I}\cdot\mathrm{MTF}_N$$

where N_r is the resolving power in TV lines, $\bar{I}$ is the gray-scale current in nA, and MTF_N is the product of the response factors of the camera lens, the vidicon, and the display tube, assuming no aperture correction.

Resolving-power functions computed for this vidicon camera system are plotted in Fig. 26. The video pass band must, of course, be wide enough to pass the line numbers N and $0.2N$ of the test object under observation in respective coordinates.

Amplifier noise is independent of the gray-scale level for any given line number. As a result, the maximum resolving power occurs in the high-light region, whereas it occurs for photographic film (Fig. 25) in the shadow region where the highest product of SNR and film gamma is obtained.

The resolving power of a motion picture is somewhat different from that of a still photograph. The noise is decreased by frame integration in the eye and may be increased by a positive process, whereas the MTF of the system is reduced by additional transfer stages.

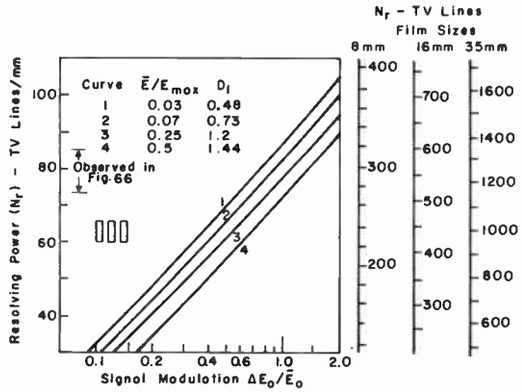

Fig. 25—Resolving power computed for the projection prints Figs. 64, 66, and 68 from 15.7 × 21 mm, 7 × 9 mm, and 3.7 × 5 mm, Plus X negatives taken with a 35-mm camera.

It should also be pointed out that the resolving-power functions of TV systems using return-beam vidicons or camera tubes with intensifier stages have a different shape and may have higher resolving powers at low gray-scale levels, because they are not amplifier-noise limited.[19,20] The resolving power of standard TV systems is, of course,

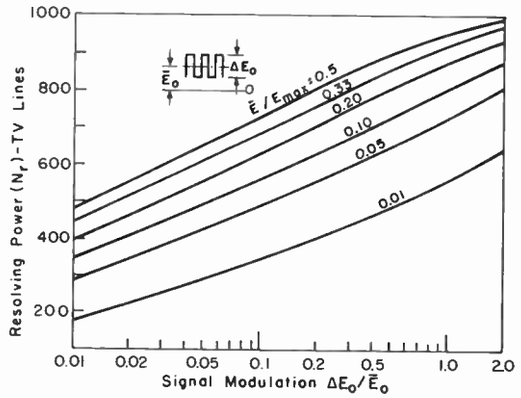

Fig. 26—Resolving power computed for a television system with a lead oxide vidicon camera operating at 30 frames/s with a peak signal current of 300 nA.

bandwidth limited by the electrical video channel. The resolving power, provided it is observed or computed as a function of gray scale and contrast,[19] is an excellent measure of the information content of an image.

References:

[1] O. H. Schade, Sr., "Image Gradation, Graininess, and Sharpness in Television and Motion Picture Systems. Part I: Image Structure and Transfer Characteristics," *J. SMPTE,* Vol. 56, p. 137, Feb. 1951.

[2] O. H. Schade, Sr., "Image Gradation, Graininess and Sharpness in Television and Motion-Picture Systems. Part III: The Grain Structure of Television Images (Raster Processes)," *J. SMPTE,* Vol. 61, p. 97, Aug. 1953.

[3] O. H. Schade, "Vertical Aperture Correction," U.S. Patent No. 3,030,440, Nov. 1958, issued April 17, 1962.

[4] O. H. Schade, Sr., "Electro-Optical Characteristics of Television Systems," published in *RCA Review,* Vol. 9, in four parts, "Part I: Characteristics of Vision and Visual Systems," p. 5, March 1948; "Part II: Electro-Optical Specifications for Television Systems," p. 245, June 1948; "Part III: Electro-Optical Characteristics of Camera Systems," p. 490, Sept. 1948; and "Part IV: Correlation and Evaluation of Electro-Optical Characteristics of Imaging Systems," p. 653, Dec. 1948

[5] O. H. Schade, Sr., "A New System of Measuring and Specifying Image Definition," Optical Image Evaluation Symp. at NBS, Oct. 1951, April 1954.

[6] O. H. Schade, Sr., "Image Gradation, Graininess, and Sharpness in Television and Motion-Picture Systems. Part IV: Image analysis in Photographic and Television Systems (Definition and Sharpness)," *J. SMPTE,* Vol. 64, p. 593, Nov. 1955.

[7] W. G. Gibson and A. C. Schroeder, "A Vertical Aperature Equalizer for Television," *J. SMPTE,* Vol. 69, p. 395, June 1960.

[8] O. H. Schade, Sr., "Optical and Photoelectric Analog of the Eye," *J. Opt. Soc. Amer.,* Vol. 46, p. 721, Sept 1956.

[9] L. A. Riggs, "Measurement of Normal Ocular Tremor by Corneal Reflection," *J. Opt. Soc. Amer.,* Vol. 42, p. 287, April 1952; G. C. Higgins and K. F. Stultz, "The Frequency and Amplitude of Ocular Tremor," *J. Opt. Soc. Amer.,* Vol. 22, p. 872, Nov. 1952.

[10] M. W. Baldwin, Jr., "The Subjective Sharpness of Simulated Television Images," *Bell. Syst. Tech. J.,* Vol. 19, p. 563, Oct. 1940.

[11] O. H. Schade, Sr., "Modern Image Evaluation and Television (The Influence of Electronic Television on the Methods of Image Evaluation," *Appl., Optics,* Vol. 3, p. 17, Jan. 1964.

[12] O. H. Schade, Sr., "Wide Angle High Definition Television Systems," Contract N60NR-23606, Final Report by RCA Laboratories for Office of Naval Research, Special Devices Center, Port Washington, N. Y., pp. 1–88, Aug. 1952.

[13] J. C. Norris, "An MTF Analysis of the Contribution of Motion-Picture Printing to Image Sharpness," *J. SMPTE,* Vol. 79, p. 706, Aug. 1970.

[13a] O. H. Schade, Sr., "Image Gradation, Graininess, and Sharpness in Television and Motion Picture Systems. Part II: The Grain Structure of Motion Pictures—An Analysis of Deviations and Fluctuations of the Sample Number." *J. SMPTE,* Vol. 58, p. 781, March 1952.

[14] O. H. Schade, Sr., "An Evaluation of Photographic Image Quality and Resolving Power," *J. SMPTE,* Vol. 73, p. 81, Feb. 1964.

[15] O. H. Schade, "Electron Optics and Signal Read-Out of High-Definition Return-Beam Vidicon Cameras," *RCA Review,* Vol. 31, p. 120, March 1970.

[16] O. H. Schade, Sr., "High-Resolution Return-Beam Vicidon Cameras: A Comparison with High-Resolution Photography," *J. SMPTE,* Vol. 79, p. 694, Aug. 1970

The references cited above refer to publications in which many of the photographs reproduced in this book have appeared. Many other references are given in the above publications and in two volumes edited by Lucien N. Biberman and Sol Nudelman entitled, *Photoelectronic Imaging Devices,* Plenum Press, N. Y., N. Y. (1971) and in the book, *Perception of Displayed Information,* edited by Lucien M. Biberman, Plenum Press, N. Y., N. Y. (1973).

[17] A. Rose, "The Sensitivity Performance of the Human Eye on an Absolute Scale," *J. Opt. Soc. Amer.,* Vol. 38, p. 196, Feb. 1948.

[18] D. O. North, "Analysis of the Factors Which Determine Signal/Noise Discrimination in Pulsed-Carrier Systems," *Proc. IEEE,* Vol. 51, p. 1016, July 1963.

[19] Otto H. Schade, Sr., "The Resolving Power Functions and Quantum Processes of Television Cameras," *RCA Review,* Vol. 28, p. 460, Sept. 1967.

[20] O. H. Schade, Sr., "Resolving Power Functions and Integrals of High-Definition Television and Photographic Cameras—A New Concept in Image Evaluation," *RCA Review,* Vol. 32, p. 657, Dec. 1971.

Photographs

The photographs of television pictures reproduced on the following pages were made under laboratory conditions in which equipment limitations were minimized insofar as possible. The pictures permit an evaluation of the three principal factors that determine picture quality—(1)gray scale, (2)noise, and (3)definition, or sharpness.

The standards under which a television system operates impose a basic limitation on the maximum sharpness that a picture can have. The standards for broadcast are established by governments. They are designed to give a flicker-free picture with reasonable sharpness, with the transmitted signal contained within a specified radio-frequency-channel width. The most widely used sets of standards at the present time are (1) 525-line picture, 4.25-megahertz video channel width, at 30 pictures per second, and (2) 625-line picture, 5-megahertz video channel width, at 25 pictures per second. The first is used in the United States, Canada, Mexico, and Japan, while the second is used in a number of Western European countries.

The sharpness limitation imposed by the standards is comparable to a slight defocusing of an optical system. However, in broadcast television as seen in the home, any loss of sharpness attributable to the standards under which the system operates is frequently masked by a much greater loss of sharpness due to less than ideal receiving conditions. In the photographs shown here, picture degradation due to equipment operation has been essentially eliminated, so that the effect of the standards alone can be observed. Some of the pictures were made using the U.S. 525-line standards. Others were made using non-standard specifications, and include 625-line, 1000-line, and 1800-line pictures.

Three sources of video signal were used—a flying-spot scanner for transparencies and either a 4½ inch image orthicon or a return-beam vidicon for direct pickup. The television pictures were displayed on a monitor with a high-quality picture tube and photographed with a 4 × 5 inch camera. For comparison purposes when the source was a transparency, the picture was projected onto a white screen and photographed with the same camera.

The reproductions were made by offset printing, using a 150-line screen. No special precautions were taken to avoid moiré effects.

Fig. 27 2×2-inch slide reproduced by photographing optical projection image.

Figures 27–30

Gray Scale

Fig. 28 2X2-inch slide reproduced by standard 525-line, 4.25-MHz TV system using flying-spot scanner and gamma correction; photograph of 16-inch cathode-ray-tube image.

Fig. 29 2X2-inch slide reproduced by photographing optical projection image.

Figures 27–30
Gray Scale

Fig. 30 2X2-inch slide reproduced by standard 525-line, 4.25 MHz TV system using flying-spot scanner and gamma correction; photograph of 16-inch cathode-ray-tube image.

Fig. 31 Live pick-up with 4½-inch image orthicon, 525-lines, 8-MHz, 30 frames/sec; photograph of 16-inch cathode-ray-tube image.

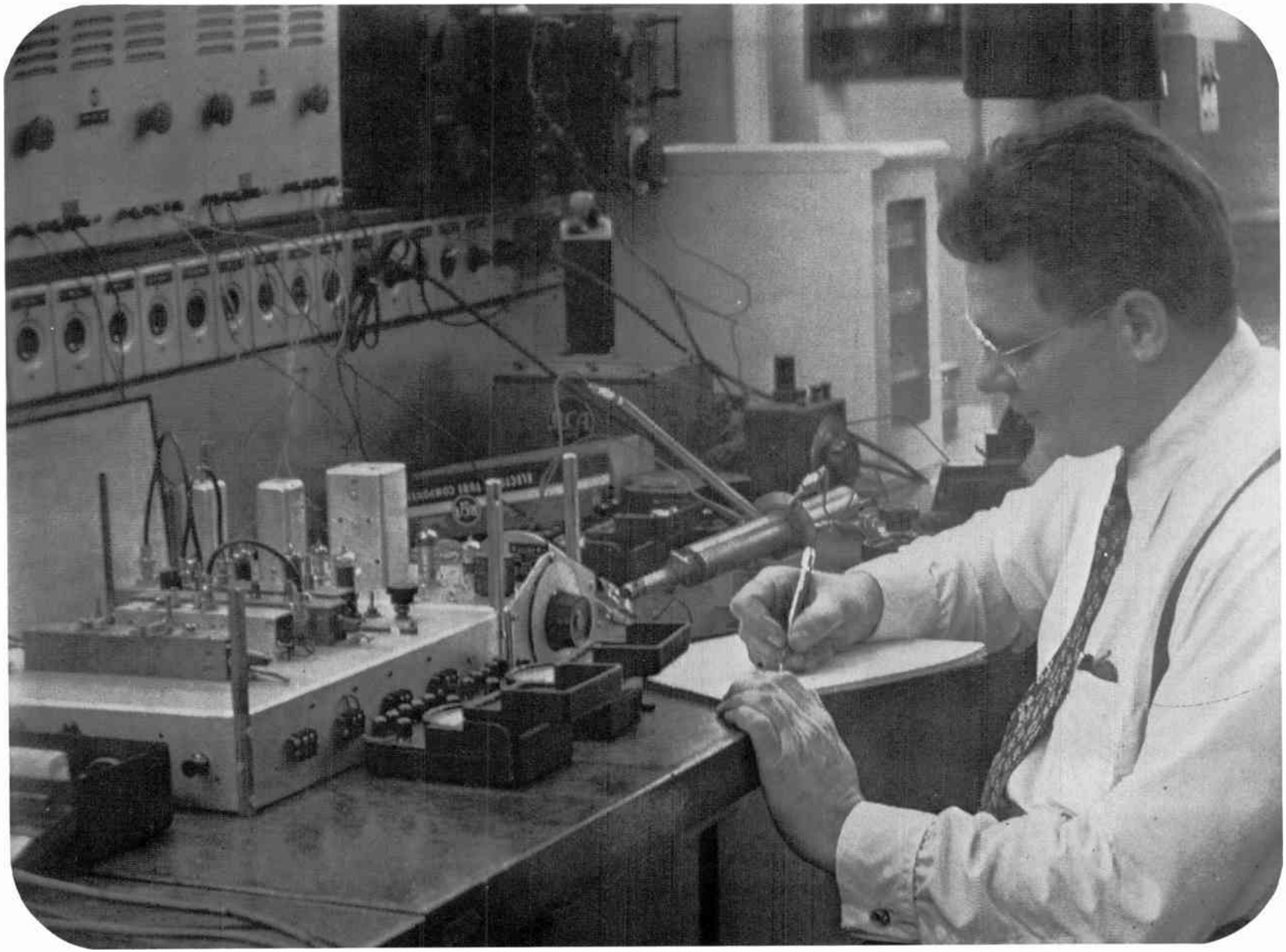

Fig. 32 Live pick-up with 4½-inch image orthicon, 625-lines, 8-MHz, 30 frames/sec; photograph of 16-inch cathode-ray-tube image.

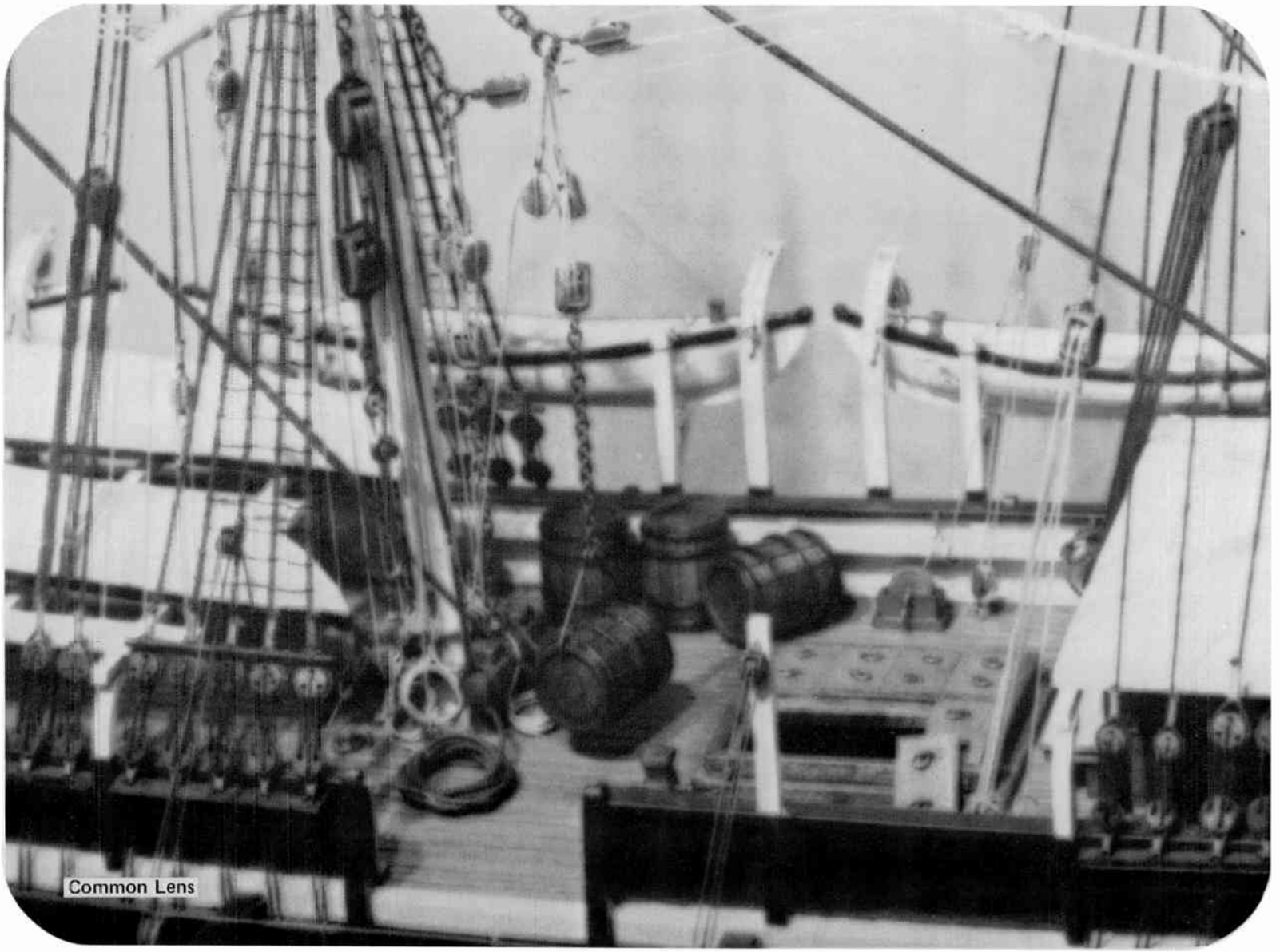

Fig. 33 Enlarged section of photograph made with a common lens; MTF, equivalent pass band (N_e), and edge transition are given in Fig. 4.

Fig. 34 Subject of Fig. 33 reproduced by an equivalent cos^2 aperture yielding the same N_e value as in Fig. 33. The N_e values of the two lenses are the same. It is seen that the sharpness is determined by N_e rather than the limiting resolution, which is substantially higher for the common lens (see Fig. 4). While Fig. 34 may appear to be slightly sharper, Fig. 33 actually contains "texture" not present in Fig. 34. The strands in some of the ropes can be seen in Fig. 33 but not in Fig. 34.

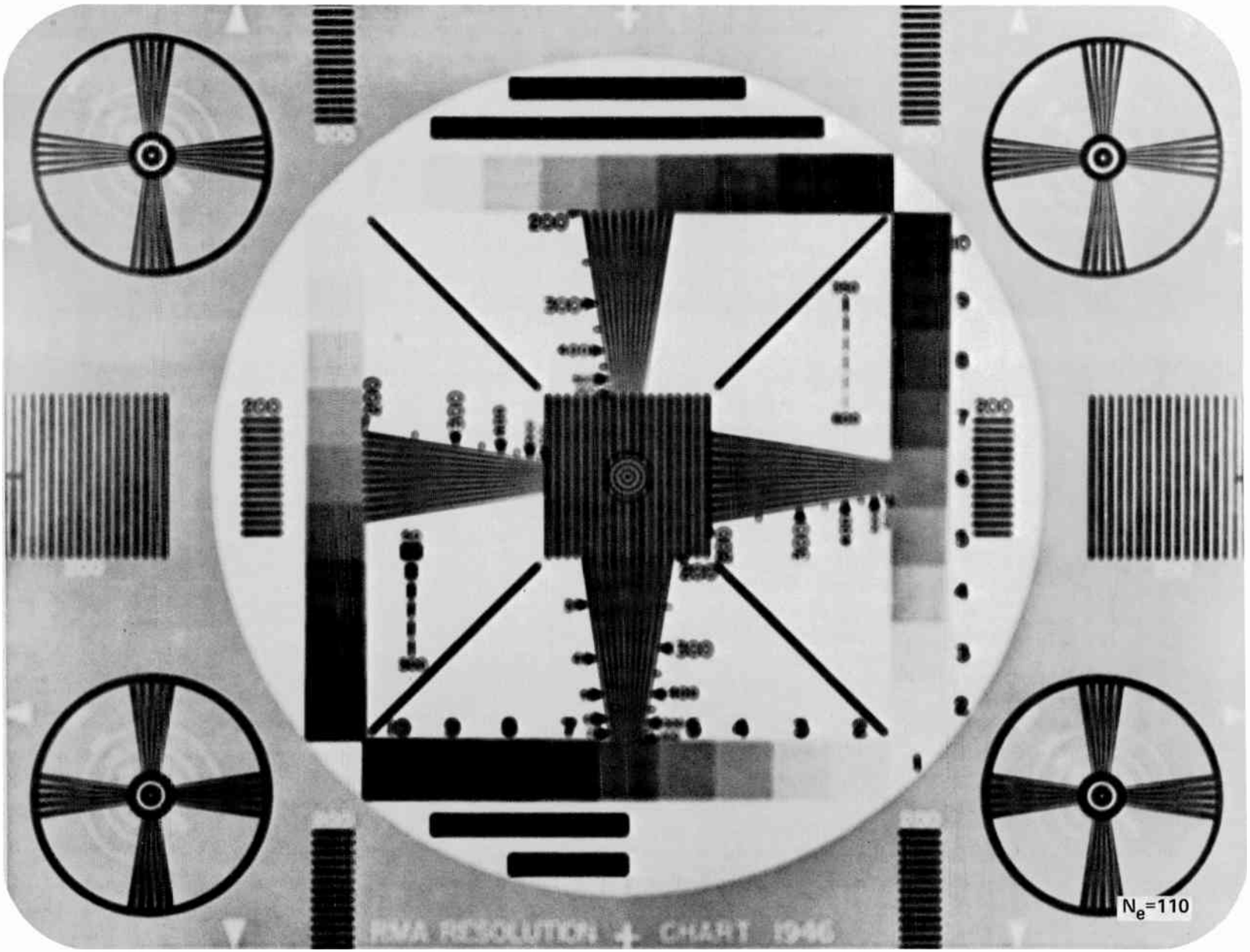

Fig. 35 (a) Photographic reproduction of test pattern with camera defocused to give N_e = 110 lines.

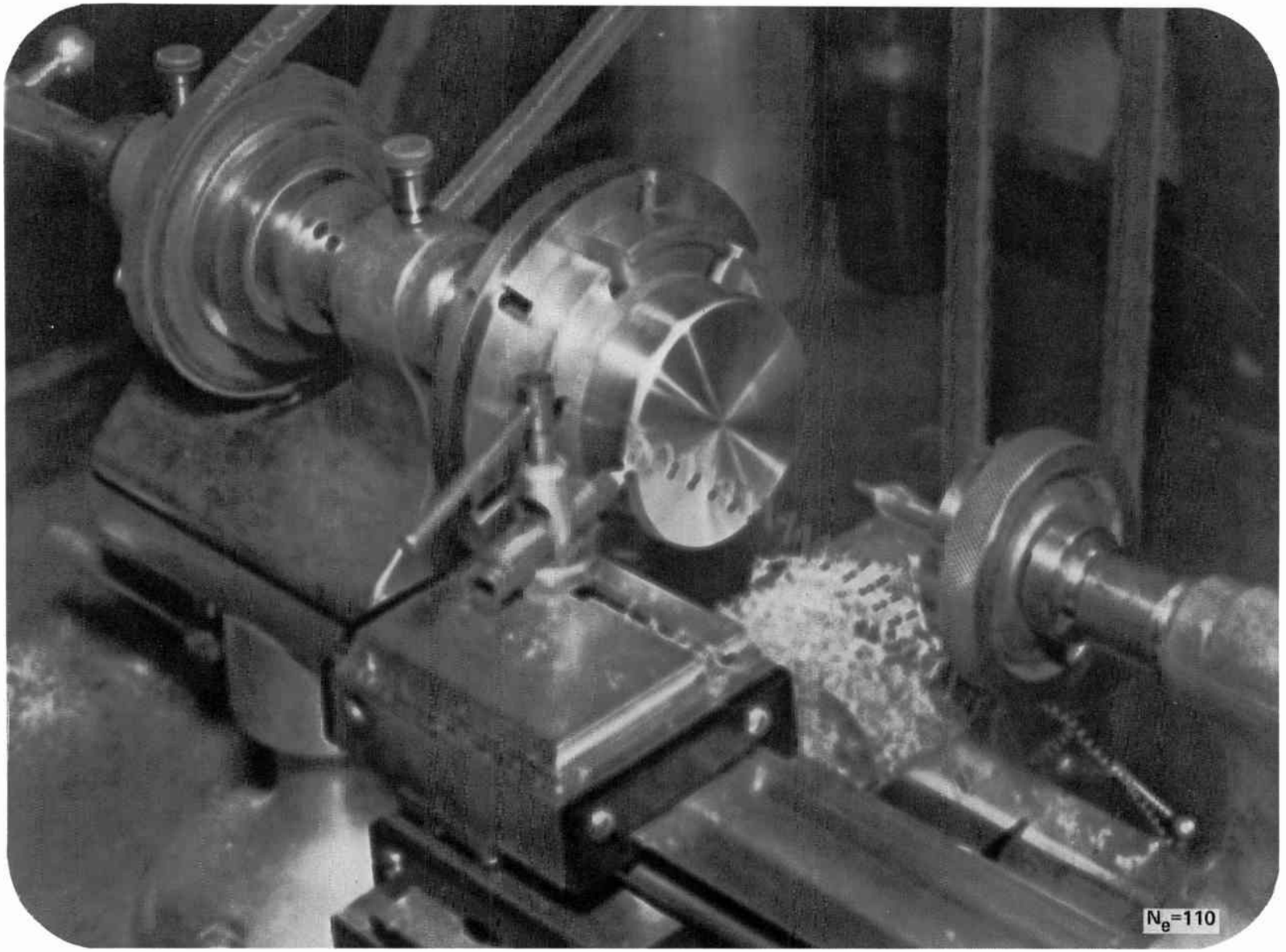

Figures 35–41
Sharpness
Ratings

(b) Photographic reproduction of a photograph with camera defocused to give N_e = 110 lines.

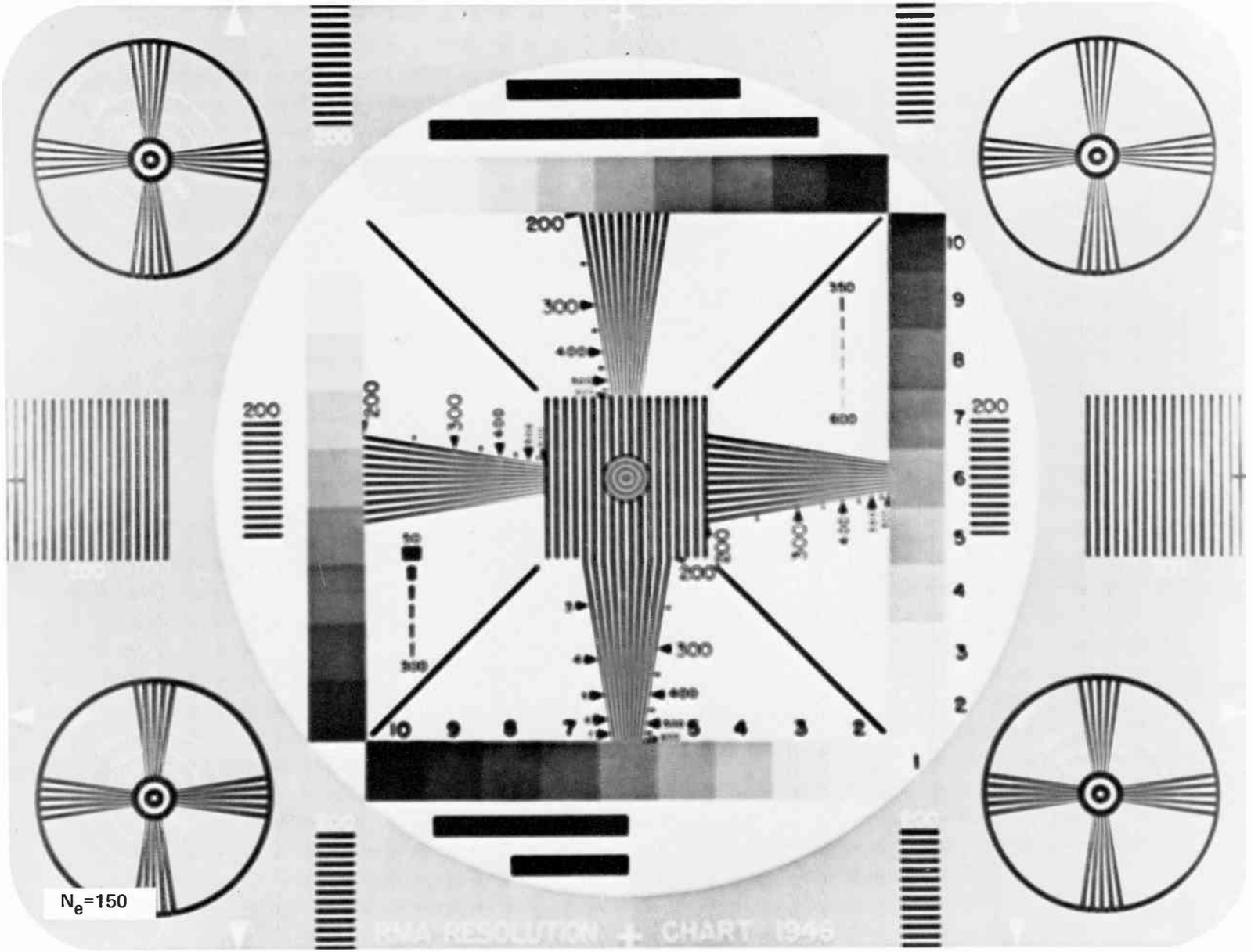

Fig. 36 (a) Photographic reproduction of test pattern with camera defocused to give N_e = 150 lines.

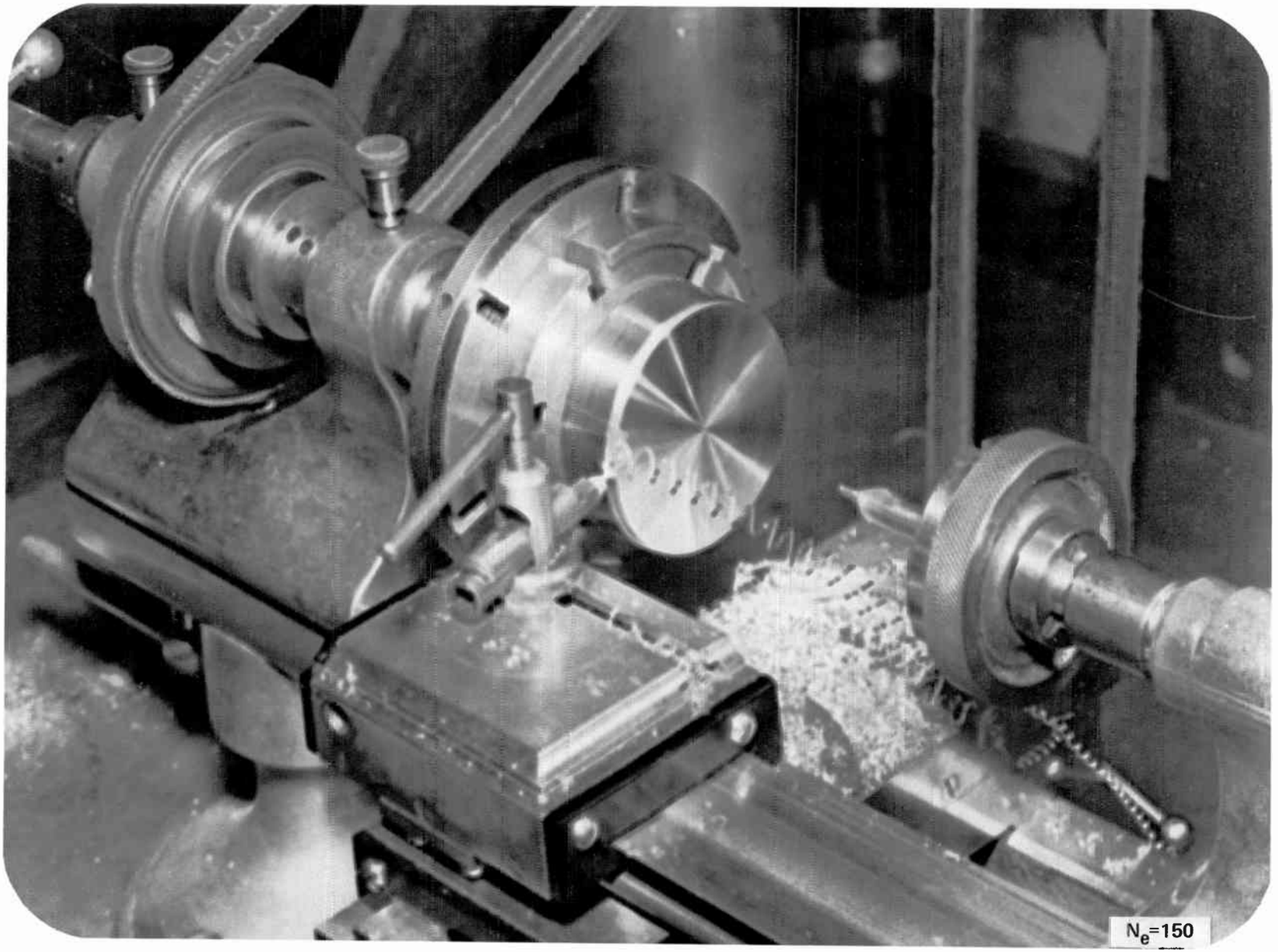

Figures 35–41
Sharpness
Ratings

(b) Photographic reproduction of a photograph with camera defocused to give N_e = 150 lines.

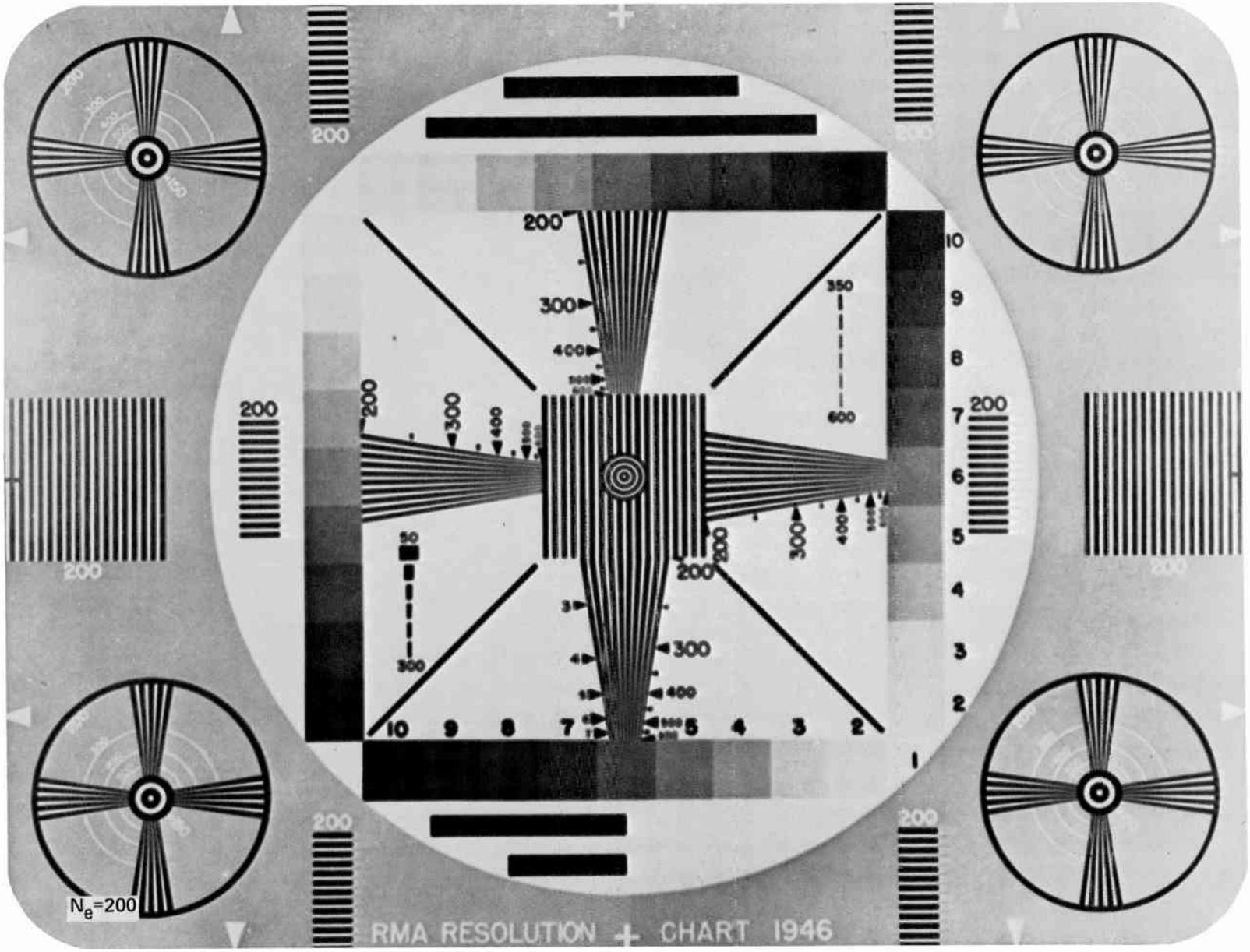

Fig. 37 (a) Photographic reproduction of test pattern with camera defocused to give N_e = 200 lines.

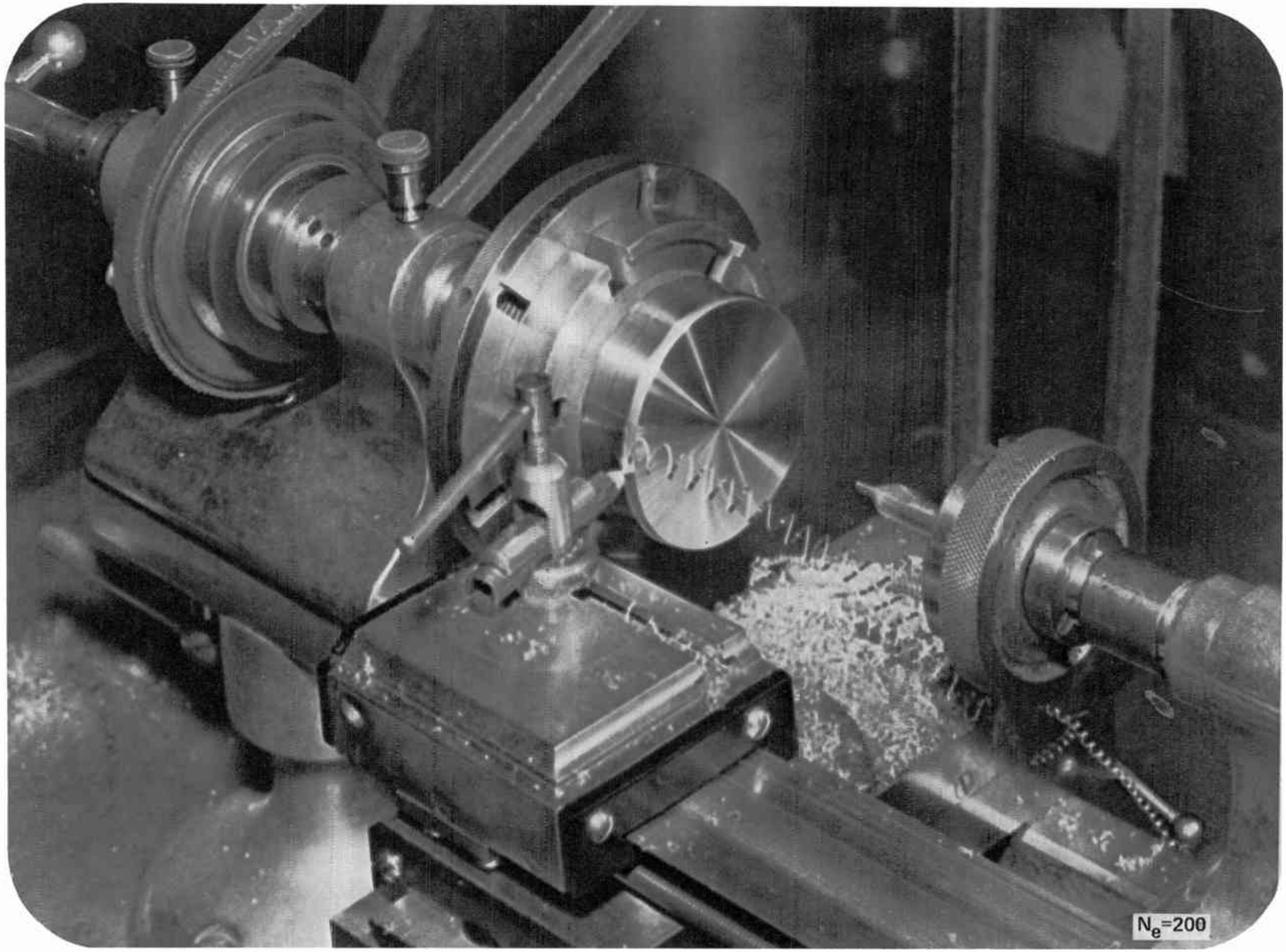

Figures 35–41
Sharpness
Ratings

(b) Photographic reproduction of a photograph with camera defocused to give N_e = 200 lines.

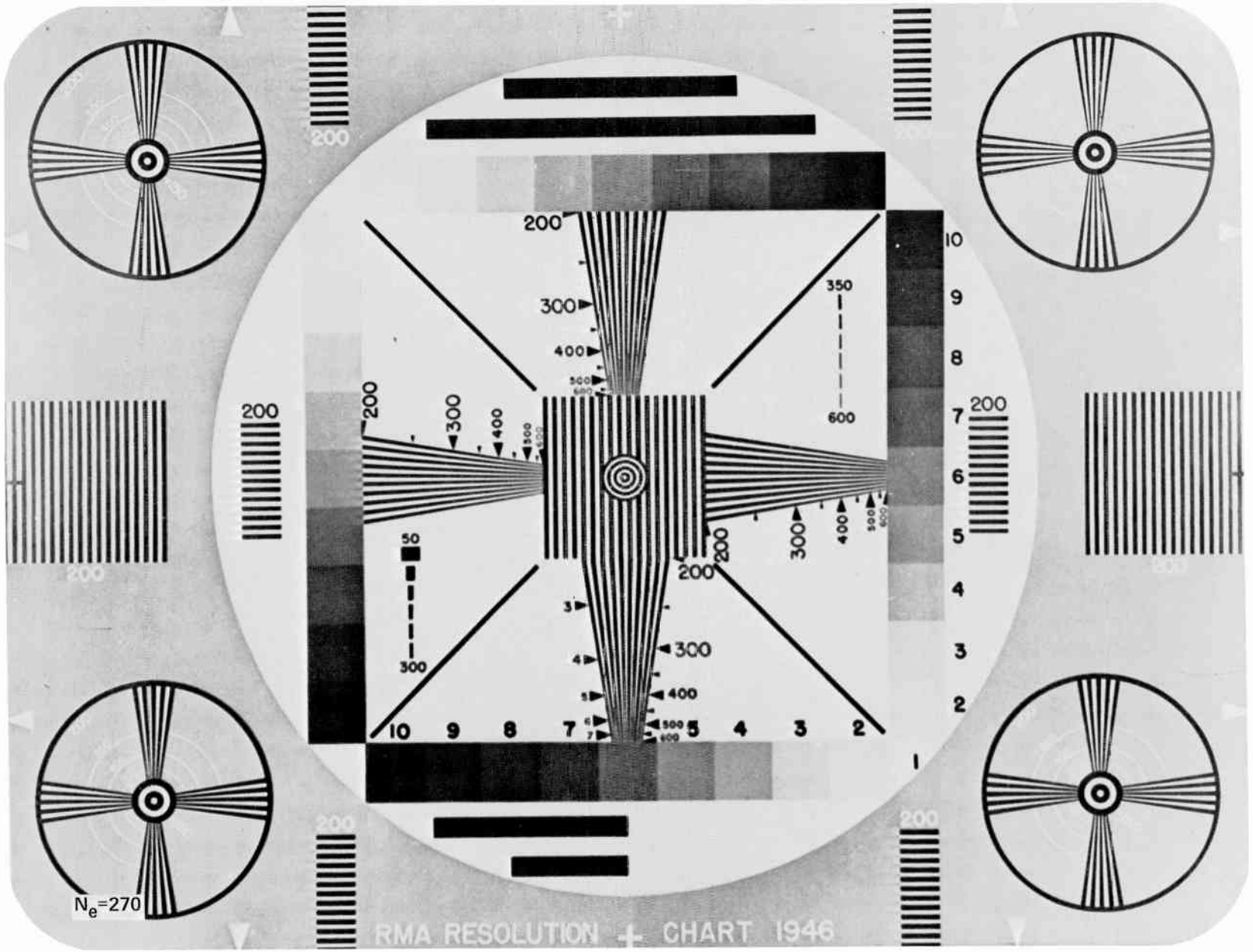

Fig. 38 (a) Photographic reproduction of test pattern with camera defocused to give N_e = 270 lines.

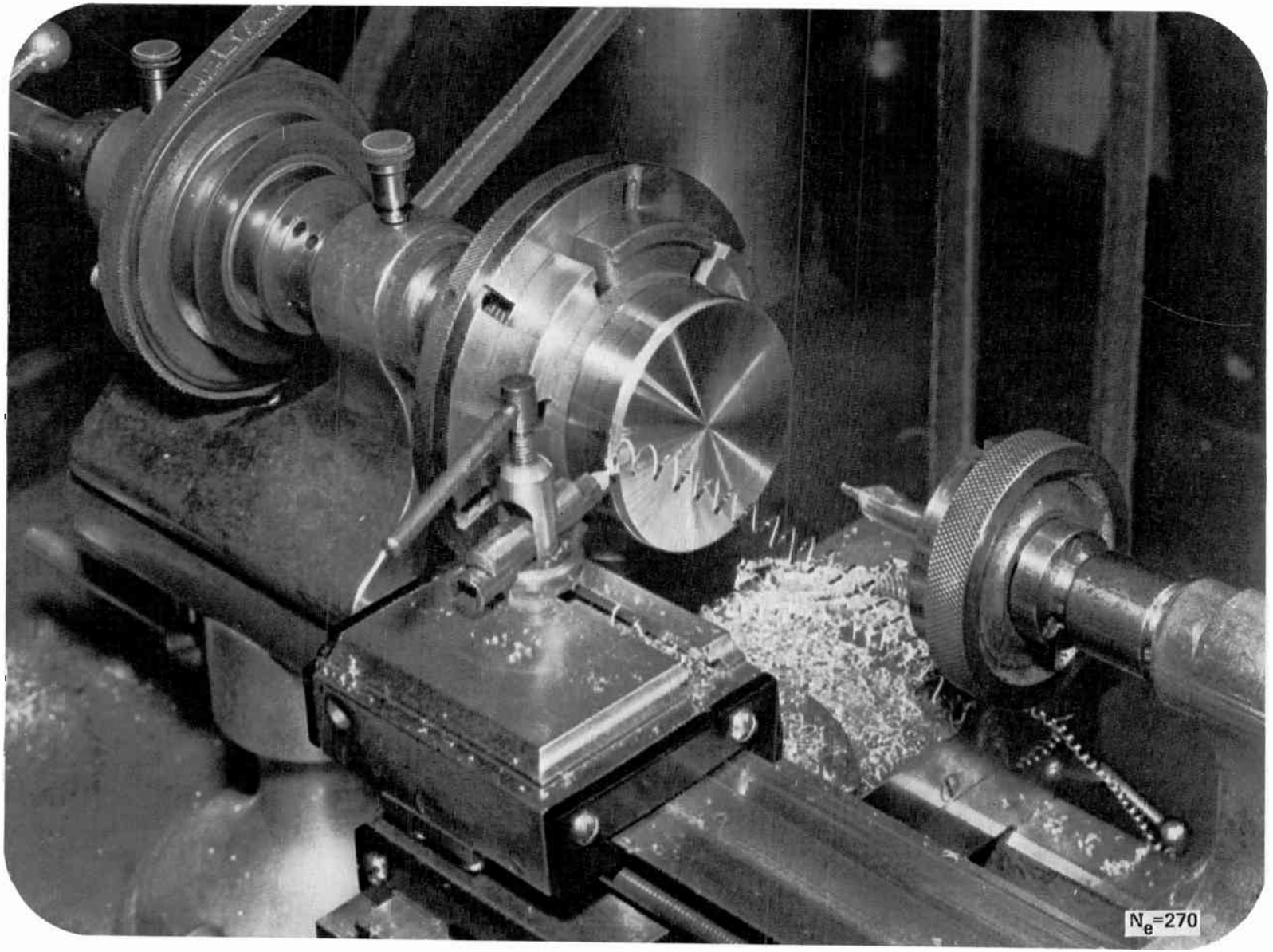

Figures 35–41
Sharpness
Ratings

(b) Photographic reproduction of a photograph with camera defocused to give N_e = 270 lines.

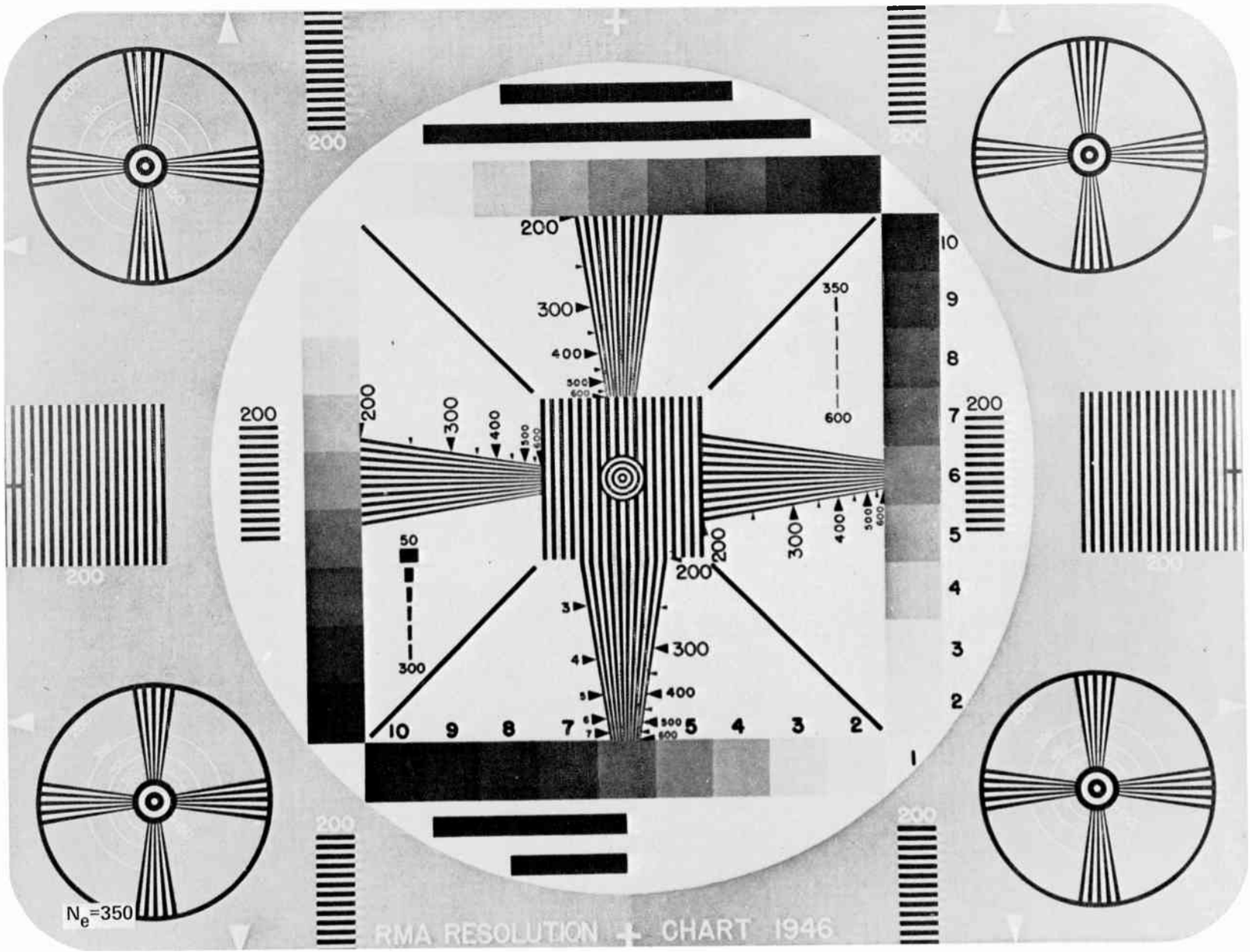

Fig. 39 (a) Photographic reproduction of test pattern with camera defocused to give N_e = 350 lines.

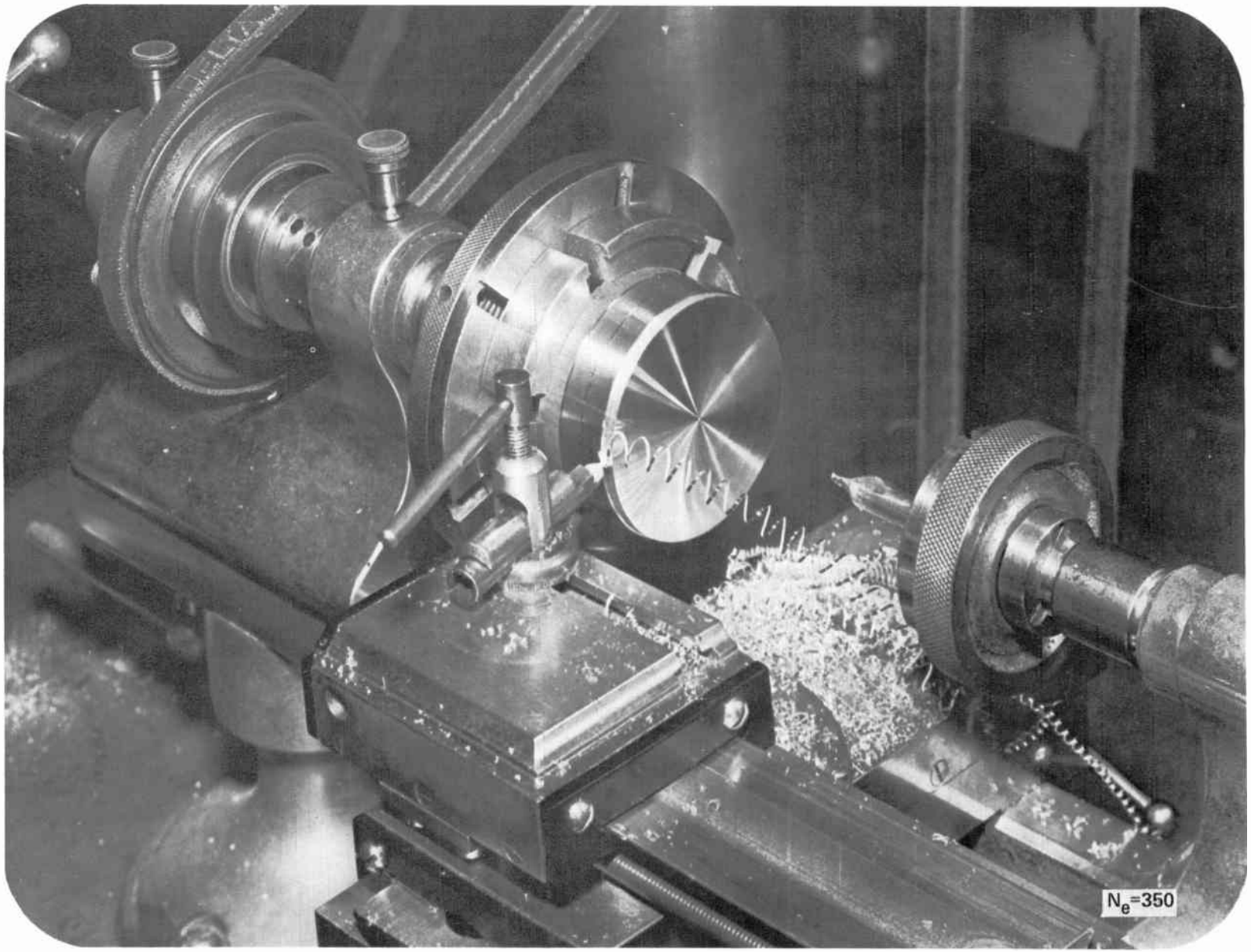

(b) Photographic reproduction of a photograph with camera defocused to give N_e 350 lines.

Figures 35–41
Sharpness
Ratings

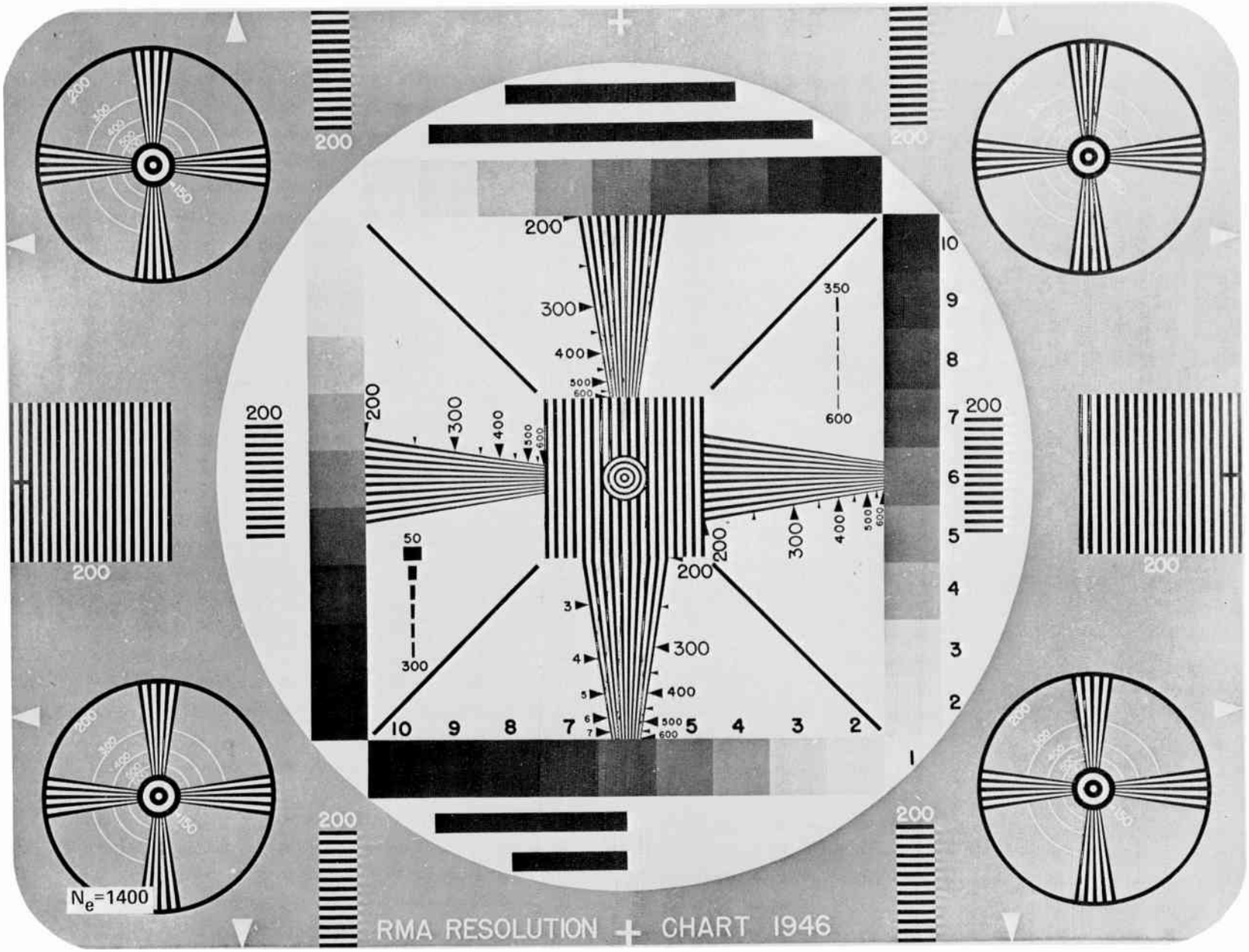

Fig. 40 (a) Photographic reproduction of test pattern with camera focused to give N_e = 1400 lines.

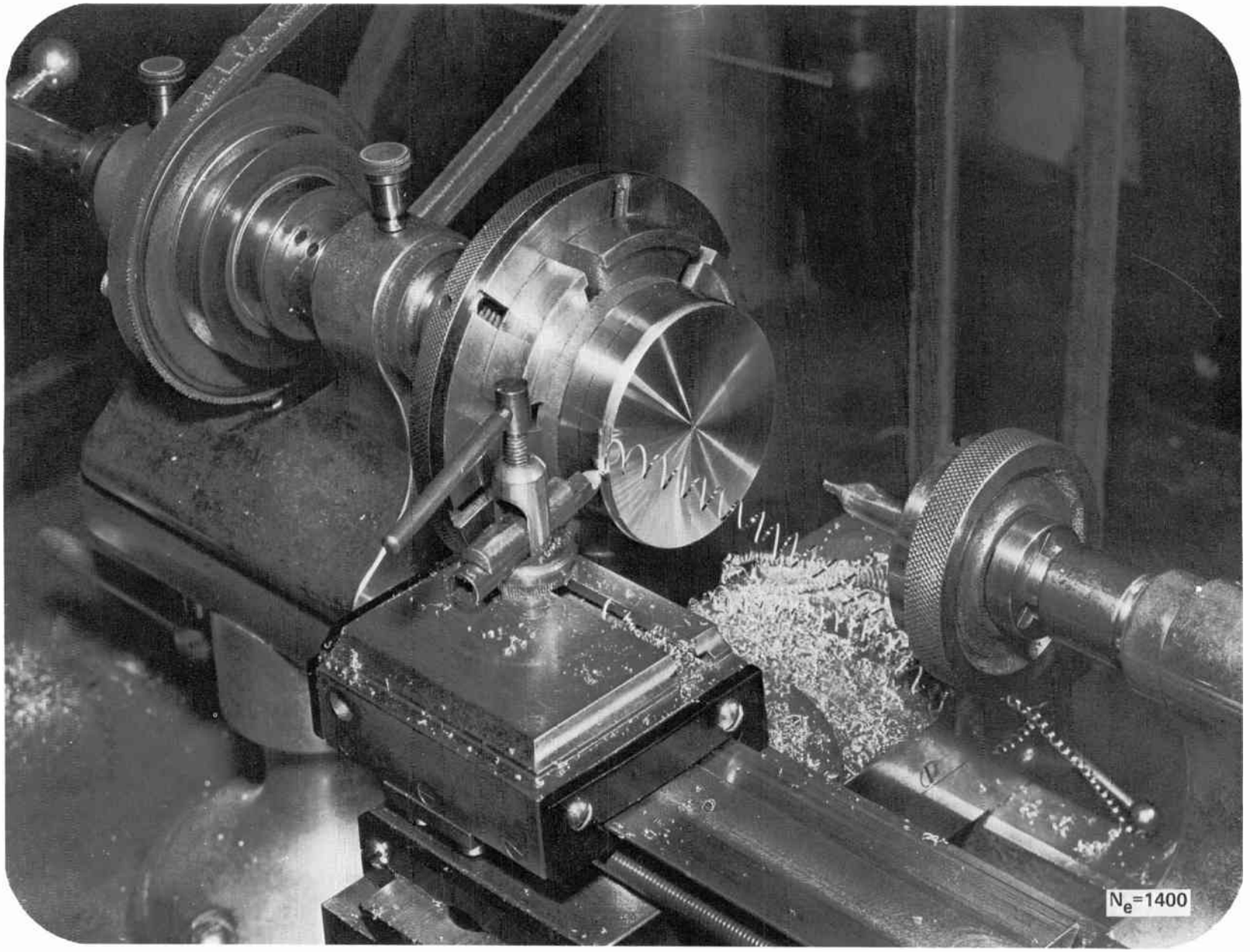

Figures 35–41
Sharpness
Ratings

(b) Photographic reproduction of a photograph with camera focused to give N_e = 1400 lines.

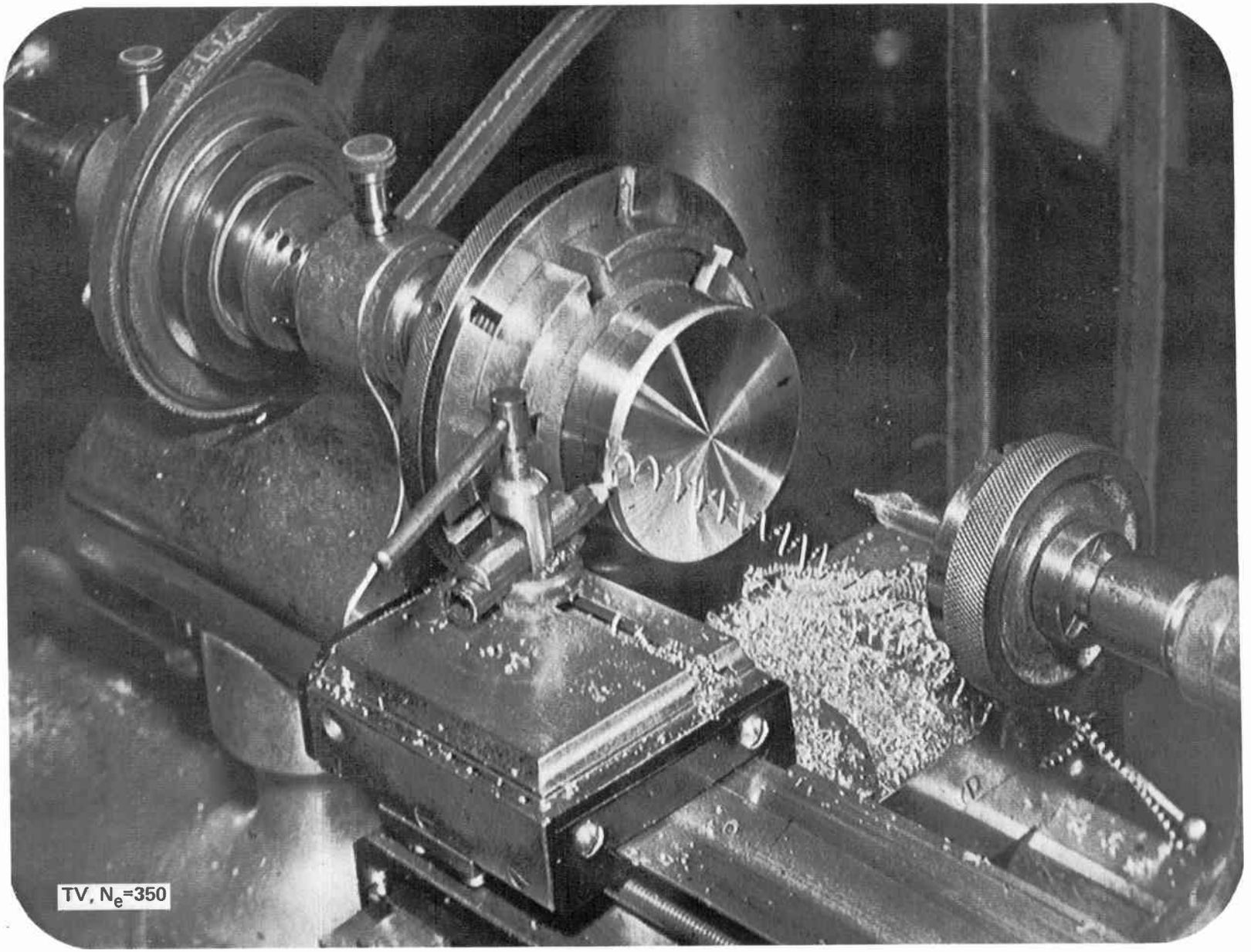

Fig. 41 Television reproduction of a photograph; 625 lines, 8 MHz bandwidth, 30 frames/sec, N_e = 350 lines. Compare with Fig. 39b.

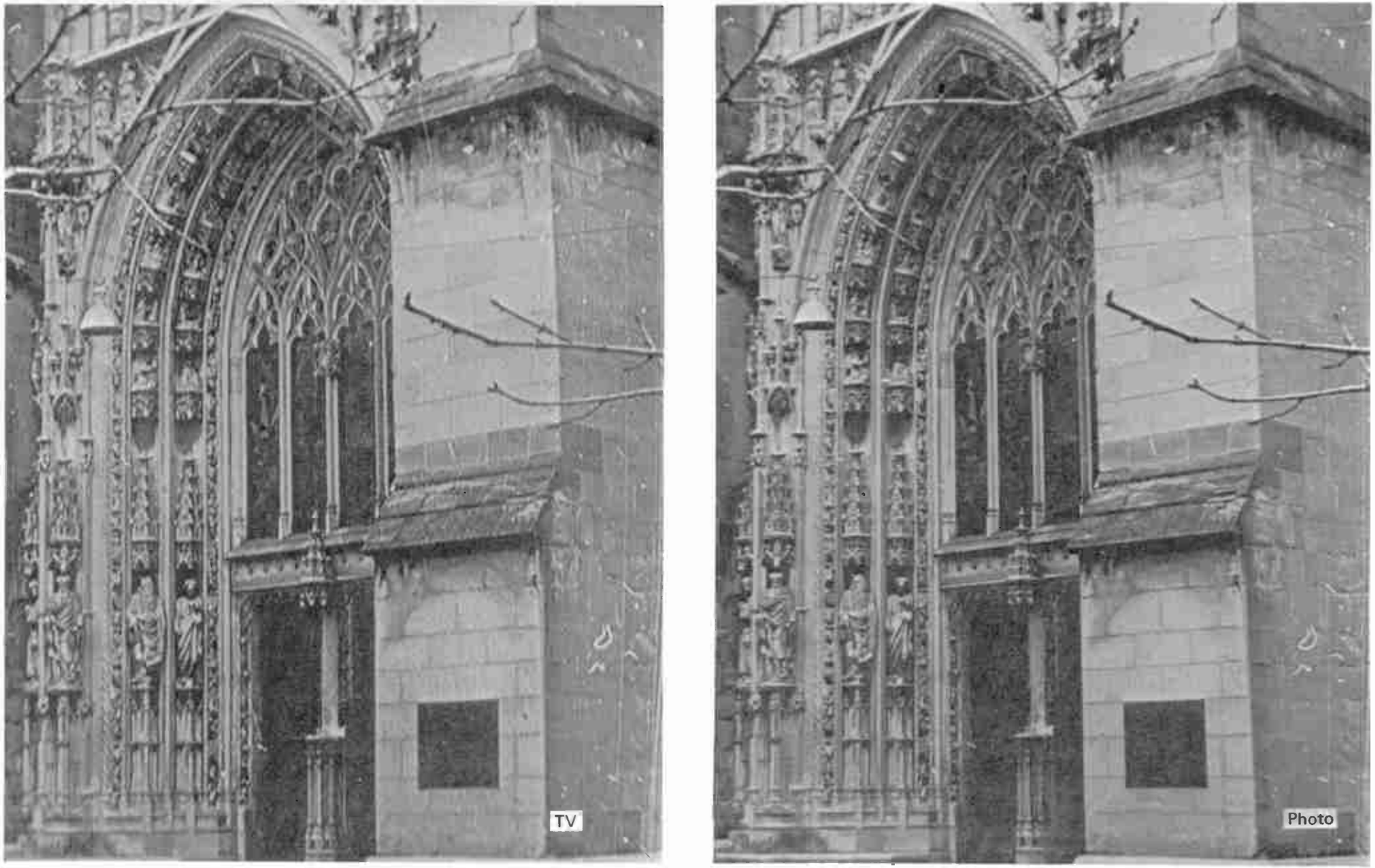

Fig. 42 TV image (625 lines, 8 Mhz, 30 frames/sec) (left) and simulated 35-mm motion picture image (right) having equal equivalent pass band ($N_e = 286$); see Fig. 9.

Fig. 43 (a) TV image of text material (625 lines, 8 MHz, 30 frames/sec) made under conditions indicated in Fig. 9 (N_e = 286).

(b) Simulated 35-mm motion picture image of text material made under conditions indicated in Fig. 9 (N_e = 286).

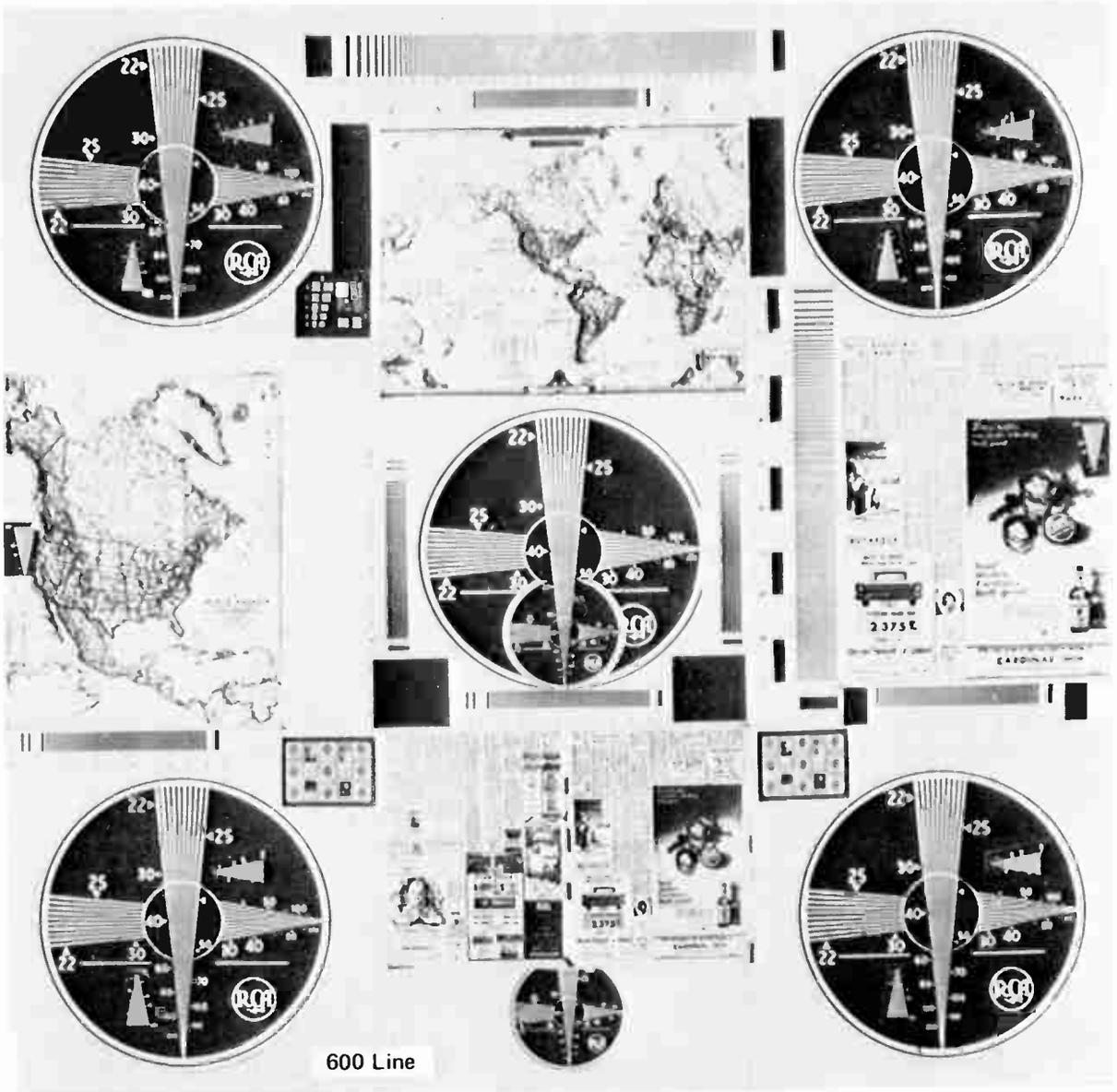

Fig. 44

Reproduction of a high-resolution test pattern by a 600-line TV system with spot wobble.

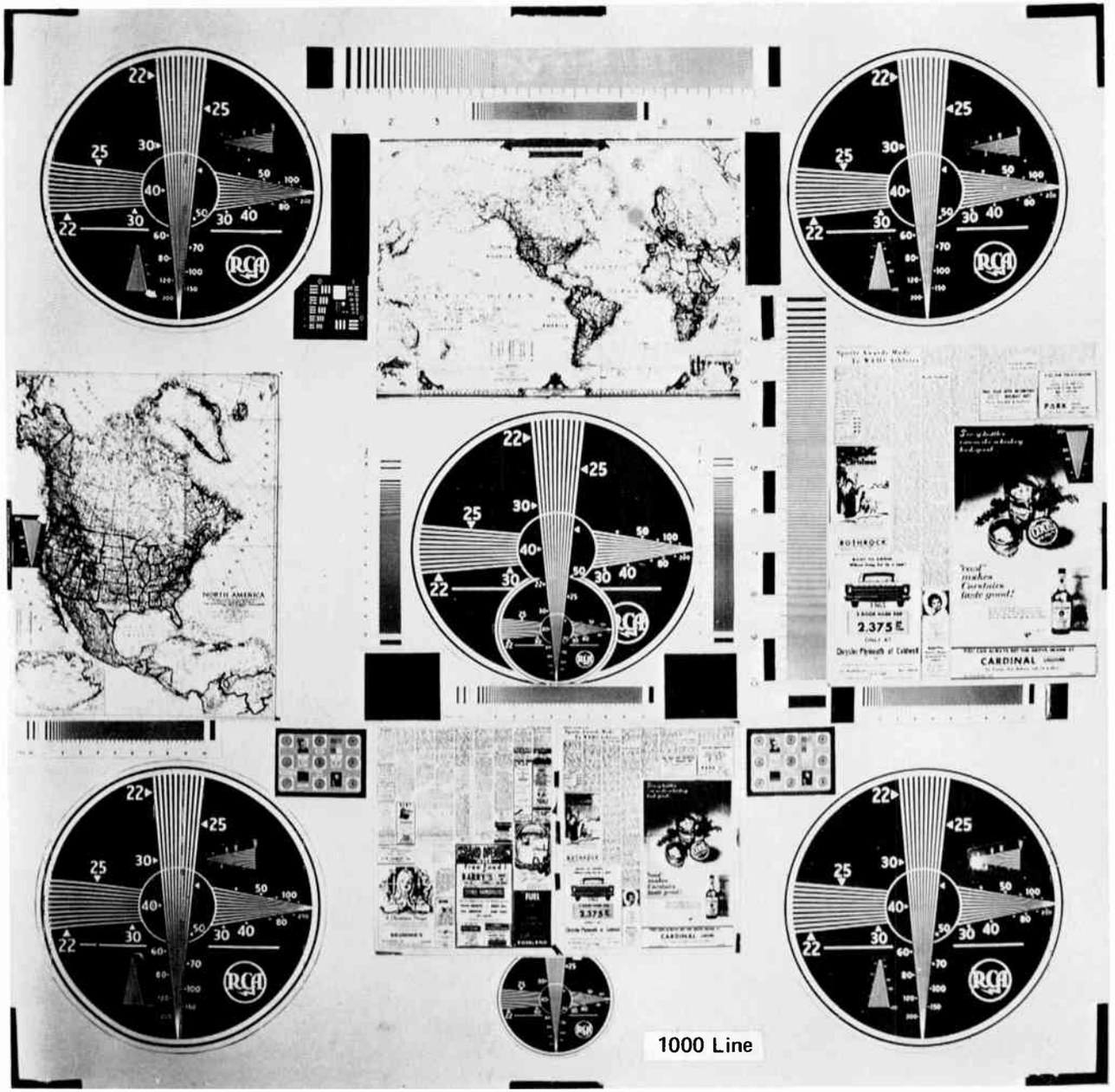

Figures 44–63
Resolution

Fig. 45

Reproduction of a high-resolution test pattern by a 1000-line TV system with spot wobble.

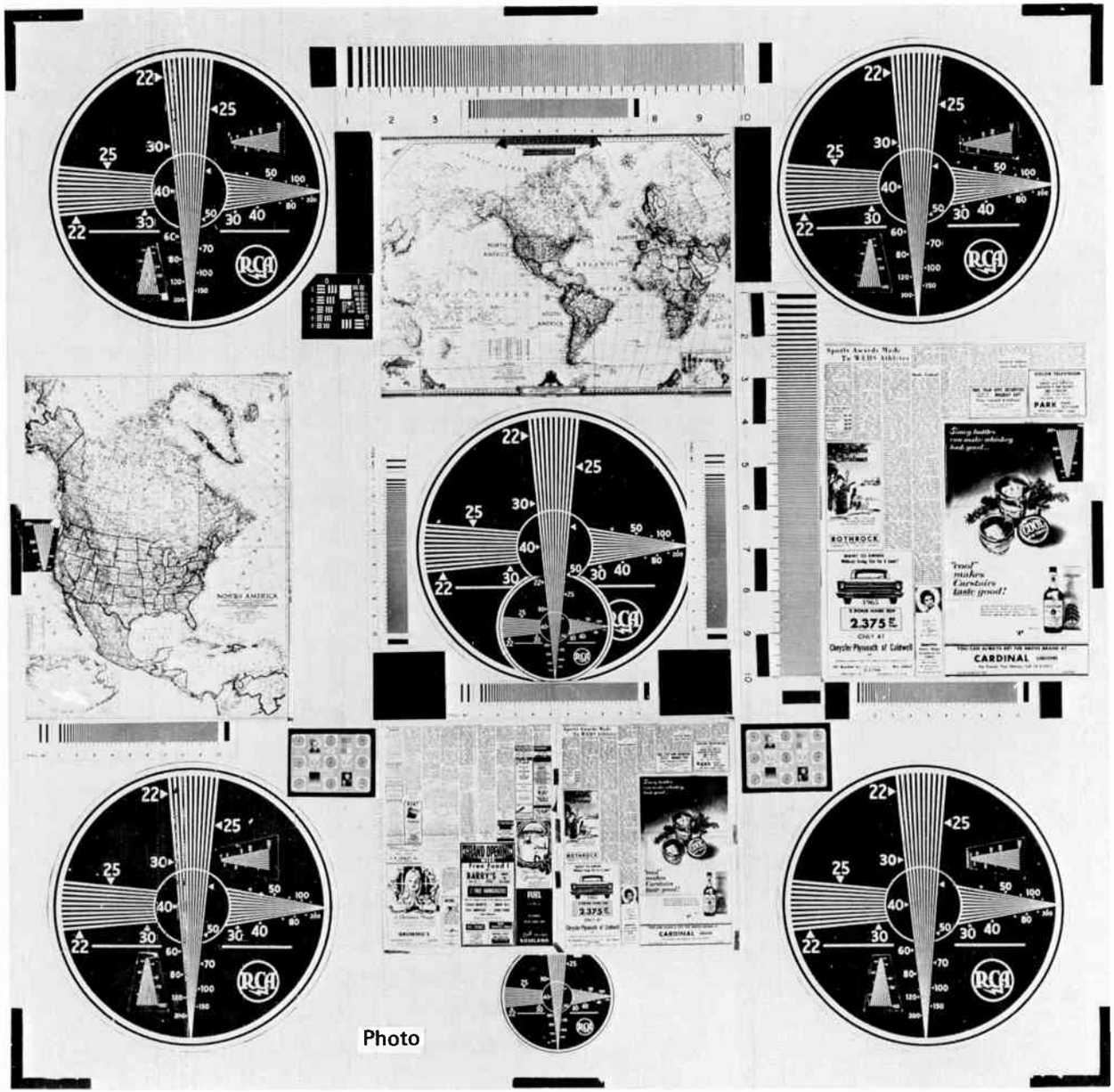

Fig. 46

Direct photograph on 65X65-mm Linagraph Shellburst film, 4500 lines limiting resolution.

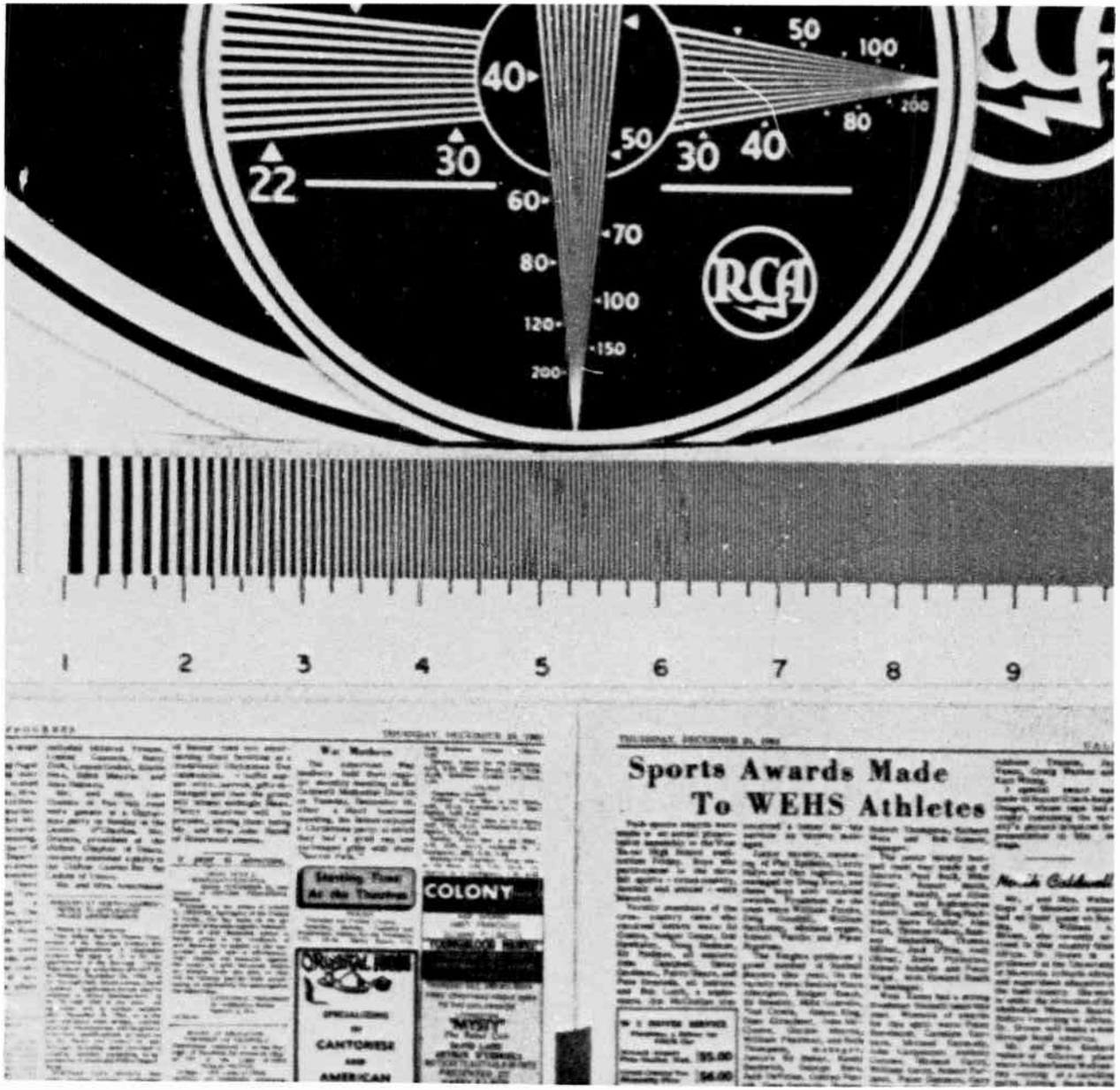

Figures 44–63
Resolution

Fig. 47

Enlargement of Fig. 46, showing newspaper not readable.

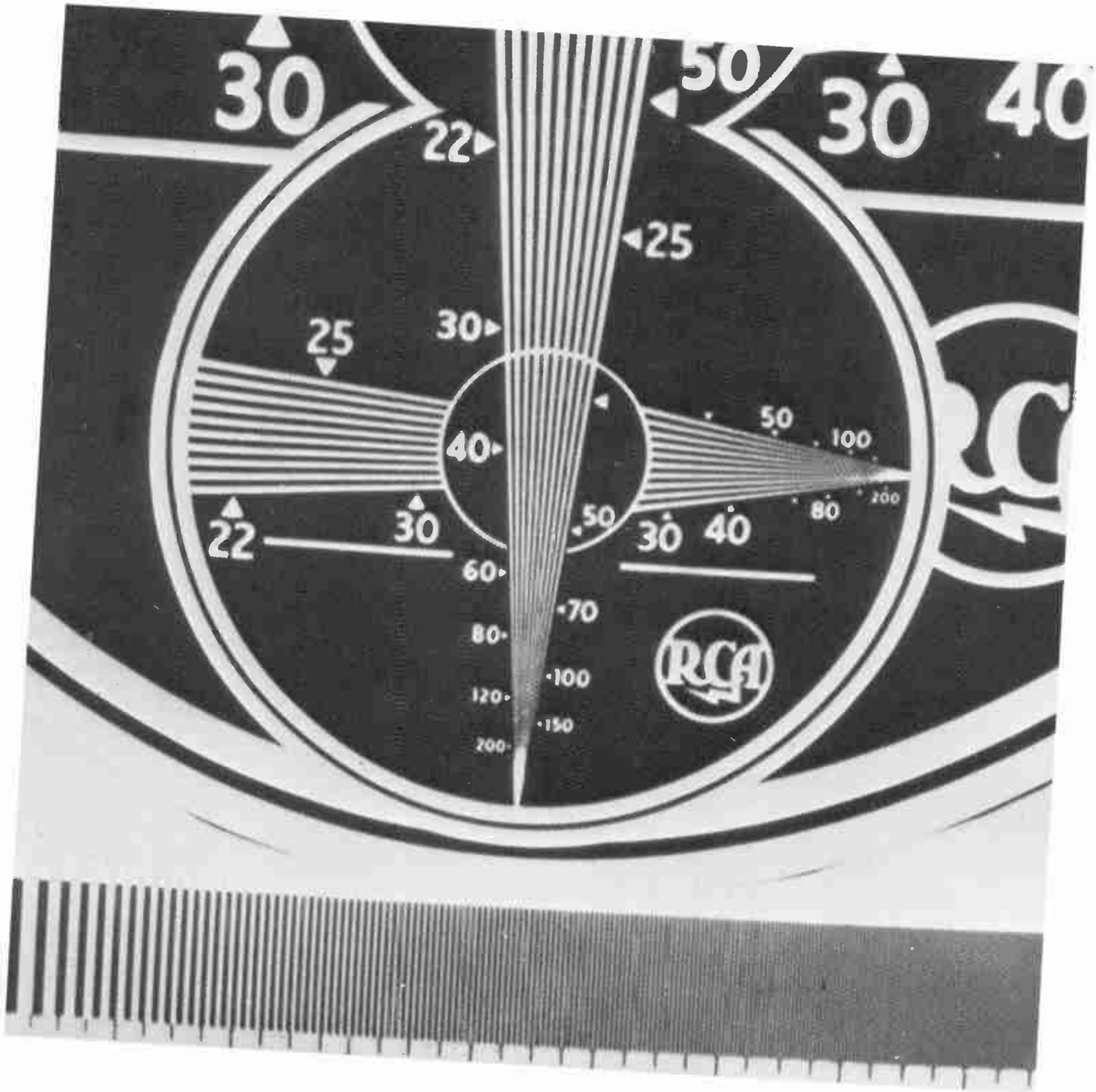

Fig. 48

Readout of a small section of the 50×50-mm image in a return-beam vidicon showing a resolution of 100 cycles per mm. A pattern generated by the beat of the raster with the field mesh of the vidicon is visible.

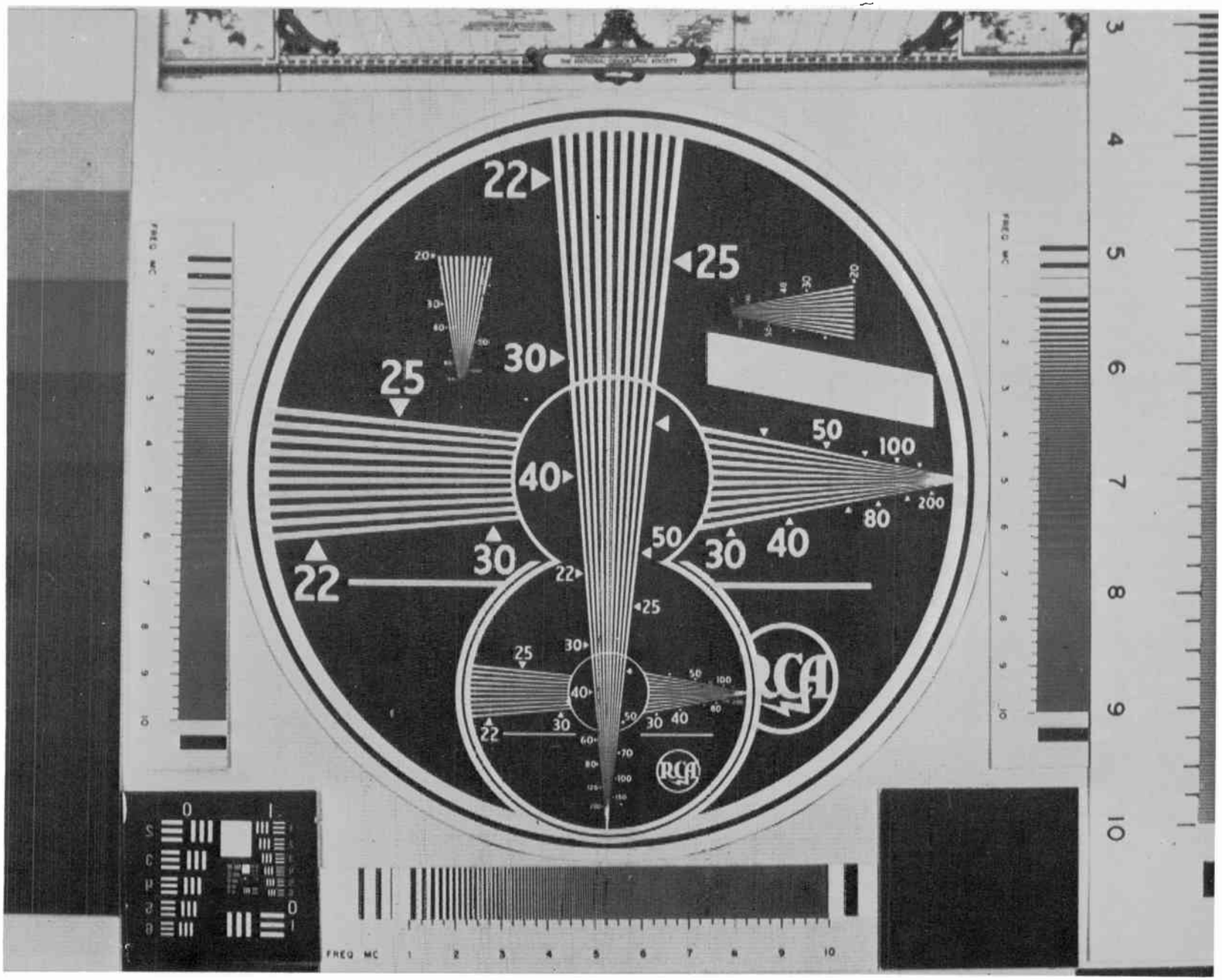

Fig. 49 Enlargement of CRT display of 50×50-mm image from a 4½-inch return-beam vidicon, read out with 100-MHz video channel (1870 lines, 20 frames/sec, 3:1 interlace) showing bandwidth-limited resolution of 3600 lines.

Figures 44–63
Resolution

ports Awards Made To WEHS Athletes

orts awards were an annual presen- sembly in the West igh School audi- riday. Boys who ial in the three s - cross country, nd soccer - were

members of the untry team who letters were: Ed lodger Coupe, Don , Doug Hedman, nan, all seniors; Campbell, Danny , Perry Neare, and reda, all juniors. Leith, a sopho- n McClellan also

received a letter for his service as varsity manager.

Junior varsity, consisting of Phil Epifanio, Larry Hulyo and Dan Ingerto, was managed by Doug Kerr, and these boys also received awards. Freshmen on the team were William Fricke, Doug Goodhill, William Hawksley, Michael Hogan, Robert Petillo and Peter Rigolosso.

The Knights produced a great number of football players this year. On the varsity were: Seniors Vince Albergato, Rodger Beach, Ed Beesley, Mike Costello, Paul Crotta, James King, Dean Kirschner, John McCleeve, Gordon Morris, William Pharmer, and Rich Thompson, manager. Juniors Ed Baker, Randy Beckwith, George Betz, Jack DeVries, Conrad Fenick, Gene Garguilo, Rodger Johnson, Carl Maffei, Mike Kalafer, George Mears, Joseph O'Brien, Charles Roveda, Francis Rice, Chris Unger, and Kent Smith, manager, and sophomores Mike Furey, William Kaiser, Richard McCleeve, Robert Thompson, Richard Weis and Bob Connor, manager.

The junior varsity football team was made up of Juniors Paul Berk, Mike Oliver, Robert Smith, George Wakely, and Allan Walker, and Sophomores Robert Comley, Bing Heckman, Steve Kalafer, Alan Koch, Thomas Kukoc, Ramsey Mahadeen, Thomas Miller, Jack O'Hea, Andy Oliver, Steve Polverino, Robert Schafer and Peter Vogel, with Howard Heath as manager.

West Essex had a strong freshman football team this year. Winners of awards for this sport were: Peter Bernhardt, Carmine Carnaca, Michael Carmody, John Carpentier, Anthony Cottone, Michael Curry, William Eaton, Robert Ferlanti, Peter Gennaro, Gary Glass, Gary Hannon, William Kerr, Jeff Kuebler, George Lincoln, William Martin, Ron McAllister, William Minutti, Joseph Mullen, Greg Park, Steve Scarano, Greg Varley, Charles Voelker, Byron Walker, Kenneth Walter, and managers Melvin Bellott, Robert Dughi, and Albert German.

WEHS soccer team, co-champions of the state in Group II, came up with the best record of fall sports. Members of the 1964 soccer team who received varsity awards were: Seniors Bob Conkling, Paul Galusha, Harold Habermas, Glen Intile, Jon Knoop, Alvin Konner, Bruce Mc Kaba, Richard Meier, Tom Nelson, John Pullia, Greg Schneider, Jeff Smith, Gene Yarnchak and Bob Svehla; Juniors Jack Bruckah, Richard Goodman, Elmar Habermas, Fred MacNamara, Charles Partington, and managers Charles Bachellor and John Jehl.

Junior varsity consisted of: Juniors Fred Giltzow, Joe Jeremias, Roger Jones, Ralph Kelly, Richard Kurkewicz, Greg Lukemier, Tom Shelhamer, Bob Stevens, Kevin Wronko, Sophomores Russel Battye, Addison Truxton, Jay Vesce, Craig Warner and Kurt Wittig.

A special award was made to Soccer Coach Ralph Dougan, whose team had a trophy containing the varsity's picture prepared for presentation to him on stage.

North Caldwell

Mr. and Mrs. Walter Kops of Mountain avenue had as their guest on Sunday, Dr. William A. Brown, who recently arrived in this country from Africa. Dr. Brown is a professor at the University of Monrovia in North Africa and supervises education in the bush country. His work is under the direction of the Methodist Mission Board. Before returning to Africa, Dr. Brown will make a tour through South America.

Mr. and Mrs. Richard Nelson of Hillcrest place were holiday hosts Wednesday evening at a carolling party. Joining them for the joyous occasion were Mr. and Mrs. Benjamin Stanley, Mr. and Mrs. Robert Griffith, Mr. and Mrs. Oakley Roark, Mr. and Mrs. James Richards, Mr. and Mrs. Richard Wagner, Mr. and Mrs. Francis Dean, Mr. and Mrs. Ned Kehoe of North Caldwell, Mr. and Mrs. John Jacobsen of Cedar Grove and Dr. and Mrs. Joseph Fleming of Montclair. They all returned to the Nelson home late in the evening for refreshments.

Mr. and Mrs. Hyman Goldman of Mountain avenue were in the group who returned for a party after the recent presentation of Dickens' "Christmas Carol". The party was held for the cast and crew members at the Firemen's Building.

Miss Judith Goodman, daughter of Mr. and Mrs. Morris Goodman of Mountain avenue, returned home on Friday from Douglass College for the holidays.

Mr. and Mrs. Paul Bender of Pine place expect their son home for the holidays, from the University of Miami.

The Garden Club of North Caldwell has been busy [illegible] holiday arrange-

mother, Mrs. Alice Paules of Red Lion, Pa.

Mr. and Mrs. Robert Spinner of Deer Trail road with friends, Mr. and Mrs. Kenneth Diamond of Millburn, recently journeyed to New York to see the show, "Owl and the Pussy Cat."

Mr. and Mrs. Charles L. Jaeger of Grandview avenue are entertaining this evening Mrs. Jaeger's parents, Mr. and Mrs. Joseph C. Mergner of Belleville, who will remain overnight. Tomorrow, Mr. and Mrs. Jaeger will have as guests also Mr. Jaeger's parents, Mr. and Mrs. Charles Jaeger of Newark. Recent guests at the Jaeger home were Mr. and Mrs. Robert Kessler of South Acton, Mass., who formerly resided in Montclair.

Harry De Old, Jr., son of Mr. and Mrs. Harry De Old of Hillside avenue, is now at home for the holidays from Franklin College.

On January 14, Men's night will be celebrated by the Garden Club of North Caldwell. The annual Christmas tree burning will take place and following that a covered dish supper will be held at the Gould Avenue School. Speaker for the evening will be Roy De Boer of Rutgers University.

Mr. and Mrs. Wilbur Dean Fairley of Springfield, Mass., entertained Friday evening at a dinner party in honor of the bridal party of Miss Virginia Hamlin, daughter of Mr. and Mrs. Mahlon Hamlin of White Oak drive, who was

Fig. 50

Enlargement of small portion of the high-resolution test pattern. The enlargement was obtained by scanning a small area of the 50X50 mm target of the 4½-inch return-beam vidicon so as to remove the bandwidth limitation. The width of one newspaper column is approximately one millimeter on the target.

Fig. 51 →

TV reproduction of 9X9-inch print of aerial photograph; 4½-inch return-beam vidicon, 1870 lines, 20 frames/sec, 3-to-1 interlace, 60-MHz bandwidth; photographed from 17-inch cathode-ray tube. Resolution is bandwidth limited. Scanning lines are not visible because of spot-wobble applied to the beam of the CRT.

Figures 44–63
Resolution

Fig. 52

TV reproduction of aerial photograph; 4½-inch return-beam vidicon, 1870 lines, 20 frames/sec, 3:1 interlace, 60-MHz bandwidth; photographed from 17-inch cathode-ray tube. Resolution is bandwidth limited. Scanning lines are not visible because of spot-wobble applied to the beam of the CRT.

Fig. 53

An enlargement of part of Fig. 52 obtained by scanning a small portion (approximately 1/30) of the format area in the pickup-tube sensor. This gives an indication of the amount of detail actually stored in the sensor.

Fig. 54 TV reproduction of aerial photograph; 4½-inch return-beam vidicon, 1870 lines, 20 frames/sec, 3:1 interlace, 60-MHz-bandwidth; photographed from 17-inch cathode-ray tube. Resolution is bandwidth limited. Scanning lines are not visible because of spot-wobble applied to the beam of the CRT.

Figures 44–63

Resolution

Fig. 55 Electronic enlargement of part of Fig. 54 obtained by scanning a small portion (approximately 1/30) of the format area in the pickup tube sensor. This gives an indication of the amount of detail actually stored in the sensor.

Fig. 56 Photographic copy of 8×10-inch master print (resolution 5400 lines, N_e = 2200). The copy, which was made with a 4×5-inch camera, has a resolution of 3000 lines, N_e = 1200. The printing process used in this book (150-line-per-inch screen) reduces the N_e of this print to roughly 800 lines.

Fig. 57 TV reproduction of master print, 1760 lines, 60 MHz, photographed with 4.5-inch return-beam vidicon on 17-inch CRT. The photographic copy used to make the reproduction shown here has a resolution of 1500 lines, $N_e = 600$.

Fig. 58 Electronic enlargement of Fig. 57 obtained by scanning a portion of the target of the return-beam vidicon.

Figures 44–63
Resolution

Fig. 59 Composite 1000-line TV picture (N_e = 650) assembled from four 500-line 7 MHz, 30 frames/sec. TV pictures.

Fig. 60 TV reproduction of master print, 625 lines, 9 MHz, 30 frames/sec, 4.5-inch image orthicon. Photographed from 17-inch CRT.

Figures 44–63
Resolution

Fig. 61 TV reproduction of master print, 525 lines, 7 MHz, 30 frames/sec, 4.5-inch image orthicon. Photographed from 17-inch CRT.

Fig. 62 TV reproduction of master print, 625 lines, 5 MHz, 25 frames/sec, 4.5-inch image orthicon. This is the broadcast standard in Western Europe. Photographed from 17-inch CRT.

Figures 44–63
Resolution

Fig. 63 TV reproduction of master print, 525 lines, 4.25 MHz, 30 frames/sec, 4.5-inch image orthicon. This is the U.S. broadcast standard. Photographed from 17-inch CRT.

Fig. 64 Reproduction of 8X10-inch master print by 35-mm motion-picture frame; medium-speed Plus-X film (ASA 120). Magnification from film to reproduction shown here: 10.5.

Fig. 65 Reproduction of 8X10-inch master print by 35-mm motion-picture frame; medium-speed Plus-X film (ASA 120). Magnification from film to reproduction shown here: 10.5.

Fig. 66 Reproduction of 8×10-inch master print by 16-mm motion-picture frame; medium-speed Plus-X film (ASA 120). Magnification from film to reproduction shown here: 24.

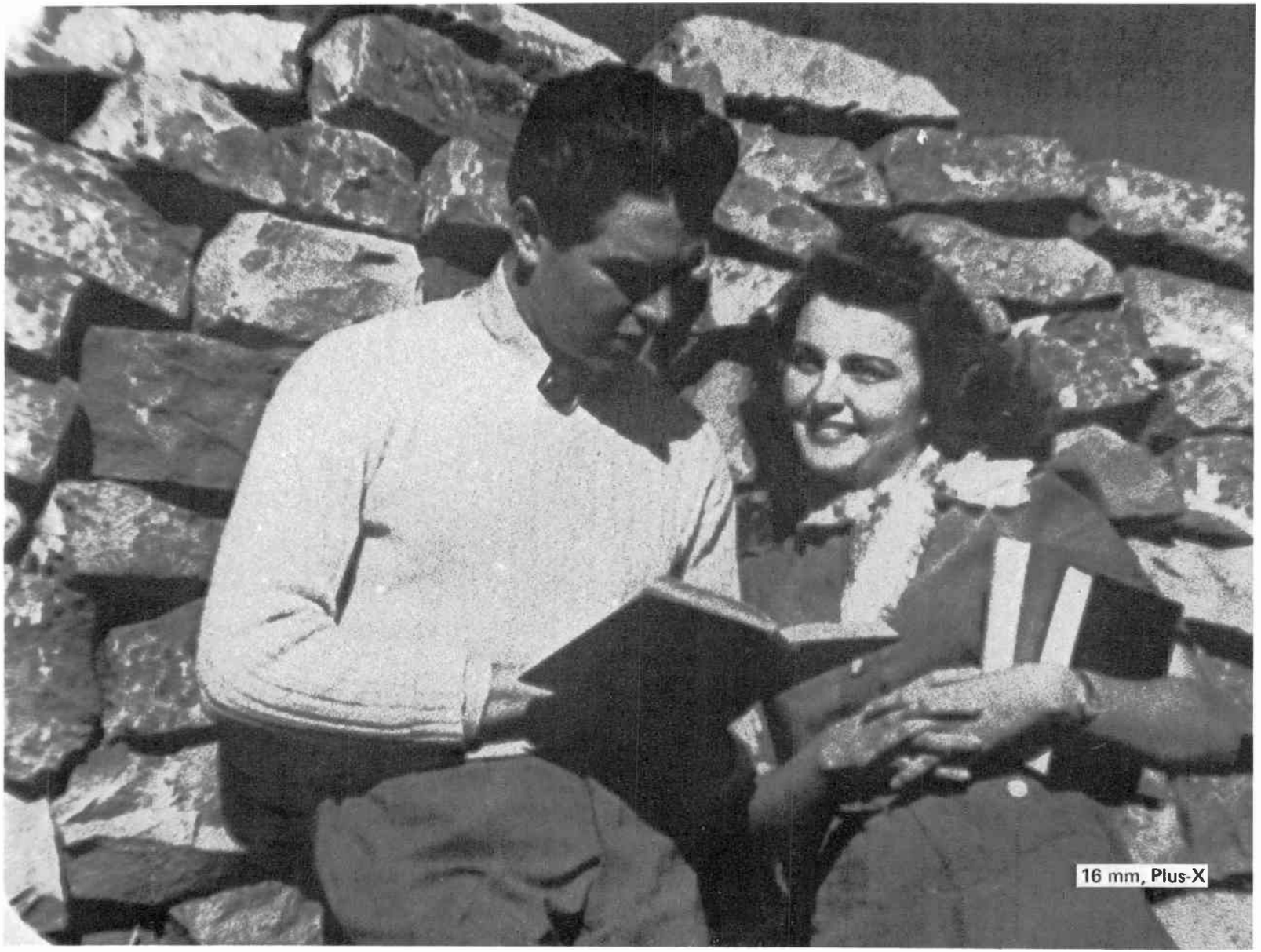

Figures 64–72
Film

Fig. 67 Reproduction of 8×10-inch master print by 16-mm motion-picture frame; medium-speed Plus-X film (ASA 120). Magnification from film to reproduction shown here: 24.

Fig. 68 Reproduction of 8X10-inch master print by super-8-mm motion-picture frame; medium-speed Plus-X film (ASA 120). Magnification from film to reproduction shown here: 43.

Figures 64–72
Film

Fig. 69 Reproduction of 8X10-inch master print by super-8-mm motion-picture frame; medium-speed Plus-X film (ASA 120). Magnification from film to reproduction shown here: 43.

Fig. 70 Reproduction of 8×10-inch master print by 35-mm motion-picture frame; high-speed Tri-X film (ASA 400). Magnification from film to reproduction shown here: 10.5.

Fig. 71 Reproduction of 8X10-inch master print by 16-mm motion-picture frame; high-speed Tri-X film (ASA 400). Magnification from film to reproduction shown here: 24.

Fig. 72 Reproduction of 8X10-inch master print by super-8-mm motion-picture frame; high-speed Tri-X film (ASA 400). Magnification from film to reproduction shown here: 43.